

Finding bioactive compounds in plant extracts by HPLC-coupled assays: novel approaches to natural product-based drug discovery

Ph.D. Thesis

Árpád Könczöl

Semmelweis University
Doctoral School of Pharmaceutical Sciences



Supervisor: Dr. György Tibor Balogh, Ph.D.
Consultant: Dr. Ágnes Kéry, Ph.D.

Official Reviewers: Dr. Huba Kalász, D.Sc.
Dr. Dezső Csupor, Ph.D.

Chair of Exam Committee: Dr. Kornélia Tekes, Ph.D.
Exam Committee: Dr. Éva Lemberkovics, Ph.D.
Dr. József Balla, Ph.D.

Budapest, 2013

Contents

CONTENTS	2
ABBREVIATIONS AND SYMBOLS	5
1. INTRODUCTION	7
1.1. Paradigm and challenges of the current drug discovery	7
1.2. Status and relevance of natural products in drug discovery	8
1.3. Novel approaches to natural product lead finding: profiling by coupled techniques	11
1.4. Review of targets and methods used in the screening and profiling of the plant extract library	15
1.4.1. Free radicals, oxidative stress and antioxidants	16
1.4.1.1. The DPPH (2,2-diphenyl-1-picrylhydrazyl) method	18
1.4.1.2. The peroxyxynitrite anion (ONOO ⁻): biochemistry and methodologies for measurement of ONOO ⁻ scavenging activity	21
1.4.2. The blood-brain barrier (BBB)	23
1.4.2.1. Methodologies for measurement of blood-brain barrier transport	25
1.4.2.2. The parallel artificial membrane permeability assay for blood-brain barrier (PAMPA-BBB)	26
1.4.2.3. Rationale of studying natural products and plant extracts by PAMPA-BBB	27
2. OBJECTIVES	28
3. MATERIALS AND METHODS	30
3.1. Chemicals and reference compounds	30
3.2. Plant material	30
3.2.1. Plant extract library	30
3.2.2. <i>Artemisia gmelinii</i> Webb. ex Stechm. (Asteraceae)	31
3.2.3. <i>Salvia miltiorrhiza</i> Bunge (Lamiaceae)	32
3.2.4. <i>Tanacetum parthenium</i> (L.) Sch. Bip. (Asteraceae)	32
3.2.5. <i>Corydalis cava</i> (L.) Schweig. & Kört. (Papaveraceae)	33
3.2.6. <i>Salvia officinalis</i> L. (Lamiaceae)	33
3.2.7. <i>Vinca major</i> L. (Apocynaceae)	34
3.3. Instrumentation	34
3.3.1. High performance liquid chromatography – mass spectrometry	34
3.3.2. Nuclear magnetic resonance spectroscopy	35
3.4. Cytotoxicity screening campaign	35
3.4.1. Cell line	35

3.4.2. Procedure of screening	36
3.4.3. Data handling.....	36
3.5. Antioxidant activity screening campaign	37
3.5.1. Procedure of screening	37
3.5.2. Data handling and IC ₅₀ measurement.....	38
3.6. Antioxidant activity-guided phytochemical investigation of <i>Artemisia gmelinii</i>	39
3.6.1. HPLC-based DPPH scavenging assay.....	39
3.6.2. Isolation of compounds 7a and 8a with preparative HPLC	39
3.6.3. High resolution mass spectrometry analysis	40
3.6.4. NMR spectroscopy	40
3.7. HPLC-based peroxynitrite scavenging assay	41
3.7.1. Synthesis of the peroxynitrite anion	41
3.7.2. Preparation of the <i>Salvia</i> specific model mixture.....	41
3.7.3. HPLC conditions	41
3.7.4. Peroxynitrite scavenging activity measurement in 96-well plate.....	42
3.8. Blood-brain barrier permeability screening campaign and related methods.....	43
3.8.1. PAMPA-BBB procedures	43
3.8.2. HPLC-MS analysis.....	44
3.8.3. Gas chromatography – flame ionization detector analysis of PAMPA-BBB co-solvents.....	46
3.8.4. NMR spectroscopy	46
3.9. Statistical analysis.....	47
4. RESULTS.....	48
4.1. Cytotoxicity screening.....	48
4.2. Antioxidant activity screening.....	49
4.3. HPLC-based antioxidant activity profiling of the methanolic extract of <i>Artemisia gmelinii</i>	51
4.3.1. Introduction	51
4.3.2. Phytochemical and antioxidant characterization	52
4.4. HPLC-based peroxynitrite scavenging activity profiling of <i>Salvia</i> spp.	56
4.4.1. Introduction	56
4.4.2. Optimization of the chromatographic conditions	59
4.4.3. Calibration for pyrogallol red.....	60
4.4.4. Validation of the assay with a <i>Salvia</i> specific model mixture.....	61
4.4.4.1. Comparison of degradation kinetics in mixture to individual scavenging activities.....	63
4.4.4.2. Validation of the assay parameters with structure – activity relationships	65
4.4.5. Demonstration of the assay performance on the methanolic extract of <i>Salvia miltiorrhiza</i>	65

4.5. Blood-brain barrier (BBB) permeability screening and HPLC-based hit profiling	67
4.5.1. Introduction	67
4.5.2. Validation of the PAMPA-BBB assay for natural products.....	68
4.5.3. Characterization of the effective BBB-permeability potential of major phytochemical compound classes.....	69
4.5.4. Co-solvent retention profile of the PAMPA-BBB assay.....	71
4.5.5. Screening of the plant extract library and tentative physicochemical characterization of BBB+ and BBB- plant extracts by LC-MS	72
4.5.6. Application of the PAMPA-BBB/LC-MS/NMR procedure to four BBB+ plant extracts.....	74
4.5.7. Evaluating the CNS-activity of the identified BBB+ compounds.....	80
5. DISCUSSION.....	81
5.1. HPLC-based antioxidant activity profiling of the methanolic extract of <i>Artemisia gmelinii</i>	81
5.2. HPLC-based peroxynitrite scavenging activity profiling of <i>Salvia</i> spp.	81
5.3. Blood-brain barrier (BBB) permeability screening and HPLC-based hit profiling	82
6. CONCLUSIONS.....	84
7. SUMMARY	87
8. ÖSSZEFOGLALÁS	88
9. REFERENCES	89
10. LIST OF PUBLICATIONS	108
10.1. Publications related to the thesis	108
10.2. Further scientific publications	109
11. ACKNOWLEDGEMENTS	110
12. APPENDIX	111

Abbreviations and Symbols

Abs	Absorbance
BBB	Blood-brain barrier
Caco-2	Human epithelial colorectal adenocarcinoma cell line
CHO	Chinese hamster ovarian cell line
CNS	Central nervous system
DAD	Diode array detector
DCQA	Dicaffeoylquinic acid
DMSO	Dimethylsulfoxide
DPPH	2,2-diphenyl-1-picrylhydrazyl radical
ESI	Electrospray ionization
ESR	Electron spin resonance spectroscopy
FCCP	Carbonyl cyanide- <i>p</i> -(trifluoromethoxy)phenylhydrazone
FID	Flame ionization detector
GCOSY	Gradient correlation spectroscopy
GHMBCAD	Gradient heteronuclear multiple bond coherence spectroscopy (adiabatic version)
GHSQCAD	Gradient heteronuclear single quantum coherence spectroscopy (adiabatic pulse version)
HPLC	High-performance liquid chromatography
HRMS	High-resolution mass spectrometry
HSCCC	High-speed counter current chromatography
HTS	High-throughput screening
I%	Inhibition percentage
IC ₅₀ /EC ₅₀	Half maximal inhibitory/effective concentration
LC	Liquid chromatography
LOD	Limit of detection
log BB	Logarithm value of brain tissue to plasma concentration ratio of a given drug
log <i>D</i>	Logarithm value of distribution coefficient

log k	Logarithm value of chromatographic retention factor
log <i>P</i>	Logarithm value of partition coefficient (measure of lipophilicity)
LOQ	Limit of quantitation
MS	Mass spectrometry
MDCK	Madin-Darby canine kidney epithelial cell line
MW	Molecular weight (dalton)
NCE	New chemical entity
NMR	Nuclear magnetic resonance (spectroscopy)
NP	Natural product
ONOO ⁻	Peroxynitrite anion
PAMPA-BBB	Parallel artificial membrane permeability assay for blood-brain barrier
PBL	Porcine brain lipid extract
PBS	Phosphate buffered saline
<i>P_e</i>	Effective permeability (cm/s)
PR	Pyrogallol red
PTFE	Polytetrafluoroethylene (teflon)
QQQ	Triple-quadruple mass analyzer
ROS	Reactive oxygen species
RP	Reversed phase
RSD	Relative standard deviation
SE	Standard error
SIM	Single ion mode
SPE	Solid phase extraction
TFA	Trifluoroacetic acid
TLC	Thin layer chromatography
TMS	Tetramethylsilane
<i>t_R</i>	Retention time (min)
UHPLC	Ultra-high pressure liquid chromatography
UV	Ultraviolet light

Note that bolded compound numbering refers to chromatographic retention order and indexes within are plant specific.

1. Introduction

1.1. Paradigm and challenges of the current drug discovery

Drug discovery is defined as the multidisciplinary process by which new medications for human diseases are discovered or designed. The complex process of modern drug discovery involves several distinct phases, such as the target identification (e.g., enzyme, receptor or ion channel, presumably involved in the pathological phenomenon of interest), the hit generation, and finally the lead generation and optimization. Hit generation can be based on a number of strategies, however since the advent of large chemical libraries produced by combinatorial synthesis in the 1990s, the high-throughput screening (HTS) became the mainstream (primary) approach to identify chemical starting points for drug discovery programs. In parallel with the expansion of these two technologies, the practice of the “olden” natural product (NP)-based drug discovery has been increasingly de-emphasized by the pharmaceutical industry. Causes and consequences of this partly controversial situation have been extensively discussed and analyzed in the recent literature [1-5], and have been briefly summarized in the next chapter of this thesis.

Nevertheless, it must be pointed out, that despite the significant advances in molecular biology, genomics, medicinal and analytical chemistry, the attrition rate and costs of drug development have reached an extremely high level: out of the 10 000 compounds evaluated in discovery efforts, only 250 (2.5%) enter preclinical testing, 5 (0.05%) move forward into clinical trials, and only 1 (0.01%) is granted approval by the Food and Drug Administration at a cost that is estimated between US\$ 1.3-1.6 billion [6]. Combining this fact with the lengthening of the overall R&D time at around 12-15 years, it has been concluded that the pharmaceutical industry is currently in a productivity crisis [7]. In such a difficult scenario, new and alternative methodological approaches and concepts that endeavor to accelerate and improve the drug discovery process are particularly needed. It is noteworthy that some of these innovative efforts have been clearly directed to harmonize and reintegrate the “conventional” NP-based lead generation within today’s fast-paced, HTS-utilizing drug discovery paradigm.

1.2. Status and relevance of natural products in drug discovery

Chemical substances derived from animals, plants and microbes (i.e., natural products) have been used by mankind to treat diseases since the dawn of medicine: fossil records date use of plants as medicines at least to the Middle Paleolithic age some 60 000 BC [8], while the oldest record on the use of NPs in medicine was written in cuneiform in Mesopotamia on clay tablets approx. 2600 BC [9]. Chemical and pharmacological investigation of traditional medicines in the 19th century, which were derived predominantly from plants, led to the discovery of most early drugs such as aspirin, digitoxin, codeine, morphine, quinine, and pilocarpine [1]. Turning to present times, as Fig. 1 clearly shows, NPs have served as an important source and inspiration for a significant fraction (approx. 40%) of the current pharmacopeia. In certain therapeutic areas the contribution is even higher: approx. 60% of anticancer remedies and 75% of drugs for infectious diseases are NPs or derivatives thereof [11].

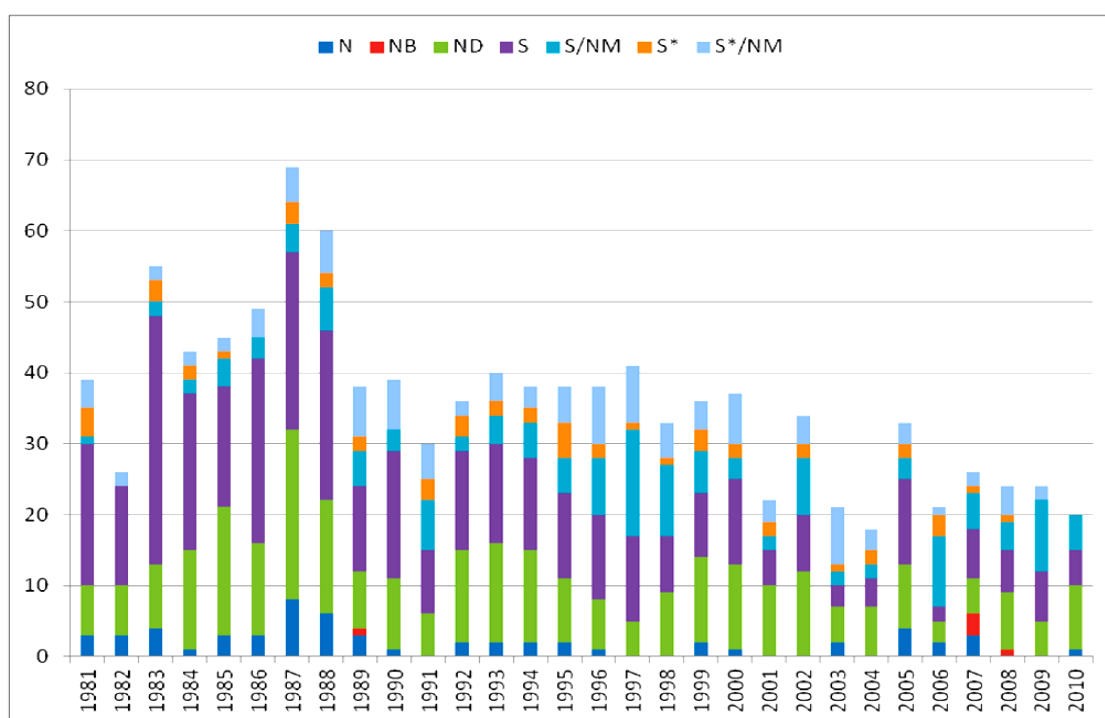


Figure 1. Sources of small molecule new chemical entities (NCEs) by source/year from 1981 to 2010. **N**: Natural product; **NB**: Natural product “Botanical” (defined mixtures); **ND**: Derived from a natural product and is usually a semisynthetic modification; **S**: Totally synthetic drug; **S***: Made by total synthesis, but the pharmacophore is/was from a natural product; **NM**: Natural product mimic. (Adapted from [10] without modification).

Nevertheless, it has also been demonstrated on Fig. 1, that the number of NCEs reaching the pharmaceutical market has shown a downward trend over most of the past two decades. It was supposed that beside many other commercial factors, the coincided decreasing emphasis in the mainstream pharmaceutical industry on NPs as the source of novel lead compounds has contributed to this decline [12, 13]. What were the underlying reasons for this trend in the past, and what changes are taking place today?

The advent of the HTS approach, followed by the introduction of combinatorial chemistry has fundamentally shifted the drug discovery paradigm in the 1990s. Practice of the NP-based lead generation has become incompatible, and thus uncompetitive with the HTS of large and pure synthetic compound libraries. First, NP extracts tend to be complex mixtures of secondary metabolites, containing hundreds or thousands of compounds, often including constituents (so called “nuisance compounds”) such as tannins, fatty acids, colored or autofluorescent chemicals, which are specifically interfering with routinely applied bioassays [14]. Thus, crude NP extracts cannot be screened directly in HTS campaigns. Second, once a NP extract has been identified as active, the principle responsible for the bioactivity must be isolated by a time-consuming and laborious bioactivity-guided fractionation. This step is further burdened and lengthened by the identification and elimination of already known compounds (dereplication), to avoid the duplication of effort. Third, after a single biologically active compound has been obtained from an extract, the *de novo* structure determination of the novel NP lead must be carried out (Fig. 2).

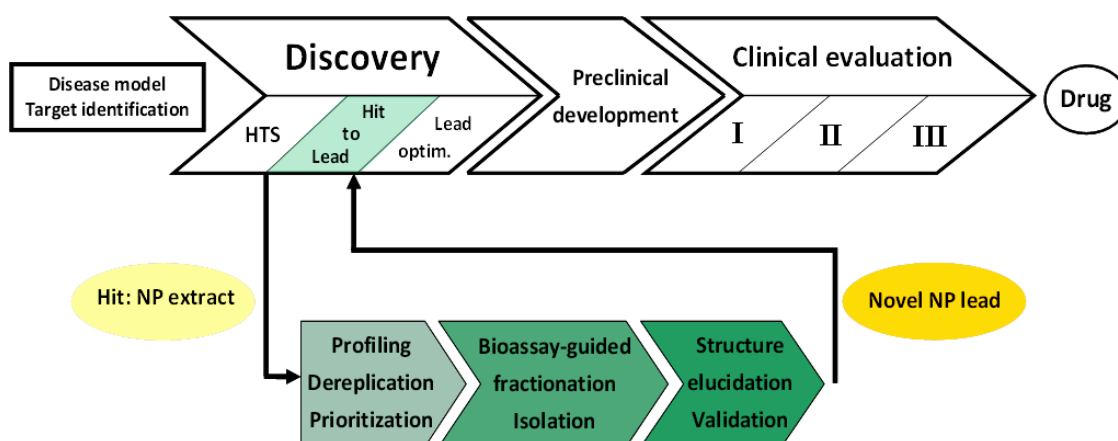


Figure 2. General scheme of HTS-based drug discovery and development. Unique processes of the NP-based approach within the hit-to-lead phase are enlarged and highlighted.

Furthermore, the complex nature of some NP chemical structures may present an obstacle for synthetic medchem modifications during the lead optimization phase and for total- or semi-synthesis in case of limited supply of the lead compound [1-3]. One can conclude, reviewing the above summarized drawbacks and concerns, that the NP-based drug research has not kept pace with the modern HTS approach and thus is not worthy of being practiced in today's drug discovery environment.

However, the success (hit rate) of any HTS campaign is inherently dependent on the quality of the screened library and the quality is determined by three factors: chemical diversity, lead-likeness, and biological relevance [15, 16]. Without a more detailed discussion, in terms of these features, NPs are considered as superior to any synthetic chemical collection: NPs offer high and unique chemical diversity [17, 18], combined with high probability of lead-likeness (or even drug-likeness) [19], and of affinity to biological macromolecules [20].

Moreover, recent advancements in separation and structure elucidation technologies, and particularly in the hyphenation thereof, have greatly improved the processes of isolation, dereplication, and structure elucidation. Owing to reliable and robust ionization interfaces (e.g., electrospray ionization), directly coupled high performance liquid chromatography (HPLC) - mass spectrometer (MS) systems have assumed a pivotal role in this area [21]. In the field of nuclear magnetic resonance (NMR) spectroscopy, the advent of multidimensional pulse methods and sensitivity improvements (e.g., micro-probe technologies) have dramatically lowered the amount of material needed (in the sub-milligram range) for structural analysis [22-24]. Combining the above mentioned techniques with purification (e.g., solid phase extraction) and liquid handling solutions has led to the development of automated, high-throughput fractionation systems, which were also capable of generating pure NP libraries in an efficient way [25-27]. Last but not least, innovative approaches, coupling of bioassays of interest to analytical procedures (typically to LC-MS) permitting the rapid and simultaneous separation and dereplication of active constituent(s) in NP extracts (i.e., activity profiling) have recently gained popularity as well. As the work presented in this thesis has focused on the same topic, detailed review of these profiling-like concepts and technologies is provided in the next chapter.

1.3. Novel approaches to natural product lead finding: profiling by coupled techniques

The major bottleneck (i.e., the rate limiting step) in the NP-based drug discovery is still the procedure of isolation and purification of the active principle (defined as the lead compound in this context) from an exceptionally complex matrix [2]. As can be seen in Fig. 3A, progression in the conventional bioactivity-guided route depends on the number of “cycles” of subsequent fractionation and bioassay steps required. As a result, the overall time needed to obtain a pure enough NP lead is the sum of the turnaround times of the three single steps multiplied by the number of cycles. In contrast, Fig. 3B depicts an alternative way: through simultaneous assessment and rapid correlation of the biological responses (e.g., on-line) to each constituent of the mixture, the synergistic melding of the bioassay and the analytical cascade is capable of shortening significantly the time needed to identify and/or isolate the bioactive agent(s).

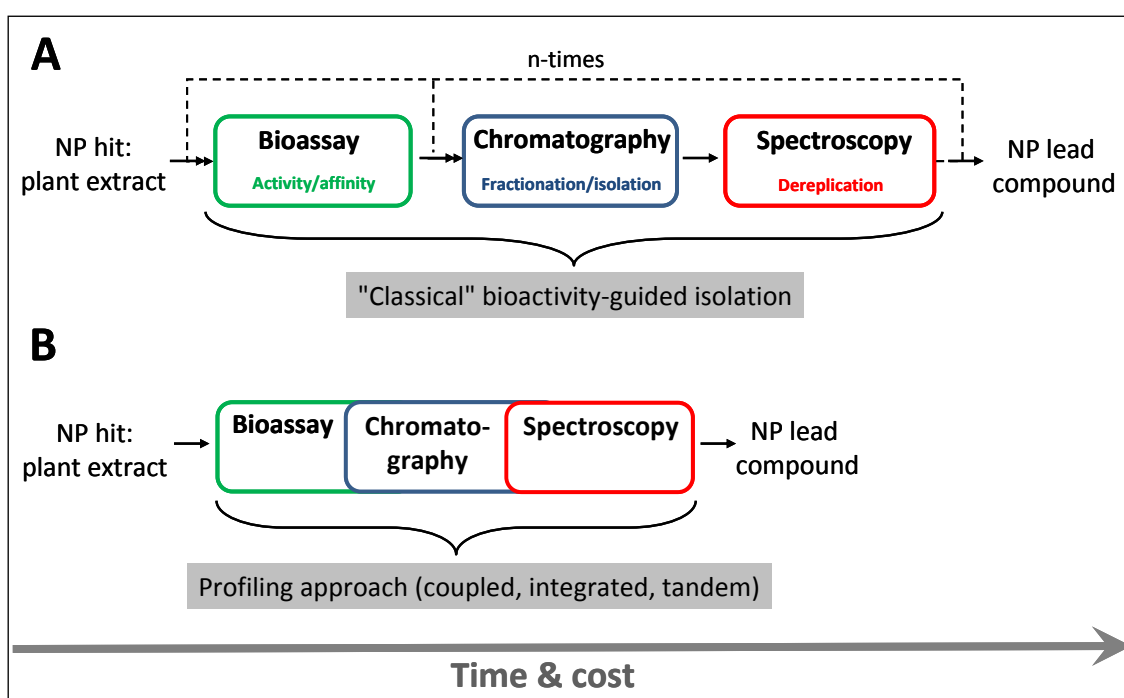


Figure 3. Comparison of the working schemes of the sequential (iterative) (A), and the more rapid and cost effective profiling approaches (B).

In addition, coupling of such techniques/assays to biological screens can improve the quality and information content of the assay result. Interaction (e.g., synergism) between mixture constituents or lack thereof could also be revealed by such

methods. It must be noted, however, that this type of coupling may represent a significant challenge in practice and must be carefully validated from several aspects before it is used. Depending on the studied biological phenomenon, the separation and detection technique, a number of different terms have been created in the literature for these types of approaches. In practice, the coupling follows basically three major strategies (Table 1 and Fig. 4).

Table 1. Summary of different types and setups of approaches applied for the profiling of complex mixtures (e.g., plant extracts) in NP-based drug discovery.

Type of assay coupling (setup and example)	Term and concept	Application
at-line (Fig. 4A)	HPLC-based activity profiling (microfractionation) [14] or small-scale bioprofiling [28]	<ul style="list-style-type: none"> • enzyme inhibition <ul style="list-style-type: none"> - COX-2 [29] - MAO-A [30] • receptor binding <ul style="list-style-type: none"> - GABA_A [31] - β₂AR [32]
off-line (Fig. 4B)	biological target interaction chromatography (“before-after” approach) [33] or ligand fishing [34]	<ul style="list-style-type: none"> • plasma protein binding [35] • DNA binding [36] • interaction with tubulin [37]
on-line <ul style="list-style-type: none"> • on-column (Fig. 4C) • post-column (Fig. 4D) 	affinity chromatography with immobilized targets: biological fingerprinting analysis (BFA) [33], missing peak chromatography [38] high-resolution screening (HRS) by biochemical detection (BCD) [42, 43]	<ul style="list-style-type: none"> • liposome and biomembrane affinity [39] • plasma protein affinity [40] • receptor binding [41] • free radical scavenging <ul style="list-style-type: none"> - DPPH [44] - ABTS [44] • enzyme inhibition [45] • receptor binding [45]

COX-2: cyclooxygenase-2; MAO-A: monoamine oxidase-A; GABA_A: γ-aminobutyric acid; β₂AR: β₂ adrenergic receptor; DPPH: 2,2-diphenyl-1-picrylhydrazyl; ABTS: 2,2'-azino-bis(3-ethylbenzothiazoline-6-sulphonic acid).

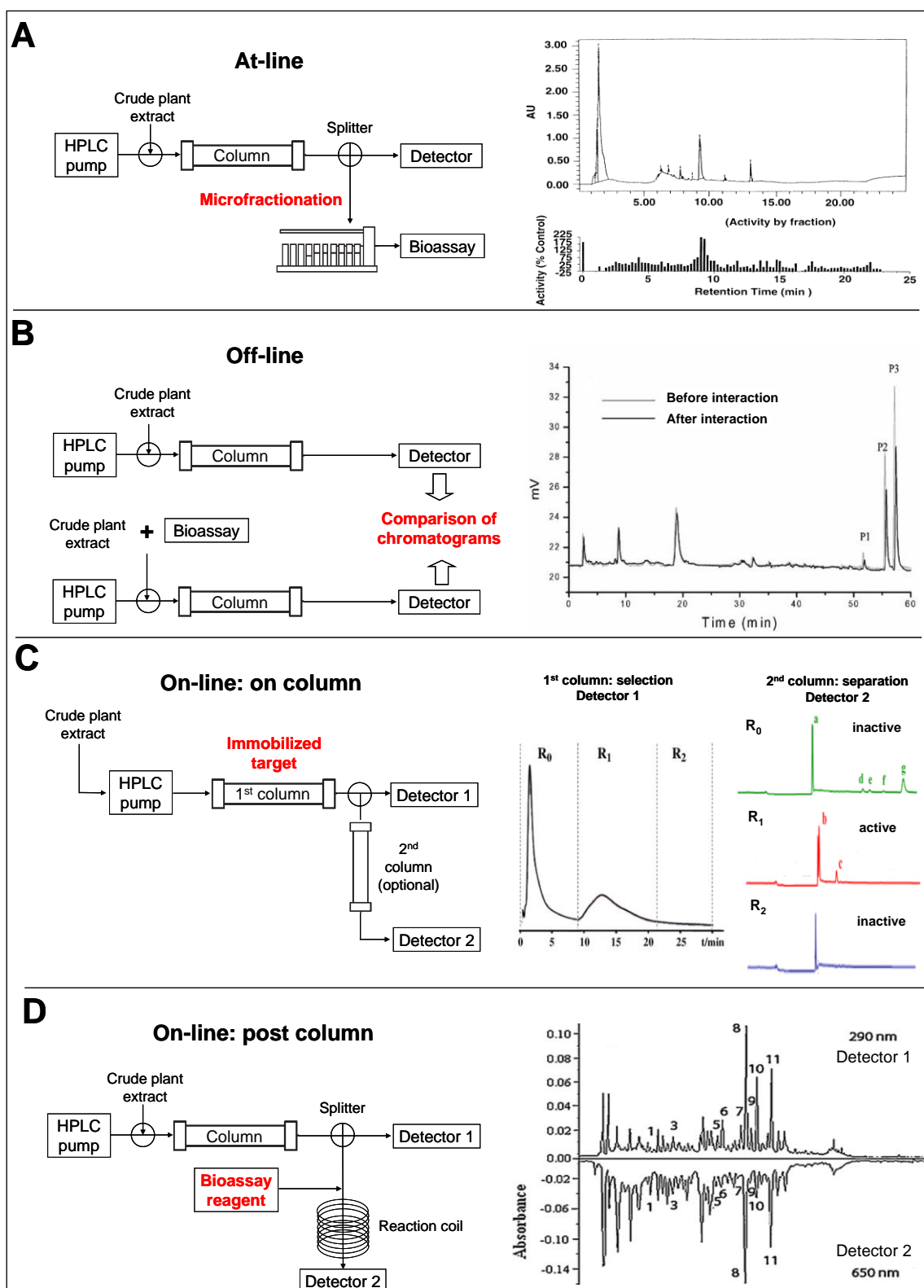


Figure 4. Instrumental configuration and one example from the literature of each profiling approach. (A) HPLC-based activity profiling [21], (B) Biological target interaction chromatography [36], (C) Affinity chromatography [41], (D) High resolution screening by post-column biochemical detection [53].

According to the first and simplest one, crude extracts are subjected to analytical or semi-preparative HPLC, and a portion of the effluent is collected into microplates (Fig. 4A). These microfractions are dried under vacuum, redissolved and assayed separately for bioactivity. The chromatogram and the activity profile are matched to identify active peaks [14]. Thus, this approach represents the miniaturized format of the conventional bioactivity-guided fractionation.

In the second approach, the multi-component NP extracts are allowed to interact with the targeted biomacromolecule prior to the chromatographic step (Fig. 4B). Next, comparison of chromatograms of the sample before and after being treated with the target indicates clearly the “biointeractive” constituents of the extract [33].

The most integrated and complex solution has been achieved by the development of the so called on-line assay configurations. In some of these systems the targets are immobilized on the stationary phase of a column and the mixture is continuously infused through of this (Fig. 4C). Compounds with the highest affinity for the target will have the longest breakthrough times (frontal affinity chromatography) [2, 33, 46].

Another group of on-line assays represents the high-resolution screening (HRS) methods (Fig. 4D), which utilizes continuous-flow biochemical detection in a so called post-chromatographic way: activity assessment of HPLC eluate is carried out in a post-column reaction chamber [42-45].

Moving to techniques used for the steps of separation and dereplication in these setups, literature reflects on the unequivocal dominance of HPLC-coupled spectroscopic systems, such as LC-DAD-MS/MS [44], and LC-NMR [47]. It must be noted, however, that most profiling/fingerprint analysis have been developed with Reversed Phase-LC using a simple UV detector. Furthermore, the recent advent of ultra-high performance liquid chromatography (UHPLC) [48], and the spreading of analytical columns packed with fully porous sub-2 μm and superficially porous particles have created ideal conditions for conducting such studies in terms of superior separation efficiency and sensitivity [49]. Finally, NP-specific, comprehensive chemical and biological databases, such as the NAPRALERT [50], the Dictionary of Natural Products (DNP) [51], and the Plant Profiler of Sigma-Aldrich [52] are supporting even more efficiently the critical step of dereplication in these workflows. For example, the database of DNP documents

and organizes every, virtually known natural product in a searchable form up to date (approx. 230 000 compounds).

Detailed analysis of strengths and limitations of the discussed approaches is beyond the scope of this thesis. Anyway, the following has been concluded in a very recent in-depth review: “Fully integrated systems represent technically impressive achievements, their implementation in other laboratories could be somewhat intricate. As a consequence many on-line assays have not been adopted outside of the lab where they were originally conceived. Compared to on-line assays, at-line and off-line approaches are more versatile, robust and probably have higher potential for broad implementation in NP-based drug discovery programs” [54]. In conclusion, the overall performance of a coupled system relies basically on two factors: on the resolving power/selectivity of the chromatographic separation as well as on the robustness/compatibility of the coupled bioassay.

1.4. Review of targets and methods used in the screening and profiling of the plant extract library

In this chapter, the biological background, the therapeutic impact and the methodological aspects of the two distinctive areas investigated in our screening and hit profiling studies are discussed:

- First, general biochemistry of free radicals and antioxidants is shortly summarized (Chapter 1.4.1.). It is followed by the detailed bibliographic presentation of the *in vitro* radical scavenging assay (2,2-diphenyl-1-picrylhydrazyl (DPPH)) used in our primary antioxidant screen. Next, an other reactive species (the peroxynitrite anion (ONOO^-)), and the related methodologies used in a secondary/focused antioxidant screen are introduced.
- Second, a biological barrier (the blood-brain barrier, (BBB)), with exceptional impact on the CNS drug discovery, and methodologies (*in vitro* mainly) investigating the permeation of molecules (e.g., drugs) through this barrier are reviewed (Chapter 1.4.2.). Finally, the last part of this chapter is devoted to the evaluation of the studied and applied permeability assay (parallel artificial membrane permeability assay for blood-brain barrier (PAMPA-BBB)).

Since our entire work focused on the screening of the plant extract library of Gedeon Richter Plc., much emphasis was placed on the potential role and relevance of plant metabolites in both of the above mentioned two topics. Moreover, where it was available from the literature, particular case studies related to the coupling of the bioassays used by us to analytical processes (typically to HPLC or LC-MS) are summarized as well.

1.4.1. Free radicals, oxidative stress and antioxidants

Free radicals (species with one or more unpaired electrons), such as reactive oxygen species (ROS) are generated by normal metabolic processes in all aerobic organisms due to the incomplete reduction of molecular oxygen in the electron flow chain (Fig. 5).

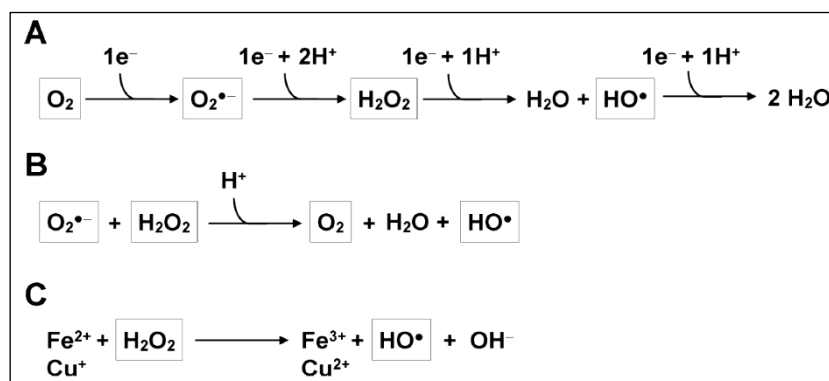


Figure 5. Production of ROS. (A) The stepwise transfer of electrons to O_2 leading to the generation of superoxide anion ($O_2^{\cdot-}$), then hydrogen peroxide (H_2O_2), and finally the highly toxic hydroxyl radical (HO^{\cdot}). (B) The Haber-Weiss reaction, and (C) the Fenton reaction for the formation of HO^{\cdot} . (Adapted from [55] without modification).

As the so formed ROS are highly reactive and deleterious towards other substances within cells (e.g., lipid membranes, proteins, and nucleic acids), endogenous antioxidant defense systems have been evolved during the course of evolution to minimize and repair free radical-induced damages [56]. These defensive mechanisms and molecular networks include enzymatic as well as non-enzymatic components, which are acting in concert to maintain the redox homeostasis of cells. For instance, superoxide dismutase, catalase, glutathione peroxidase, and glutathione reductase are enzymatic antioxidants in human plasma and erythrocytes, while bilirubin, melatonin, uric acid, glutathione, and ubiquinol belong to the group of small molecule antioxidant agents (i.e., radical scavengers) [56]. The efficiency, however, of this endogenous defence is considered as

incomplete, particularly under some pathophysiological conditions such as UV-irradiation, heavy metal exposure, inflammation, and ischemia/reperfusion [56]. As a result, oxidative stress develops, in which free radicals are produced in excess and at the wrong time and place. This leads to the oxidative damaging of cellular macromolecules, promoting ultimately cell death.

It has been shown and confirmed recently that oxidative stress is involved in aging [57] and several degenerative diseases, including cancer [58], cognitive dysfunction [59], diabetes mellitus [60], and atherosclerosis [61]. Therefore, considerable efforts have been paid to the quest for effective, exogenous antioxidants in the pharmaceutical industry: it was found that more than 300 000 papers associated with antioxidants were published from 1980 to 2008 [62]. Some of these works are devoted to synthesize antioxidants with novel structures [63-65], and characterize the radical scavenging properties of existing drugs to enlarge the therapeutic application of these drugs as antioxidants [66, 67]. Other works focus on the screening and extraction of antioxidant compounds from natural products to identify and isolate the valid and most potent scavengers in these mixtures [68-70]. It must be noted at this point, that the research for radical scavenger agents in the pharmaceutical and food industry has been partially merged into each other (see nutraceuticals), since many dietary compounds, such as vitamins A, C, and E, carotenoids, and plant phenoloids play important role in the maintenance of human health as well as in the prevention and treatment of diseases [56, 71].

Nevertheless, as phytotherapy and medicinal plant research are mainly focused on the areas of cancer and inflammatory diseases, huge number of studies have been published which are dealing with the screening and evaluation of the antioxidant/anti-inflammatory potential of plant extract collections/libraries [68, 72-77]. First, a common feature of these investigations was the use of robust *in vitro* bioassays (photometric-based) in the screening experiments. Second, it was revealed by mean of bioactivity-guided isolation that phenoloid compounds, such as flavonoids, simple phenols and caffeic acid derivatives were basically responsible for the measured radical scavenging activities of the extracts. Third, it can be concluded that the IC₅₀ values of crude or fractionated plant extracts which were considered as actives/hits in these screens fell in the range of 1-10 µg/mL.

1.4.1.1. The DPPH (2,2-diphenyl-1-picrylhydrazyl) method

DPPH is a stable N-centered radical discovered by Goldsmith and Renn in 1922 [78], and later utilized by Blois as a colorimetric reagent to evaluate the direct radical scavenging properties of small molecule antioxidants such as ascorbic acid, cysteine, and hydroquinone [79]. It is a paramagnetic compound with an odd electron and exhibits a strong absorption band at 517 nm, resulting a deep violet color in its alcoholic solution. Upon reduction by an antioxidant, the odd electron of DPPH becomes paired off (forming the stable, corresponding hydrazine): the violet color changes to yellow and the absorption of the solution decreases or vanishes (i.e., bleached out) (Fig. 6). This reaction is intended to mimic reactions taking place in oxidizing systems *in vivo*, such as the peroxidation of membrane lipids.

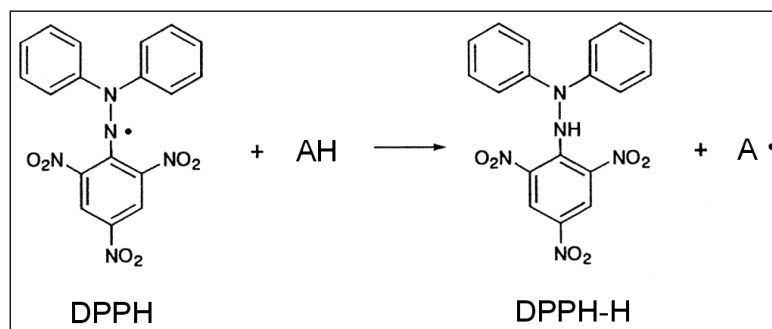


Figure 6. Reaction scheme for scavenging the DPPH radical by an antioxidant (AH) through hydrogen atom transfer.

Because of the relative simplicity and robustness of the colorimetric assay based on this reaction, now it has gained widespread use in the free radical scavenging activity assessment: it has become a primary method to measure the total antioxidant potential (hydrogen donating ability) of natural compounds, plant extracts, foodstuffs or other biological sources [80]. Moreover, it is also widely implemented to elucidate the redox properties of newly synthesized compounds [81, 82]. As a result, several modification, extension, improvement, and hyphenation of the original assay setup have been published [80]. Developments of the DPPH method, with particular focus on the antioxidant screening of plant extracts by chromatographic techniques are reviewed briefly in the following.

Combination of thin layer chromatography (TLC) with the DPPH method was reported first by Glavind and Holmer in 1967: after TLC separation of the analyte,

radical scavengers (tocopherols) were detected visually by spraying the TLC plates with DPPH solution [83]. Owing to its cost-effectiveness, this approach became very popular: Cieřla et al. have optimized and standardized it recently [84]. Since the spectrophotometric assay suffers from the interference with colored compounds frequently found in foodstuffs and plant extracts, HPLC-based quantitative methods have been proposed as alternatives to the original colorimetric assay to study such complex mixtures: Yamaguchi et al. developed a reversed phase HPLC method to selectively detect at 517 nm the remaining DPPH radical after off-line reaction of standard antioxidants with the probe [85]; while Boudier et al. optimized HPLC conditions to simultaneously quantify the reagent (DPPH) and the reaction product (DPPH-H) of the assay at 330 nm [86].

In addition, off-line LC-MS approaches have been developed to rapidly identify the most potent radical scavenger constituents of plant extracts by simply monitoring the reduction or disappearance of the corresponding peaks after addition of the active radical to the samples (see Fig. 4B for the corresponding instrumental setup): by evaluating the radical scavenger properties of 14 phenolic compounds in the extract of *Lonicerae japonica*, Tang et al. demonstrated that compounds with peak areas significantly decreasing were natural antioxidants, whereas those with peak areas not changing presented no activities [87]; Helmja et al. applied the same “spiking” test to the analysis of a *Solanum melongena* extract, and revealed the radical scavenging ability each of the identified single 11 compounds as a contribution to the total activity of the extract [88]. For this purpose, an opposite calculation of EC₅₀ was performed: compounds were characterized by the concentration of DPPH radical (mM) necessary to oxidize 50% of a compound in competition with all other oxidizable compounds in the mixture (Fig. 7). It was found that cinnamic acid derivatives corresponding to peaks 5-9 in Fig. 7 possessed low EC₅₀ values, thus, were mainly responsible for the antioxidative activity of the extract.

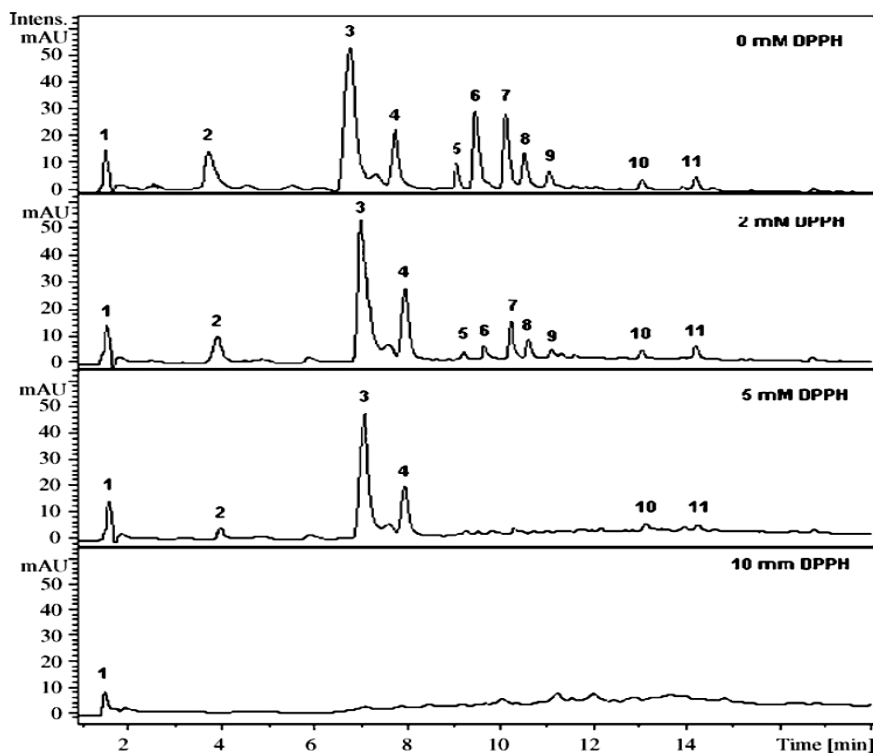


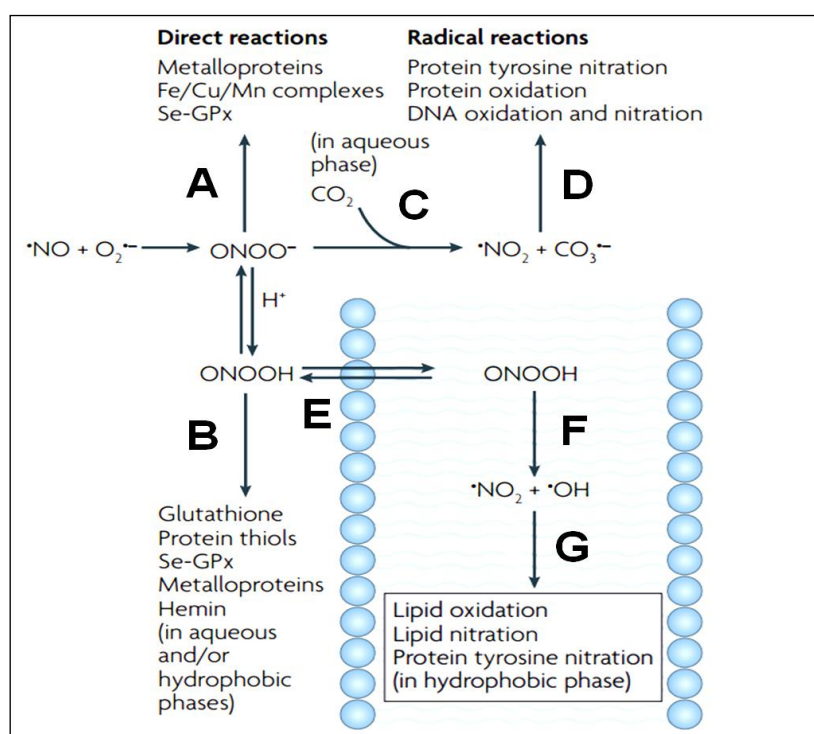
Figure 7. The HPLC–UV chromatograms of *Solanum melongena* extract and reaction products after treated with increasing concentrations of DPPH recorded at 280 nm. (Adapted from [88] without modification).

In contrast, van Beek and coworkers have created an on-line setup using the DPPH assay: a solution of the radical is added post-column and a second chromatogram is recorded parallelly at 517 nm. Thus, active compounds appeared as negative peaks (see Fig. 4D for the corresponding instrumental setup) [89]. Since then, a lot of successful examples of application have been reported [42, 90-93]. However, Zhang et al. have compared the performance of the on-line setup, to the pre-column off-line (spiking) method or to the at-line approach (microfractionation), and concluded that the reaction with DPPH prior to the separation gave the best resolution [94].

Off-line and on-line coupling of the prosperous high speed counter current chromatography (HSCCC) to the DPPH assay have also been solved recently by Chinese research groups. Numerous antioxidants have been rapidly identified and isolated from complex plant extracts by the guidance of DPPH-HPLC assays [95-98]. It must also be noted that the DPPH method has been adopted to microplate format, thus it became convenient to HTS [99].

1.4.1.2. The peroxynitrite anion (ONOO⁻): biochemistry and methodologies for measurement of ONOO⁻ scavenging activity

The peroxynitrite anion (ONOO⁻), typically produced by the rapid diffusion-controlled reaction of nitric oxide ([•]NO) with superoxide radical (O₂^{•-}) *in vivo*, is implicated in the pathogenesis of a wide variety of human diseases, such as atherosclerosis, obesity, diabetes mellitus, and Alzheimer-disease [56, 100]. Although not a free radical by chemical nature (it is an unstable structural isomer of the nitrate anion), ONOO⁻ is considered as a powerful oxidizing and nitrating species. Fig. 8 summarizes the major biochemical reactions (direct as well as indirect ones), which are leading to the complex and deleterious/cytotoxic effects of ONOO⁻ [101]. It must be pointed out, however, that only minor part of ONOO⁻ is transformed into radicals: it is mostly trapped *in vivo* by thiols and metalloproteins (Fig. 8A and B) [101].



Se-GPx: selenium-containing glutathion peroxidase, DNA: deoxyribonucleic acid.

Figure 8. Biochemical reaction pathways of peroxynitrite. Peroxynitrite anion (ONOO⁻) is in equilibrium with peroxynitrous acid (ONOOH; pK_a=6.8) and either one can undergo direct reactions with biomolecules as indicated (A and B). A fundamental reaction of ONOO⁻ in biological systems is its fast reaction with carbon dioxide (C), which leads to the formation of carbonate (CO₃^{•-}) and nitrogen dioxide ([•]NO₂) radicals, which are good one-electron oxidants (D) that can readily oxidize amino acids such as cysteine and tyrosine to yield the corresponding cysteinyl and tyrosyl radicals. In addition, [•]NO₂ can undergo diffusion-controlled termination

reactions with biomolecule-derived radicals, resulting in nitrated compounds (**D**). Alternatively, ONOOH can undergo homolytic fission to generate one-electron oxidants hydroxyl ($\cdot\text{OH}$) and $\cdot\text{NO}_2$ radicals (**E**). However, this reaction is slow in biological systems compared with the other reactions of ONOO^- and ONOOH and therefore is a modest component of the *in vivo* reactivity of peroxynitrite in aqueous compartments. However, ONOOH readily crosses lipid bilayers (**F**) and its decomposition to $\cdot\text{OH}$ and $\cdot\text{NO}_2$ radicals seems to become relevant in hydrophobic phases to initiate lipid peroxidation and lipid and protein nitration processes (**G**). Moreover, ONOOH in the membranes may undergo direct reactions with metal centres such as hemin or membrane associated thiols. (Adapted from [101] without modification).

Since its half-life is less than a second under physiological conditions, direct detection of ONOO^- in biological systems is really difficult. Beside electron spin resonance (ESR) assays [102], fluorescent and luminescent spectroscopic probes have been used frequently for this purpose [103-105]. In addition, indirect approaches have focused on the detection of endogenous biomolecules modified by a ONOO^- -dependent reaction, e.g., quantification of 3-nitro-tyrosine as a marker product of ONOO^- -specific aromatic nitration of tyrosine by HPLC has gained popularity [106, 107]. Anyway, the specificity of these techniques is considered controversial due to several interfering factors.

In contrast, due to the relatively simple generation procedure and stability of ONOO^- at laboratory conditions [108], numerous *in vitro* assays (with lower biological significance obviously) assessing ONOO^- scavenging activity of single compounds or biological samples have also been developed. Among those, the most accepted method is based on the oxidation of dihydrorhodamine by ONOO^- to fluorescent rhodamine [109]. Being less sensitive, however, colorimetric bleaching assays have also been published: Balavoine and Geletii have developed a simple and robust colorimetric assay based on pyrogallol red dye bleaching for screening of ONOO^- scavenging activity of plant extracts and foodstuffs [110, 111].

Turning to the analyses of naturally occurring peroxynitrite scavengers, it can be concluded that a great number of biological samples and natural compounds have been reported as effective ONOO^- scavengers *in vitro*, however the number of comprehensive screening studies on this topic is rather limited. It was found that representative compounds of flavonoids (e.g., quercetin, kaempferol, luteolin, epicatechin) [112, 113], phenylpropanoids and derivatives thereof (e.g., caffeic acid, sinapinic acid, chlorogenic acid, and curcumin) [107, 114, 115], carotenoids [116], and

tocopherols [116] possessed significant ONOO^- eliminating activity. In the case of phenoloids, structure activity relationships have been revealed in further mechanistic studies (Fig. 9): it has been shown that the ortho-hydroxyl structure, especially the catechol group in the ring B seems essential for ONOO^- scavenging activity, and the 2,3-double bond also plays an important role, while *O*-glycosilation reduces the radical scavenging activity (reviewed extensively in [117]). As a conclusion, two possible mechanisms for phenoloid-mediated ONOO^- scavenging have been proposed: monohydroxylated structures act as alternative substrates for nitration, whereas catechol moieties are oxidized to *o*-quinones (electron donation).

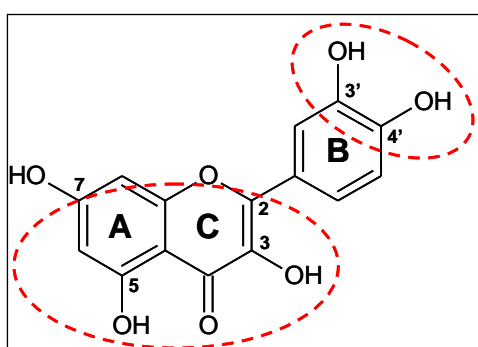


Figure 9. Structural features of quercetin responsible for ONOO^- scavenging activity.

Although significant efforts have been made in medicinal plant research to identify and isolate compounds with ONOO^- scavenging potential from plant extracts, little or no attention has been paid to the effective coupling of antioxidant activity assays with advanced separation techniques (HPLC). Recent studies are still reporting the practice of the conventional bioassay-guided (sequential) isolation approach [118-120], thus giving up the chance to characterize the contribution of the single components to the total activity.

1.4.2. The blood-brain barrier (BBB)

The BBB is a unique physical and metabolic barrier formed by brain capillary endothelial cells joined by tight junctions. It serves to isolate the cerebral parenchyma from the systematic circulation and helps to maintain the homeostasis of the brain microenvironment by allowing the entry of selected nutrients and macromolecules, while restricting the penetration of polar molecules [121, 122]. Features that distinguish the brain endothelium from that of other organs include complex tight junctions,

relatively low pinocytotic activity, and the expression of a number of specific uptake and efflux transport systems and metabolic enzymes (such as P-glycoprotein and cytochrome P450 enzymes) [123]. These properties greatly limit the transcellular and paracellular movement of drugs and xenobiotics to the CNS and make the BBB a highly selective regulatory interface: only 2% of the possible CNS therapeutic compounds can pass the BBB and reach their therapeutic targets [124]. It means that the BBB poses a major challenge for today's CNS drug discovery, since CNS drugs must permeate the barrier, whereas compounds targeting peripheral tissues should be impaired in the passage.

The main molecular transport mechanisms, such as passive and active pathways across the BBB are summarized and illustrated in Fig. 10.

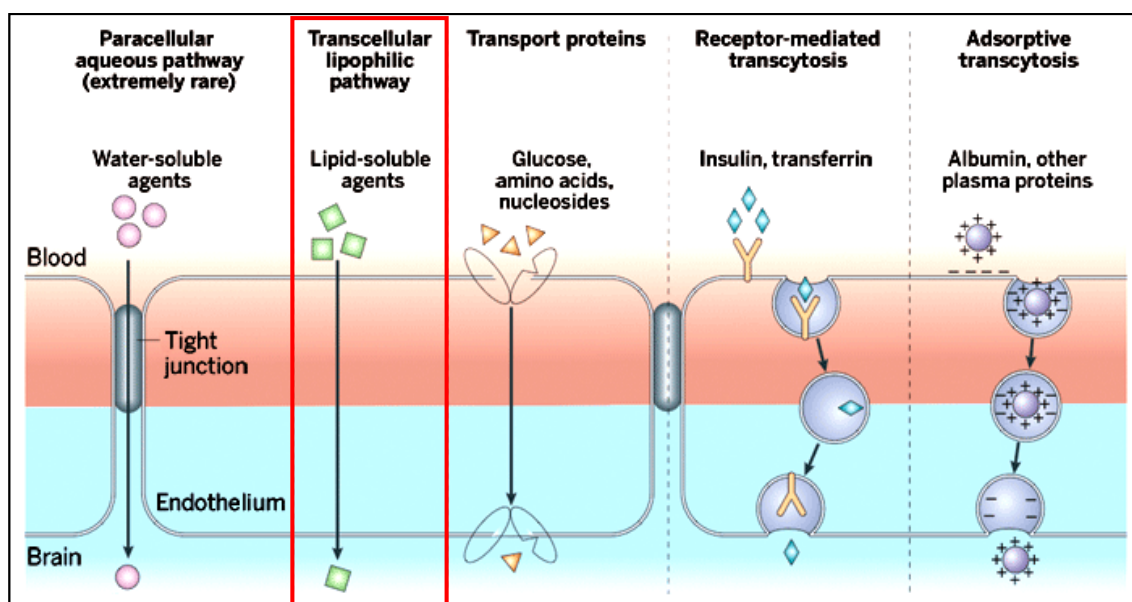


Figure 10. The main routes for molecular traffic across the BBB. Note that most CNS drugs enter the brain by transcellular passive diffusion (also called the “pharma route”, highlighted in red bracket). (Adapted from [125] with minor modification).

Since paracellular permeation is practically restricted by tight junctions in the BBB, and uptake transporters are basically intended to enhance the transport of nutrients and cofactors, most small molecule drugs enter the brain by transcellular passive diffusion. This process is driven by a concentration gradient between the blood and the brain, and is inherently affected by the physicochemical properties of discovery compounds, such as molecular size, lipophilicity ($\log P$ or $\log D$), flexibility, and total

polar surface area (TPSA). The brain exposure of an individual drug, however, always needs to be considered as a resultant of multiple permeation and distribution mechanisms, including efflux transport, metabolism, and plasma protein binding [126]. As a consequence, the implemented methodology used for the assessment of brain penetration must appropriately reflect on these processes.

1.4.2.1. Methodologies for measurement of blood-brain barrier transport

Owing to the prominent role of BBB transport in CNS drug research, a wealth of new approaches and assays have been established over the years to measure and predict the brain penetration of drugs and discovery compounds (comprehensively reviewed in [126-129]). Among these, the cost-effective *in silico* models, based on correlations between compound permeation and physicochemical descriptors, have gained popularity in the early phase of drug discovery. However, their scope and predictive power are limited only to aid the design of synthetic libraries and to classify compounds with high and low brain penetration potency. The other end of the BBB-assay spectrum in terms of reliability and cost represents *in vivo* techniques. These involve traditionally low-throughput and labor-intensive measurements, such as brain microdialysis and brain perfusion studies performed in rodents. They are designed to assess specific parameters of brain penetration, namely rate, extent and unbound drug concentration.

Since only a limited number of compounds can be evaluated by these *in vivo* techniques, robust and high-throughput *in vitro* approaches have emerged in the pharmaceutical industry. *In vitro* BBB methods could be classified into cell-based and noncell-based assays. Cell-based assays are utilizing either brain-derived (e.g., isolated brain capillaries, bovine brain microvessel endothelial cell culture) or non-brain-derived (e.g., Caco-2, MDCK) cells and are intended to indicate efflux/uptake potential and/or metabolic liabilities. In contrast, the principle of noncell-based models is strictly physicochemical by nature. Thus, they tend to mimic and predict exclusively the transcellular passive diffusion component of the whole brain disposition process. The immobilized artificial membrane chromatography (IAM), and the parallel artificial membrane permeability assay (PAMPA) form this latter group of methods [126-129].

1.4.2.2. The parallel artificial membrane permeability assay for blood-brain barrier (PAMPA-BBB)

The parallel artificial membrane permeability assay was first introduced by Kansy et al. in 1998 to model oral absorption processes [130]. Di and coworkers have modified the PAMPA system specifically for BBB application: they applied porcine brain lipid extract (PBL) dissolved in n-dodecane as PAMPA membrane, and demonstrated that using this method discovery compounds can be binned into CNS+ and CNS- classes [131]. It has also been reported that the PAMPA-BBB derived values display good correlation to cell-based models and to *in situ* brain perfusion measurements [132]. Since then, the PAMPA technique has become one of the most powerful and versatile physicochemical screening tool in early stage CNS-targeted drug discovery practice [133].

The system consists of two multiwell microtiter plates, a donor and an acceptor compartment in a “sandwich” like configuration, separated by an artificial lipid impregnated filter membrane (Fig. 11).

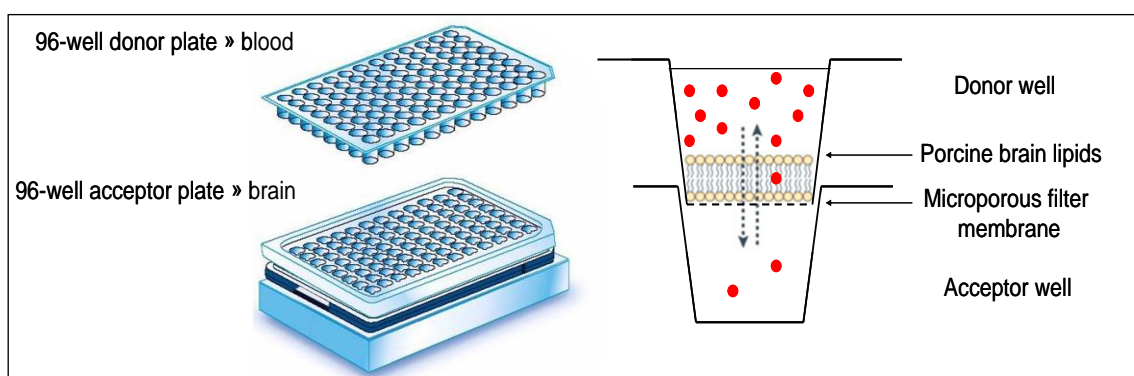


Figure 11. General scheme of the PAMPA-BBB system: setup of the “sandwich” plate (left), and schematic representation of passive diffusion in a well (right).

Initially, the test drug is added in the donor plate and allowed to diffuse across the membrane. After incubation (typically for 4 hrs at 37 °C), PAMPA sandwich plates are separated and drug concentrations in donor and acceptor solutions are determined by UV spectroscopy or LC-MS. Thus, the rate of transcellular passive diffusion can be predicted by calculating the effective permeability (P_e , cm/s) of the tested drugs.

1.4.2.3. Rationale of studying natural products and plant extracts by PAMPA-BBB

Plant extracts with traditionally known or ethnomedically proven neurobiological activity are attractive lead sources for CNS drug discovery [134-138]. However, for the vast majority of CNS-active herbal remedies the active principles and the exact molecular mechanism of action have not yet been elucidated [139]. Nevertheless, it can be assumed that certain constituents of such plant extracts are capable of crossing the BBB.

In silico calculations have been developed and validated mainly using large datasets of drugs [140, 141], and, as the NP chemical space significantly differs from that of therapeutic agents and synthetic compounds [142, 143], the predictive accuracy and reliability of these models for plant metabolites are questionable, whereas costly *in vivo* BBB techniques are considered as impractical for complex mixtures like plant extracts.

In contrast, the PAMPA-BBB assay is a single mechanism-based measurement, and when the complexity of a typical plant extract is considered, this feature has great importance, because evaluation and interpretation of multimechanism-type (i.e., active transport, metabolic transformation) assay results may be quite challenging. Moreover, PAMPA-BBB studies, conducted in cassette dosing (i.e., sample pooling, wherein the number of mixed components varies between three and 32) have indicated no significant interference or difference on effective permeabilities whether assessed with single compounds or mixtures thereof [144-148]. Tarragó et al. have evaluated earlier permeability values in a crude plant extract for baicalin and baicalein using a PAMPA-BBB assay [149]. These features of the PAMPA-BBB system stimulated us to investigate its potential use on crude and pre-fractionated plant extracts in terms of screening and identifying compounds with high brain penetration propensity.

2. Objectives

“These materials have already been prepared for humans, we should merely reach them.”

Ivan Petrovich Pavlov

The primary aim of our work was to design, adopt and/or validate, and perform screenings of a plant extract library. The screening assays included a cytotoxicity, an antioxidant, and a BBB permeability screening campaign. As the plant extract hits emerged from the latter two screenings proved to be complex mixtures of secondary plant metabolites, we attempted to couple the bioassays of particular screens to HPLC-based analytical procedures. While doing this, our motivation was to shorten the bioassay-guided isolation route of the active principle(s), particularly in the lead compound identification and dereplication step. Therefore, much emphasis was placed on the methodological aspects of the assay couplings: analytical features such as resolution, throughput and applicability were studied and optimized in detail. Moreover, by mean of the case studies presented in this thesis, we have endeavored to contribute to the phytochemical and pharmacological characterization of the investigated plant species.

The specific aims were the followings:

- To screen the plant extract library for cytotoxic activity, and to analyze the dependence of the cytotoxic activity of plant extracts on the type (polarity) of the solvent extraction procedure.
- To screen the plant extract library for antioxidant activity and to analyze the dependence of the antioxidant activity of plant extracts on the type (polarity) of the solvent extraction procedure.

- To analyze and prioritize (dereplicate) the resulted plant extract hits by LC-MS, and to develop a LC-MS method that can be coupled with the DPPH assay in order to effectively identify the radical scavenger constituents in one antioxidant plant extract hit, namely in the methanolic extract of *Artemisia gmelinii*.
- To isolate and elucidate the chemical structure of the most active radical scavenger compounds in the methanolic extract of *Artemisia gmelinii*.
- To adopt and validate the pyrogallol red bleaching test for HPLC in order to screen and characterize chemical constituents with peroxynitrite (ONOO⁻) scavenging activity in alcoholic extracts of *Salvia* species, since *Salvia* extracts proved to be predominant among the antioxidant hits.
- To demonstrate the performance of the developed HPLC-based ONOO⁻ scavenging assay on the methanolic extract of *Salvia miltiorrhiza* Bunge.
- To investigate the applicability of the PAMPA-BBB assay for NPs and plant metabolites, and to screen the plant extract library for NP compounds with high brain penetration propensity.
- To couple the PAMPA-BBB assay to NMR experiments and to demonstrate the feasibility of this type of coupling on BBB+ plant extract hits (exemplified by the extracts of *Tanacetum parthenium*, *Vinca major*, *Salvia officinalis*, and *Corydalis cava*).

In conclusion, our entire workflow focused on the acceleration of the lead generation phase in the NP-based drug discovery by coupling (integrating) bioassays with advanced separation and spectroscopic techniques in a valid and efficient way.

3. Materials and Methods

3.1. Chemicals and reference compounds

All solvents used were LC-grade. Acetonitrile (MeCN), ethanol (EtOH), methanol (MeOH), chloroform (CHCl₃), dimethyl sulfoxide (DMSO), trifluoroacetic acid (TFA), acetic acid, glycine, sodium nitrite, hydrochloride were purchased from Merck (Darmstadt, Germany). All other reference compounds and reagents were analytical grade and purchased from Sigma-Aldrich (St Louis, MO, USA), except for adhyperforin, α -solanine, apigenin-7-*O*-glucoside, aucubin, betulin, chamazulene, catalpol, (+)-catechin, cynarin, galantamine, harpagoside, hyperforin, lupeol, luteolin-7-*O*-glucoside, nicotinic acid, parthenolide, protopine, salvianolic acid A, scopolamine, sinapic acid, solasodine, and stigmasterol, which were obtained from PhytoLab (Vestenbergsgreuth, Germany). BBB specific porcine brain lipid (PBL) extract was purchased from Avanti Polar Lipids (Alabaster, AL, USA). Purified water (18 M Ω ·cm) was obtained from a Millipore (Bedford, MA, USA) Milli-Q water-purification system and used for all aqueous solutions and eluents.

The reference compound collection used in the hit characterization and dereplication studies (LC-MS for antioxidant hits, LC-MS/MS for PAMPA-BBB hits) consisted of ubiquitous representatives of carboxylic acids, flavonoids, alkaloids, and terpenes and was identical with the list of Table A2 (Appendix). In addition to that list, gallic acid, caftaric acid, 4-*O*-caffeoylquinic acid (cryptochlorogenic acid), salvianolic acid B, cynarin, 5-hydroxyflavone, myricetin, carnosol, curcumin, and ursolic acid were included in the used reference substance collection (N=82).

3.2. Plant material

3.2.1. Plant extract library

The plant extract library of Gedeon Richter Plc. was assembled mainly between 1999 and 2001, in the course of a contractual cooperation with (i) the Institute of Ecology and Botany of the Hungarian Academy of Sciences, Vácrátót, Hungary; (ii) the Department of Pharmacognosy, Semmelweis University, Budapest, Hungary; (iii) the Department of Pharmacognosy, University of Szeged, Szeged, Hungary; and (iv) the Medicinal Plant

Research Institute, Budakalász, Hungary. This cooperation resulted in 4400 randomly collected individual extracts, originated from ca. 500 drugs of 300 plant species endemic or to-grow in the Carpathian Basin. The taxonomic composition of the collection shows a highly diverse profile, however, the representatives of the Lamiaceae and Asteraceae families are predominant.

The preparation of the extracts followed basically a general scheme: first, the dried and ground drug was extracted with CHCl_3 or in some case with petroleum ether (this procedure yielded the apolar crude extracts). After filtration the residual plant material was dried and extracted successively with aqueous MeOH (this procedure yielded the polar crude extracts). Finally, the crude extracts were evaporated to dryness *in vacuo*, and were fractionated by open column chromatography according to standard protocols. Stock solutions of the resulted fractions were prepared uniformly in DMSO at 40 mg/mL, filtered through 0.45 μm Millipore (Billerica, MA, USA) filters and stored at $-19\text{ }^\circ\text{C}$ in polypropylene deep-well plates (80 samples per plate, A2-H11) until required for screening experiments.

3.2.2. *Artemisia gmelinii* Webb. ex Stechm. (Asteraceae)



Aerial parts of *A. gmelinii* were collected before full blooming from the experimental field of the Institute of Ecology and Botany of the Hungarian Academy of Sciences, Vácrátót, Hungary. The plant material was identified by Dr. Vilmos Miklósi V. A voucher specimen (no. L8275) has been deposited in the Herbarium of the Institute. Dried and ground aerial parts of *A. gmelinii* (50 g) were first extracted with $1\times 200\text{ mL}$ and $1\times 100\text{ mL}$ of

Figure 12. *Artemisia gmelinii* [150]. $\text{CHCl}_3/\text{MeOH}$ 90:10 (v/v) using an ultrasonic bath for $2\times 15\text{ min}$ (this procedure yielded the CHCl_3 extract). After filtration the residual plant material was dried and extracted with 1×200 and $1\times 100\text{ mL}$ of 70% (v/v) aqueous MeOH at room temperature in an ultrasonic bath for $2\times 15\text{ min}$. The filtered and combined aqueous methanolic extracts were evaporated to dryness *in vacuo* to yield 3.7 g of brown oily material. This extract was fractionated by open column chromatography on silica gel (Kieselgel 60, 0.063-0.200 mm, 1.07734.100 Merck, Germany) (sorbent:

83 g, column size: 30 cm × 3 cm Ø) using a gradient system of CHCl₃/MeOH/H₂O (90:10:1, 90:15:1.5, 90:25:2.5, 90:35:3.5, 90:45:4.5, 90:60:6 v/v, each 200 mL). The last fraction (VI) was obtained in a yield of 705 mg. 60 mg of the obtained sample was dissolved in dimethyl sulfoxide, filtered through a 0.45-µm Millipore (Billerica, MA, USA) filter and stored at -19 °C in a deep-well plate until required for screening experiments.

3.2.3. *Salvia miltiorrhiza* Bunge (Lamiaceae)



Salvia miltiorrhiza Bunge was cultivated from seed exchange in the experimental field of the Research Institute of Ecology and Botany of the Hungarian Academy of Sciences (Vácrátót, Hungary). Herb was collected during the flowering period and was identified in the Institute, where herbarium specimen is also deposited. Air-dried and finely powdered aerial part of *S. miltiorrhiza* (50 g) was first ultra-sonicated with CHCl₃ at

Figure 13. *Salvia miltiorrhiza* [151]. room temperature and the dried residue was extracted with 70% MeOH. Methanol was evaporated under reduced pressure. The resulted sample was freeze-dried, weighed, and solved in DMSO at 2 mg/mL concentration, filtered through a 0.45 µm Millipore filter and stored at -19 °C until required for the experiments.

3.2.4. *Tanacetum parthenium* (L.) Sch. Bip. (Asteraceae)



Figure 14. *Tanacetum parthenium* [152].

Aerial parts of *Tanacetum parthenium* (L.) Sch. Bip. (Asteraceae) were cultivated as an ornamental plant in Debrecen, Hungary and collected in September 2011. The plant was identified by Prof. Ágnes Kéry, and a voucher specimen (no. TP108) was deposited at the Department of Pharmacognosy, Semmelweis University, Budapest, Hungary. The air-dried and finely powdered herb of *T. parthenium* (10.0 g) was extracted with cold 90:10 CH₂Cl₂/MeOH (3×100 mL) at room temperature. The

filtered extract was evaporated to dryness at 40 °C *in vacuo* to yield 500 mg of a brown oily material.

3.2.5. *Corydalis cava* (L.) Schweig. & Kört. (Papaveraceae)



Tubers of *Corydalis cava* Schweig. & Kört. (Papaveraceae) were collected at the hillside of the Dobogókő area near Budapest, Hungary, in May 2011. The plant was authenticated by Prof. Ágnes Kéry, and a voucher specimen (no. CC52) was deposited at the Department of Pharmacognosy, Semmelweis University, Budapest, Hungary. The air-dried and finely powdered tuber of *C. cava* (5.0 g) was extracted with boiling water

Figure 15. *Corydalis cava* [153]. (50 mL) for 3 min. After cooling, it was filtered and partitioned between H₂O and 3×50 mL CHCl₃ at room temperature. The CHCl₃ extract after concentration *in vacuo* yielded a residue (180 mg) which was redissolved in dilute H₂SO₄ (2%, 20 mL) and extracted with 3×20 mL CHCl₃ to afford a yellowish weakly basic alkaloid fraction after evaporation (50 mg). Due to its low DMSO solubility, this extract was dissolved in MeOH in the PAMPA-BBB experiments.

3.2.6. *Salvia officinalis* L. (Lamiaceae)



Leaves of *Salvia officinalis* L. (Lamiaceae) were collected in an experimental field of the Institute of Ecology and Botany, Vácrátót, Hungary, in May 1999. A voucher specimen (no. Miklóssy-S.o.-May1999) was deposited in the Institute and authenticated by Dr. Vilmos Miklóssy. The dried and ground leaves of *S. officinalis* (50.0 g) were ultra-sonicated with 2×100 mL CHCl₃ for 20 min. The filtered extract was concentrated to dryness

Figure 16. *Salvia officinalis* [154]. at 40 °C *in vacuo*, redissolved in 1:1 CHCl₃-MeOH (30 mL), and fractionated by open column chromatography on polyamide gel (ICN cat. no. 09602), using a gradient system of MeOH/H₂O (40:60, 60:40, 80:20, 90:10, each 100 mL). The third fraction (51 mg) was subjected to the PAMPA-BBB experiments.

3.2.7. *Vinca major* L. (Apocynaceae)



Figure 17. *Vinca major* [155].

Aerial parts of *Vinca major* L. (Apocynaceae) were collected at an experimental field of the Institute of Ecology and Botany, Vácrátót, Hungary, in August 1999. A voucher specimen (no. Miklóssy-V.ma.-Aug1999) was deposited in the Institute and authenticated by Dr. Vilmos Miklóssy. The dried and ground herb (50.0 g) was extracted with 1×200 mL and 1×100 mL of 90:10 CHCl₃/MeOH using an ultrasonic bath for 2×15 min. After

filtration, the residual plant material was dried and extracted with 1×200 and 1×100 mL of 70% aqueous MeOH at room temperature in an ultrasonic bath for 2×15 min. The filtered and combined aqueous methanolic extracts were evaporated to dryness *in vacuo* and fractionated by open column chromatography on silica gel (Kieselgel 60, 0.063-0.200 mm, cat. no. 1.07734.100 Merck, Germany) using a gradient system of CHCl₃/MeOH/H₂O (90:10:1, 90:15:1.5, 90:25:2.5, 90:35:3.5, 90:45:4.5, 90:60:6, each 200 mL). The second fraction (57 mg) was subjected to the PAMPA-BBB experiments.

3.3. Instrumentation

Instrumentation common in all analyses are summarized below, whereas study-specific methods and conditions are provided after the section of each screening experiment.

3.3.1. High performance liquid chromatography – mass spectrometry

All experiments were performed on an Agilent 1200 liquid chromatography system (equipped with a vacuum degasser G1379B, a binary pump G1312B, a well-plate autosampler G1367C, a column temperature controller G1316B, and a diode array detector G1315C), coupled with an Agilent 6410 triple quadrupole mass spectrometer (QQQ-MS) equipped with an ESI source (Agilent Technologies, Waldbronn, Germany). MassHunter B.04.01 was used for data acquisition, and for qualitative and quantitative analysis. All analyses were carried out at 40 °C on an Ascentis Express C₁₈ column (50 × 3.0 mm, 2.7 μm).

3.3.2. Nuclear magnetic resonance spectroscopy

All NMR measurements were performed on a Varian 800 MHz spectrometer equipped with a $^1\text{H}\{^{13}\text{C}/^{15}\text{N}\}$ Triple Resonance ^{13}C Enhanced Salt Tolerant Cold Probe operating at 800 MHz for ^1H and 201 MHz for ^{13}C . All pulse sequences were taken from the VNMRJ-3.1 or 3.2 pulse sequence library without modification.

3.4. Cytotoxicity screening campaign

Cytotoxicity screening of the full plant extract library (N=4400) was performed by the fluorescent measurement of resazurin reduction (Promega, Madison, WI, USA) on an immortalized chinese hamster ovarian (CHO) cell line. This simple assay is based on the ability of living cells to convert a redox dye (resazurin) into a fluorescent end product (resorufin). Viable cells retain the ability to reduce resazurin into resorufin. Nonviable cells rapidly lose metabolic capacity, do not reduce the indicator dye, and thus do not generate a fluorescent signal. Fig. 18 shows the mechanism of the assay and a representative profile of a 384-well screening plate.

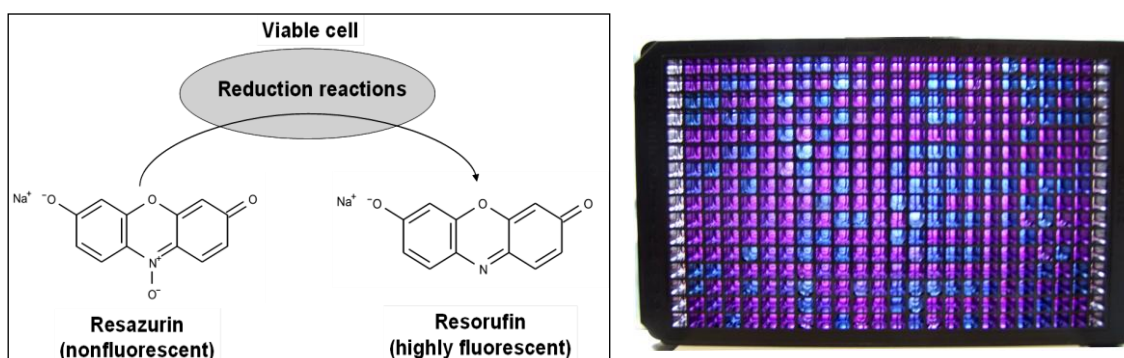


Figure 18. Principle of the cytotoxicity assay [156], and a representative profile of a 384-well screening plate. Note that blue wells were indicating cytotoxic activity.

3.4.1. Cell line

Chinese hamster ovarian (CHO) cells were cultured in Dulbecco's Modified Eagle Medium (D-MEM) (Life Technologies, Budapest, Hungary) containing 10% foetal bovine serum, 1% non-essential amino acid solution and 1% antibiotic-antimycotic solution. One day prior to treatment 2500 cells per well in 15 μL medium were seeded aseptically into tissue culture treated sterile 384-well plates (BD #353962) by a

Multidrop 384 dispenser (Thermo Labsystems). To eliminate edge effect, plates without lids were placed into sterile square Petri dishes (Nunc #166508).

3.4.2. Procedure of screening

384-well assay plates (Greiner #781 101) with diluted plant extract samples were prepared with a Biomek NX automated workstation (Beckman Coulter). 3 μ L of plant extract stock solutions (40 mg/mL in DMSO) and 97 μ L phosphate buffered saline (PBS, pH=7.4) were loaded quadrantwise into a barcoded 384-well plate. Between quadrants, tips were rinsed with DMSO and three times with distilled water. Completed sample plates were sealed and stored at 4 °C for less than 24 hrs.

On the day of the screening, 7.5 μ L of plant extract samples were transferred quadrant-wise onto cell plates by a Biomek NX, using 20 μ L tips washed once with DMSO and three times with distilled water between quadrants. Reference controls were prepared and loaded onto sample plates immediately before the Biomek transfer. Thus, the following plate/well distribution was used: in columns 3-22 320 pcs of plant extract samples; in wells A-B2, E-F2, I-L23, O-P23 8 pcs negative controls – DMSO; in wells C-D2, M-N2, C-D23, M-N23 8 pcs positive controls – 500 μ M FCCP (carbonyl cyanide-*p*-(trifluoromethoxy)phenylhydrazine; in wells G-H2, G-H23 4 pcs partial positive controls – 50 μ M FCCP. Afterwards, the 14 cell plates were returned into the Binder incubator (WTB Binder CB210) for 24-h incubation. Next day 5 μ L of CellTiter Blue reagent (Promega #G8080) was added into each well with a Multidrop Micro dispenser (Thermo Labsystems), followed by gentle shaking of the plates. Then the plates in square Petri dishes were returned into the incubator for a further 4-h incubation. Finally, fluorescence was read out in the BMG POLARstar reader (excitation 544 nm, emission 590 nm).

3.4.3. Data handling

The quality of the HTS assay was evaluated by the calculation of the dimensionless parameters Z - and Z' -factor [157].

Raw fluorescence read was taken from each well:	I_{ij}
The mean of 8 positive controls:	A
The mean of 12 negative controls:	B
The mean of 4 partial positive controls:	C

The calculation of Z (defined as the ratio of the separation band to the signal dynamic range of the assay):

$$Z = 1 - 3 \cdot \frac{SD_B + SD_C}{B - C}$$

The calculation of Z':

$$Z' = 1 - 3 \cdot \frac{SD_A + SD_B}{B - A}$$

The calculation of cytotoxic activity:

$$Activity(\%)_{ij} = 100 \cdot \frac{B - I_{ij}}{B - A}$$

As a summary, a total of 14 plant extract plates were screened in a test concentration of 400 µg/mL with 1% DMSO present. Samples with activity above 20% were considered as cytotoxic.

3.5. Antioxidant activity screening campaign

The antioxidant activity screening of the full plant extract library (N=4400) was performed according to the spectrophotometric DPPH method first described by Blois [79] and later modified for microplate format by Hu and Kitts [99]. Principle of the method was extensively discussed in Chapter 1.4.1.1.

Test parameters, such as the type of assay medium, DPPH and plant extract sample concentrations, incubation time and temperature were optimized in preliminary experiments: for avoiding the precipitation of plant extract samples in the DPPH test solution, buffer-free ethanol was used as test medium. Best reproduction of literary IC₅₀ values for two positive controls, namely quercetin and trolox, was achieved where test samples were incubated with 60 µM DPPH for 30 min at room temperature. Screening concentration of plant extract samples was set to the value of 66.7 µg/mL, after reviewing experimental conditions of analogous screening studies with crude plant extracts [68, 72-77].

3.5.1. Procedure of screening

Briefly, fresh DPPH stock solution was prepared by dissolving DPPH in ethanol on each day of analysis and kept at 4 °C in a refrigerator. On the day of the screening, 290 µL DPPH solution (60 µM) was loaded into a 96-well microtiter plate (UV-Star, Greiner Bio-One, Frickenhausen, Germany) with Eppendorf multichannel pipettes (Hamburg, Germany). Afterwards, 10 µL of positive control (quercetin, 200 µg/mL), negative control (pure DMSO), and plant extract samples (2.0 mg/mL) were loaded

onto the test plates. Appropriate mixing of test solutions was performed in the multichannel pipettes (5 cycles). Thus, the following plate/well distribution was used (Fig. 19): in the first column 8 pcs negative control, in wells A2-H11 80 pcs plant extract samples, in the last column 8 pcs positive control (quercetin). Finally, absorbance of each well was read out against a blank at 517 nm after 30 min incubation at room temperature in the dark by a UV-visible plate reader (Multiskan Spektrum, Thermo Labsystem).

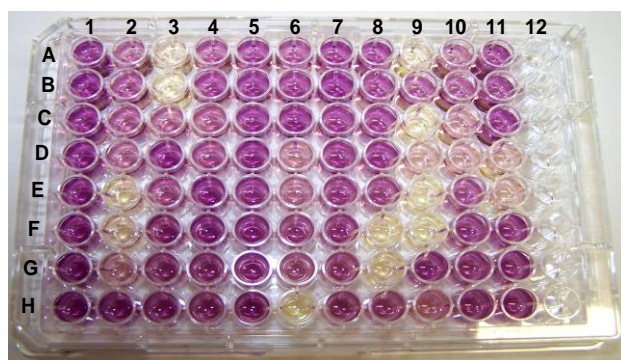


Figure 19. Representative profile of a screening plate. Note that yellow wells were indicating samples with antioxidant activity (positive control in column 12 is unfortunately missing from the picture).

3.5.2. Data handling and IC₅₀ measurement

The degree of radical scavenging activity was determined by the following formula:

$$\text{Inhibition}(\%) = 100 \cdot \frac{\text{Abs}_{\text{control}} - \text{Abs}_{\text{sample}}}{\text{Abs}_{\text{control}}}$$

where $\text{Abs}_{\text{control}}$ is the absorbance of the control reaction (containing DMSO instead of the test compound/plant extract), and $\text{Abs}_{\text{sample}}$ is the absorbance of the test compound/plant extract at 517 nm. $\text{RSD}_{\text{controls}} < 10\%$ per plate as quality control was checked in all test plates. Plant extracts with activity above 80% were considered as primary hits.

IC₅₀ values for these hits were measured in a secondary experiment: DMSO solutions of hits were diluted in six concentrations, ranging from 0.5 to 300 µg/mL, and the same protocol was repeated with these samples as described above. IC₅₀ values, the concentrations of the samples required to scavenge 50% of DPPH radical, were calculated by Prism 4 for Windows (Graph Pad Software, San Diego, USA) after sigmoidal dose–response curve fitting and were expressed as the mean of three determinations.

3.6. Antioxidant activity-guided phytochemical investigation of *Artemisia gmelinii*

3.6.1. HPLC-based DPPH scavenging assay

The modified method of Tang et al. [87] was applied to characterize the active constituents in the methanolic extract of *Artemisia gmelinii*. Briefly, 0.5 mL of *A. gmelinii* methanolic extract dissolved in DMSO and 0.5 mL of 1.5 mM DPPH stock solution were mixed and allowed to react for 30 min. The reaction mixture was then filtered through a 0.45 µm filter and injected for HPLC analysis. Ethanol was added to the extract to provide the unreacted control sample.

HPLC-MS experiments were performed on an Agilent 1200 liquid chromatography system equipped with a diode array detector and coupled with an Agilent 6120 MSD (Agilent Technologies, Palo Alto, CA, USA). Analyses were carried out at 40 °C on an Ascentis Express C₁₈ column (50 x 3.0 mm, 2.7 µm) with a mobile phase flow rate of 1.1 mL/min. The composition of eluent A was 0.1% (v/v) trifluoroacetic acid in water, eluent B was the mixture of MeCN and water in 95:5 (v/v) with 0.1% (v/v) trifluoroacetic acid. A linear gradient of 2-25% B was applied at a range of 0-8 min, then 25% B held for 1 min. This was followed by a 2 min equilibration period prior to the next injection. The UV-vis spectra were recorded between 200 to 400 nm and chromatographic profiles were registered at 320 nm. The injection volume was set to 10 µL. The MSD operating parameters were as follows: negative and positive ionization mode, scan spectra from *m/z* 100 to 800, drying gas temperature 350 °C, nitrogen flow rate 13 L/min, nebuliser pressure 50 psi, quadrupole temperature 100 °C, capillary voltage 3000 V, fragmentors were in the range 60-180 V.

3.6.2. Isolation of compounds 7a and 8a with preparative HPLC

The applied preparative chromatographic system comprised of the following parts: a Gilson 305/306 (Middleton, WI, USA) pump, a Shimadzu SPD-10A (Columbia, MD, USA) UV-vis detector and a Büchi 684 (New Castle, DE, USA) fraction collector. Preparative separations were carried out on a Waters (Milford, MA, USA) X-Terra Prep RP18 (300 mm x 30 mm, 10 µm) column using water acidified with 0.1% (v/v) acetic acid as eluent A and acetonitrile acidified with 0.1% (v/v) acetic acid as eluent B in an

optimized gradient program (5-50% B in 160 min) at a flow rate of 15 mL/min. The detection wavelengths were 220 nm and 320 nm.

The last fraction (VI) obtained from column chromatography (620 mg) was dissolved in the 1:1 (v/v) mixture of eluent A and B, and injected into HPLC. The effluent containing the solute corresponding to the observed peaks of **7a** and **8a** was collected in the fraction collector. The collected fractions were concentrated and dried under vacuum to yield purified **7a** (78 mg, t_R =102 min) and **8a** (25 mg, t_R =122 min).

Compound 7a: (1*s*,3*R*,4*s*,5*S*)-1,3-bis({[(2*E*)-3-(3,4-dihydroxyphenyl)prop-2-enoyl]oxy})-4,5-dihydroxycyclohexane-1-carboxylic acid. Pale yellow, waxy crystalline solid. UV-vis (MeCN) λ_{max} : 218, 240, 296sh, 325 nm; ^1H and ^{13}C NMR (Table A1, Appendix); $[\text{M}+\text{H}]^+$ (ESI): m/z 517.13457, calculated value for $\text{C}_{25}\text{H}_{25}\text{O}_{12}$: 517.13405 (delta: 1.0 ppm). Adduct ions of $[\text{M}+\text{Na}]^+$, $[\text{2M}+\text{H}]^+$ and $[\text{2M}+\text{Na}]^+$ can be detected at m/z 539.11654, 1033.26313 and 1055.24460, respectively. The mass accuracy was between 1.0 and 2.2 ppm for the adduct ions.

Compound 8a: Ethyl(1*s*,3*R*,4*s*,5*S*)-1,3-bis({[(2*E*)-3-(3,4-dihydroxyphenyl)prop-2-enoyl]oxy})-4,5-dihydroxycyclohexane-1-carboxylate. Pale yellow, waxy crystalline solid. UV-vis (MeCN) λ_{max} : 218, 240, 300sh, 325 nm; ^1H and ^{13}C NMR (Table A1, Appendix); $[\text{M}+\text{H}]^+$ (ESI): m/z 545.16607, calculated value for $\text{C}_{27}\text{H}_{29}\text{O}_{12}$: 545.16535 (delta: 1.3 ppm). Adduct ions of $[\text{M}+\text{Na}]^+$, $[\text{2M}+\text{H}]^+$ and $[\text{2M}+\text{Na}]^+$ can be detected at m/z 567.14793, 1089.32514 and 1111.30706, respectively. The mass accuracy was between 1.1 and 1.6 ppm for the adduct ions.

3.6.3. High resolution mass spectrometry analysis

High-resolution MS measurements were carried out on a Thermo LTQ FT Ultra mass spectrometer (ESI, 4.0 kV spray voltage, 295 °C capillary temperature, solvent: MeOH:H₂O 1:1 + 1% (v/v) cc. acetic acid, direct infusion).

3.6.4. NMR spectroscopy

All NMR measurements were performed on a Varian 800 MHz spectrometer equipped with a $^1\text{H}\{^{13}\text{C}/^{15}\text{N}\}$ Triple Resonance ^{13}C Enhanced Salt Tolerant Cold Probe operating at 800 MHz for ^1H and 201 MHz for ^{13}C . Chemical shifts were referenced to TMS used as an internal standard. ^1H - ^1H , direct ^1H - ^{13}C , long-range ^1H - ^{13}C spin-spin connectivities were established from ^1H , 2D-GHSQCAD, GCOSY and 2D-GHMBCAD experiments,

respectively. All pulse sequences were used as available in the VNMRJ 3.1 pulse sequence library. All NMR measurements were performed in DMSO- d_6 as solvent.

3.7. HPLC-based peroxynitrite scavenging assay

3.7.1. Synthesis of the peroxynitrite anion

Peroxynitrite was synthesized daily according to literature [108], and was always treated by MnO_2 to remove residual hydrogen peroxide. Briefly, a solution containing 0.5 M $NaNO_2$ and 0.5 M H_2O_2 was freshly prepared and cooled on ice, and then 1 mL aliquot of pre-cooled 1 M HCl and 1 mL aliquot of pre-cooled 1.5 M NaOH were injected simultaneously (within approximately 0.5 s) into a rapidly stirred solution. The concentration of the resulting $ONOO^-$ solution was determined by measuring the absorbance at 302 nm ($\epsilon=1670 M^{-1}cm^{-1}$). The stock solution was diluted with 0.5% NaOH and kept frozen in the dark before used. The decomposed control solution of $ONOO^-$ originated from one week long storage of the concentrated solution at room temperature.

3.7.2. Preparation of the *Salvia* specific model mixture

The artificial model mixture consisted of 17 analytical and/or chemotaxonomic marker compounds (in equimolar ratio) representative for alcoholic extracts of *Salvia* species. Gallic acid, caffeic acid and its derivatives (caftaric acid, scopoletin, sinapic acid, rosmarinic acid, salvianolic acid A, salvianolic acid B) [158-159], flavonoid aglycones (quercetin, apigenin, kaempferol, chrysin, 5-hydroxyflavone), flavonoid glycosides (rutin, luteolin 7-*O*-glucoside, apigenin 7-*O*-glucoside) and one major diterpene marker carnosol [160] were included in the mixture.

The model mixture was prepared in DMSO at a concentration of 600 μM for each phenolic component.

3.7.3. HPLC conditions

Experiments were performed on an Agilent 1200 liquid chromatography system (Waldbronn, Germany). Test solutions and samples were prepared in 96-well polypropylene plates with the total volume of 0.5 mL (Agilent, Waldbronn, Germany). Plates were sealed and incubated in the autosampler for 10 min at 20 °C before

analyzed. Analysis was carried out at 40 °C on an Ascentis Express C18 column (50 × 3.0 mm, 2.7 μm) with a flow rate of mobile phase 1.1 mL/min. Composition of eluent A was 0.1% (v/v) trifluoroacetic acid in H₂O (pH=1.9), eluent B was the mixture of MeCN and H₂O in 95:5 (v/v) with 0.1% (v/v) trifluoroacetic acid. The gradient program with two isocratic parts was the following: a linear gradient of 0-15% B with the first 2 min, then 15% B was held for 1 min, linear gradient of 15-35% B with the range of 3-5 min, then 35% B was held for 2 min, linear gradient of 35-80% B with the range of 7-10.5 min. This was followed by a 2.5 min equilibration period prior to the next injection. It gives a 13 min total analysis time per sample. The chromatograms were recorded at 220, 320 and 470 nm and the applied injection volume was 6 μL.

3.7.4. Peroxynitrite scavenging activity measurement in 96-well plate

Test solution was prepared in 96 well-plate by mixing the following reagents: 245 μL 122.4 μM solution of pyrogallol red in glycine buffer (100 mM) pH=7.00 and 50 μL stock solution of the model mixture solved in DMSO (100 μM, final concentration for each compound) and finally 5 μL ONOO⁻ in desired concentration. In case of the real sample, 50 μL of methanolic *S. miltiorrhiza* extract dissolved in DMSO (2.0 mg/mL, final concentration) was added into each test solution. The control solution contained 245 μL pyrogallol red in glycine buffer (100 μM, final concentration), 50 μL DMSO and 5 μL ONOO⁻ (1.5 mM, final concentration, =0% inhibition). The total shift of control pH, due to the addition of ONOO⁻ alkaline solution was within 0.4 unit. The blank of the assay was the same composition but mixed with 5 μL of decomposed solution of ONOO⁻ (=100% inhibition). The resulted mixture plate (containing test, control and blank solutions in triplicate) was mixed thoroughly, sealed and analyzed directly using the above described LC method.

The individual scavenging activities of the phenolic compounds were assessed the same way against 500 μM ONOO⁻ in eight concentrations between 0.2 μM and 500 μM. Appropriate controls containing no antioxidants but the decomposed ONOO⁻, were also included to estimate pyrogallol red bleaching. Inhibition percentage was calculated in both study (scavenging activity of mixture and individual compounds) as follows:

$$Inhibition(\%) = 100 \cdot \frac{[PR]}{[PR]_0}$$

where $[PR]$ was the measured pyrogallol red concentration of the sample after reaction with ONOO^- and $[PR]_0$ was the initial pyrogallol red concentration (blank). IC_{50} values were calculated as the concentration of single compounds required to protect 50% of pyrogallol red against 500 μM ONOO^- by Prism 4 for Windows (Graph Pad Software Inc., San Diego, USA) after sigmoidal dose – response curve fitting.

3.8. Blood-brain barrier permeability screening campaign and related methods

3.8.1. PAMPA-BBB procedures

A slightly modified version of the PAMPA-BBB assay was used to assess the effective permeability (P_e , cm/s) of the NP and NP-like test set [131] (Table A2, Appendix). Test compounds were dissolved in DMSO (in the case of compounds with poor solubility MeOH was used) at 10 mM, then 3 μL of this stock solution was diluted 100-fold with 297 μL 0.01 M phosphate buffered saline (PBS) at pH 7.4 to obtain the starting donor solutions (100 μM nominal concentration). Afterwards, the filter membrane of the donor (top) plate (96-well polycarbonate-based filter plate, Multiscreen-IP, MAIPN4510, pore size 0.45 μm , Millipore) was coated with 5 μL BBB specific lipid solution (16 mg PBL and 8 mg cholesterol dissolved in 600 μL n-dodecane) and the acceptor (96-well PTFE acceptor plate, Multiscreen Acceptor Plate, MSSACCEPTOR, Millipore) well was filled with 300 μL PBS buffer. The donor plate was filled with 150 μL of the starting donor solution and was carefully placed on the acceptor plate to form a “sandwich”, which was incubated at 37 $^\circ\text{C}$ for 4 h. After incubation, sandwich plates were separated and the concentrations of each test compound in the starting donor solution, and in the acceptor and donor wells were determined in triplicate by chromatographic peak areas derived from a generic LC-MS method. Using these data, the effective BBB permeability ($\log P_e$) of each test compound was calculated using the following equations [161]:

$$P_e = \frac{-2.303}{A \cdot (t - \tau_{SS})} \cdot \frac{(V_A \cdot V_D)}{(V_A + V_D)} \cdot \lg \left[1 - \left(\frac{V_A + V_D}{(1 - R) \cdot V_D} \right) \cdot \left(\frac{C_D(t)}{C_D(0)} \right) \right]$$

where P_e is the effective permeability coefficient (cm/s), A is the filter area (0.3 cm^2), V_D and V_A are the volumes in the donor (0.15 cm^3) and acceptor phase (0.3 cm^3), t is the

incubation time (s), τ_{SS} is the time (s) to reach the steady-state, $C_D(t)$ is the concentration (mM) of the compound in the donor phase at time t , $C_D(0)$ is the concentration (mM) of the compound in the donor phase at time 0, R is the membrane retention factor:

$$R = \left(1 - \frac{C_D(t)}{C_D(0)} - \frac{V_A}{V_D} \frac{C_A(t)}{C_D(0)} \right)$$

where $C_A(t)$ is the concentration (mM) of the compound in the acceptor phase at time t .

The PAMPA-BBB screening of the plant extract library was performed according to a similar protocol as described above. Thus, 180 μ L PBS buffer was added to 20 μ L of each of the 1760 stock solutions of plant extracts (10.0 mg/mL in DMSO) in 96-well polypropylene plates (Agilent, Waldbronn, Germany) (80 samples per plate, 22 plates in total, 10% (v/v) DMSO as co-solvent in donor wells). After rigorous shaking, 150 μ L of these aliquots was transferred and used in the donor plates. After incubation, 260 μ L of the acceptor solution was transferred to a 96-well UV-Star microplate (Greiner Bio-one, Germany) and analyzed using a UV-vis reader (Thermo Multiskan Spectrum). The absorbance of each well was read in the range 240-400 nm, in 10 nm stepwise increments. Verapamil was used as high permeability control and prednisone was used as low permeability control on each plate ($n = 4$). Criteria for a primary hit (considered as BBB+ extract) were: $\text{Abs}_{\text{sample}} > \text{Abs}_{\text{blank}} + 3 \times \text{SD}_{\text{blank}}$, if $\text{RSD}_{\text{controls}} < 10\%$ per plate as quality control was fulfilled.

In the case of the four BBB+ extracts studied, PAMPA-BBB experiments were repeated in deuterio PBS buffer, starting from the most concentrated samples (50 mg/mL) with 10% co-solvent. The resulting acceptor solutions were collected and 1 mL from each sample was subjected directly to NMR analysis.

3.8.2. HPLC-MS analysis

Instrumentation and experimental conditions used were as described in Chapter 3.3.1. Quantification of reference compounds in the PAMPA-BBB derived samples was achieved basically by two “generic” LC-DAD-MS methods: in the first one, eluent A was 0.1% TFA in H_2O (pH=1.9) and eluent B was the mixture of MeCN and H_2O in 95:5 (v/v) with 0.1% TFA, while in the second one 10 mM $\text{NH}_4\text{OAc}/\text{AcOH}$ buffer (pH=5.8) was used instead of TFA in the mobile phases. The applied linear gradient profile and mobile phase flow rate were the same: 0-100% B at 0-4.5 min, then 100% B

for 3 min at 0.8 mL/min. Chromatographic profiles were recorded in all cases at the UV-maxima of each test compound (210 nm was considered as minimum). Moreover, where more sensitive detection was needed, single-ion mode (SIM) MS signals were acquired (see Appendix).

BBB+ plant extracts, identified as hits in the PAMPA-BBB screen were validated in the same LC-MS system. Retention data and corresponding molecular mass of randomly selected 140-140 pcs BBB+ and BBB- compounds were extracted by MassHunter Workstation Software (Agilent, Version B.04.00) and analyzed with Statistica version 10 (StatSoft, Tulsa, OK, USA). The logarithmic value of the chromatographic retention factor extrapolated to 0% organic modifier content was calculated as follows [162]:

$$\log k_0 = (t_{R,g} - \frac{t_0}{b} \log(2.3b) - t_0 - t_D) \cdot \frac{b}{t_0}$$

where $t_{R,g}$ is the compound retention time in gradient mode (min); t_0 is the dead time of the column (the peak of DMSO was used as the unretained marker $t_0 = t_{DMSO} = 0.23$ min); t_D is the gradient delay time (0.98 min); b is the gradient steepness parameter (0.215):

$$b = \frac{V_m \cdot \Delta\phi \cdot S}{t_G \cdot F}$$

where V_m is the column dead volume (0.194 mL); $\Delta\phi$ change in the volume fraction of the strong solvent in the mobile phase during the gradient run (0.95); S is a constant for a given analyte (approx. 4.2 for small molecules), t_G is the gradient time (4.5 min); and F is the flow rate (0.8 mL/min).

For detailed analysis of the four BBB+ plant extracts, the same column, eluents, and flow rates were used as in the first generic method. For the *T. parthenium*, *V. major*, and *C. cava* samples (stock and acceptor solutions) a linear gradient of 0-30% B was applied at a range of 0-7 min, then 30-75% B at 7-9.5 min and 75-95% B at 9.5-12 min. In the case of the *S. officinalis* sample, the gradient program was: 5-30% B at 0-2.5 min, 30-75% at 2.5-10 min, 75-95% B at 10-12 min. The injection volume was set at 1 μ L for stock solutions and 10 μ L for acceptor solutions in order to compensate the dilution effect of the PAMPA-BBB assay. Chromatographic profiles were recorded at 220 nm except for the *T. parthenium* sample, where the ESI+ total ion chromatogram was

acquired. QQQ-MS conditions were: scan mode with the mass range of m/z 100-1000, drying gas temperature of 300 °C, nitrogen flow rate of 13 L/min, nebuliser pressure of 40 psi, quadrupole temperature of 100 °C, and capillary voltage of 3000 V. UV spectra were collected in the range of 190-400 nm. MS fragmentation patterns were acquired for the eight reported BBB+ compounds (**1-8**) (MS conditions with the corresponding MS spectra are provided in the Appendix).

3.8.3. Gas chromatography – flame ionization detector analysis of PAMPA-BBB co-solvents

The DMSO and MeOH content of PAMPA-BBB-derived acceptor solutions were quantified on an Agilent 6890 Gas Chromatography system (Agilent Technologies, Palo Alto, CA), equipped with a split/splitless inlet and a flame ionization detector (FID). Analytes were separated on an Agilent DB-1MS UI capillary column (30 m × 0.32 mm, 0.25 µm film thickness). Separation conditions: the oven temperature was programmed linearly from 80 °C to 230 °C at a rate of 20 °C/min and held at 230 °C for 2 min; helium was used as carrier gas at 1.1 mL/min, an injection volume of 1 µL and a split (ratio 10:1) injection mode were adopted; the injection port temperature and FID temperature were 250 °C with nitrogen as making up gas at 45 mL/min, and also hydrogen at 40 mL/min, and air at 450 mL/min. Retention times and calibration equations for DMSO and MeOH were: 3.67 min, area = 6311.6 × amount (v/v %) – 11.1 and 2.56 min, area = 3272.8 × amount (v/v %) + 109.6, respectively.

3.8.4. NMR spectroscopy

All NMR spectra were recorded in a 5 mm sample tube at 298 K, using a Varian 800 MHz NMR spectrometer equipped with a $^1\text{H}\{^{13}\text{C}/^{15}\text{N}\}$ triple resonance ^{13}C enhanced salt tolerant cold probe operating at 800 MHz for ^1H . Chemical shifts were referenced to the residual co-solvent resonances ($\delta_{\text{H}}(\text{MeOH}) = 3.34$ ppm or $\delta_{\text{H}}(\text{DMSO}) = 2.71$ ppm). ^1H -Presat and Presat-ZTOCSY spectra were recorded in all four cases while in the case of the *T. parthenium* sample an additional GHSQCAD spectrum was collected as well. All pulse sequences were taken from the VNMRJ-3.2 software library without modification.

3.9. Statistical analysis

Statistical calculations and histogram generation were carried out with the Statistica 9.0/10.0 software (StatSoft). Results are expressed as the mean \pm S.E.M. of three parallel experiments. Student's t-test was used for statistical analysis; p values > 0.05 were considered to be significant. F-test and residual analysis was performed in all linear regression analysis.

4. Results

4.1. Cytotoxicity screening

A total of 14 plant extract sample plates were screened in 384-well format. Average Z' was 0.87 ± 0.06 , and all plates displayed Z' above 0.4. Moreover, no serious positionwise inhomogeneity was observed. Thus, it can be concluded that the HTS assay was accurate and valid. More than half of the 4400 screened samples, 2508 displayed cytotoxic activity above 20% (Fig. 20). Therefore, these samples have been excluded from cell-based HTS campaigns run since that time.

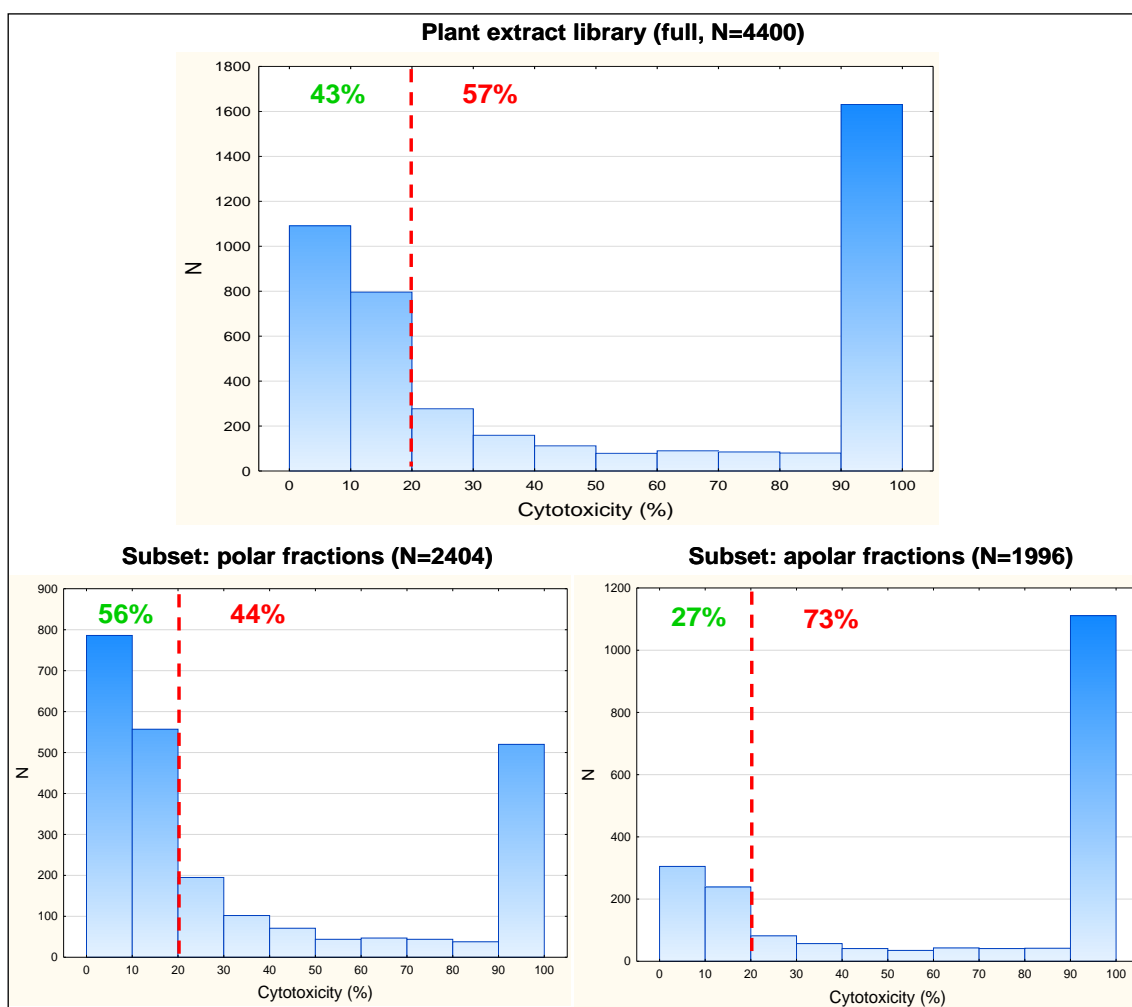


Figure 20. Results of the cytotoxicity screening: histograms of the full, and the two sub-libraries, respectively. Note that samples with activity above 20% were considered as cytotoxic.

The spectacularly bipolar nature of the resulted distribution has indirectly demonstrated that the used screening concentration (400 $\mu\text{g}/\text{mL}$ with 1% DMSO present) was adequate. Moreover, the analysis of the polar and apolar subsets' results has revealed that samples extracted with chloroform are twice as likely to show cytotoxicity, than samples originated from alcoholic extraction. This finding is in accordance with the widely accepted impact of compound lipophilicity on drug development: compounds with higher log P values are more often affected by promiscuity and toxicity issues [163, 164].

Single plant extract "hits" (with cytotoxic activity above 90%) were not studied in detail, since toxicity was considered as an excluding feature. However, by the reduction in the number of false positive plant extracts the screening efficiency in subsequent HTS campaigns (where only the non-cytotoxic subset of the plant extract library was tested) was greatly improved (data not shown due to intellectual property rights).

4.2. Antioxidant activity screening

A total of 55 plant extract sample plates were screened in 96-well format. The quality criterion ($\text{RSD}_{\text{controls}} < 10\%$ per plate) was fulfilled in all tested plates. Moreover, no serious positionwise inhomogeneity was observed. Thus, it can be concluded that the HTS assay was accurate and valid. Of the 4400 screened samples, only 251 extracts (5.7%) showed antioxidant activity above 80% (Fig. 21). In contrast to the cytotoxicity campaign, the majority of plant extracts proved to be inactive and fell below 20%. This distribution profile has indirectly demonstrated that the used screening concentration (66 $\mu\text{g}/\text{mL}$) was adequate. This conclusion is also supported by the screening results of Pezzuto et al.: the antioxidant activity of 700 plant extracts has been evaluated in the same DPPH test system at 200 $\mu\text{g}/\text{mL}$ screening concentration, and a hit rate of 14% has been obtained [68].

Moreover, analysis of the polar and apolar subsets' results has revealed that samples extracted with methanol are three times as likely to show radical scavenging activity than samples originated from chloroformic extraction.

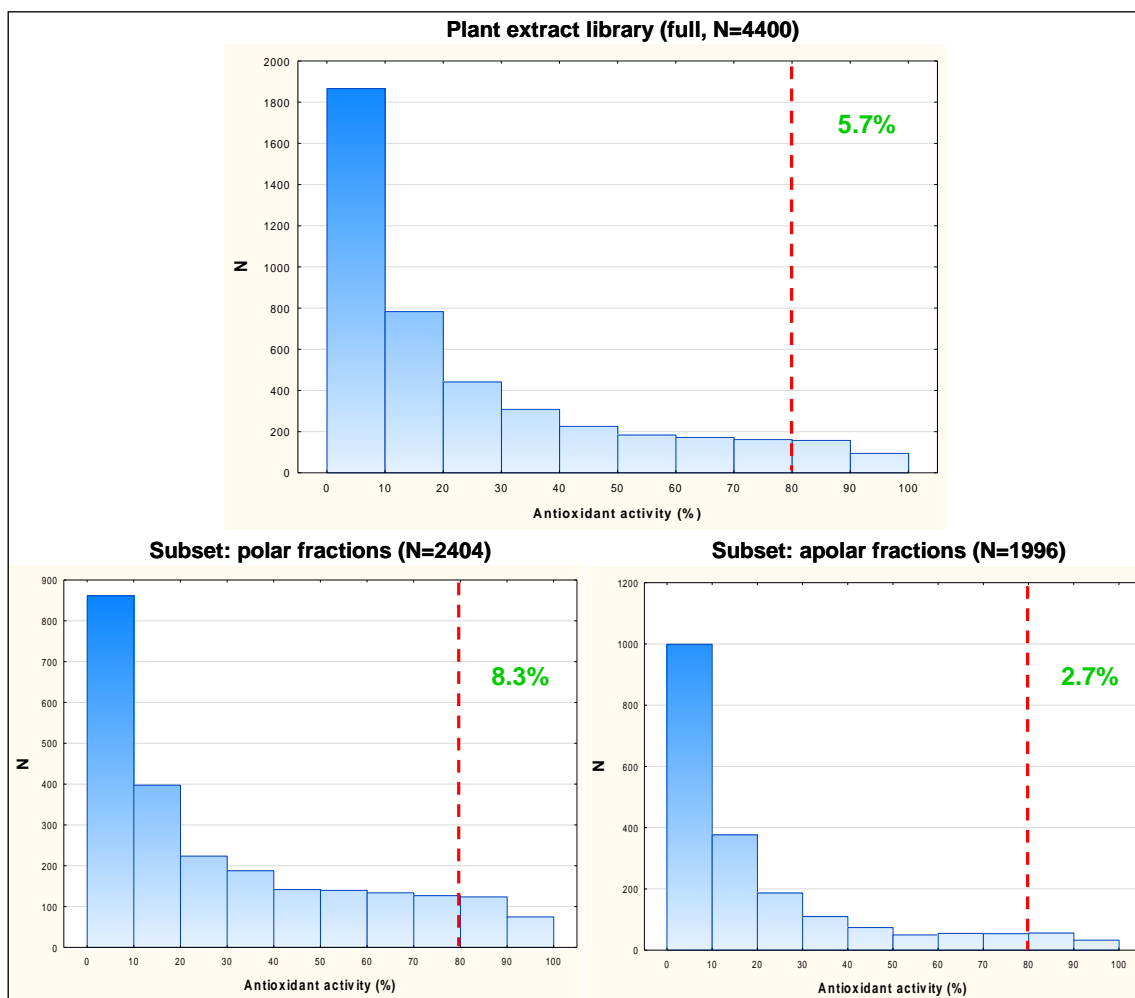


Figure 21. Results of the antioxidant activity (DPPH) screening: histograms of the full, and the two sub-libraries, respectively. Note that samples with activity (Inhibition%) above 80% were considered as actives (hits).

This trend is also somewhat predictable, since it has been demonstrated a number of times that the phenoloid content positively correlates with the antioxidant capacity in NP extracts [76, 165].

Cytotoxic antioxidant hits (N=130) have been excluded from further studies, and only non-cytotoxic antioxidant plant extracts (N=121, originated from 41 species) were characterized (dereplicated) by mean of LC-MS. Comparing the retention time, the UV and MS spectra of the major peaks with those of the reference compound library revealed that ubiquitous representatives of caffeic acid derivatives (e.g., caffeic acid, chlorogenic acid, rosmarinic acid), and flavon and flavonol glycosides (e.g., rutin) were abundant in these extracts, thus could be considered as frequent hitters in this sense.

Taxonomical analysis of the 121 hits showed that representatives of the *Salvia* genus significantly accumulated among strong radical scavenging extracts: of the 14 species of the full library (14/300=4.7%), 8 species (representing 28 extracts) were identified among the hits (8/41=19.5%).

Bearing these results in mind, our work was targeted toward two distinct objectives. First, an extract hit of a phytochemically less characterized plant, namely the methanolic extract of *A. gmelinii* was chosen to test the performance of the off-line DPPH-HPLC (spiking) assay. Second, the radical scavenging capacity of *Salvia* extracts was tested in an orthogonal antioxidant system. For this purpose, the pyrogallol red bleaching test used for ONOO⁻ scavenging activity assessment was adopted for HPLC.

4.3. HPLC-based antioxidant activity profiling of the methanolic extract of *Artemisia gmelinii*

4.3.1. Introduction

Artemisia gmelinii Webb. ex Stechm. (Asteraceae), also known as Gmelin's wormwood, is a perennial herb widespread in south and south-east Asia with several ethnopharmacological applications, however its phytochemical composition is not well studied. The leaf and stem are used in Korea to treat inflammatory liver conditions [166]; "tablets" made from flowers are taken in India to overcome cold, cough and fever [167]; pastes made from the fresh plant are used externally to cure headache, boils and pimples in Nepal [168, 169]. In contrast, the literature data regarding the chemical composition of *A. gmelinii* are limited only to three studies: caffeic acid, scopoletin, 4',7-di-*O*-methylapigenin, 4',5,7-trihydroxy-3',6-dimethoxyflavone, acacetin and velutin as phenolic compounds were isolated from the ethanolic extract [170], and some ubiquitous monoterpenes and sesquiterpenes (e.g. guaianolides) were identified in the petrol ether extract [171, 172], but no data regarding the bioactivity of the plant extracts has been reported.

We found one fraction of the methanolic extract of *A. gmelinii* as a hit in our antioxidant screening campaign (DPPH). Therefore, an LC-MS method was developed to separate and characterize the major constituents of the extract. Moreover, the LC

method was coupled offline with the DPPH assay, based on the work of Tang and co-workers [87], to indicate the free radical scavenger molecules in the mixture.

4.3.2. Phytochemical and antioxidant characterization

Six compounds (**1a-6a**) were identified on the chromatogram of the extract (Fig. 22A and Table 2) by comparing the retention time, the UV and MS spectra of the major peaks with those of authentic reference compounds. Caffeic acid (**1a**) and scopoletin (**4a**) as ubiquitous secondary plant metabolites were described earlier [170], but chlorogenic acid (**2a**), 4-*O*-caffeoylquinic acid (cryptochlorogenic acid) (**3a**), luteolin-7-*O*-glucoside (**5a**) and apigenin-7-*O*-glucoside (**6a**) are reported here for the first time in *A. gmelinii*. After spiking (i.e. overdosing) the sample with the DPPH radical solution (Fig. 22B) the peak areas of compounds **7a** and **8a** exhibited the most pronounced decrease, therefore the preparative HPLC purification was targeted to isolate **7a** and **8a**.

Afterwards, the two most active compounds (**7a** and **8a**) were isolated with preparative HPLC and were tentatively identified as dicaffeoylquinic acid (DCQA) derivatives. During the detailed structure elucidation of the two species based on NMR and molecular modeling, we were faced however with difficulties regarding the unambiguous “resolvability” of the relative stereochemistry of these structures because of their inherent structural dynamics as well as due to ambiguities in the relevant literature data. Nevertheless, after extensive analysis of the stereochemical behaviour of the two species and the analogue compound cynarin (1,5-*O*-dicaffeoylquinic acid) we concluded that **8a** is the ethyl ester derivative of **7a**, where the latter is tentatively identified as 3,5-*O*-dicaffeoylquinic acid (Table 2).

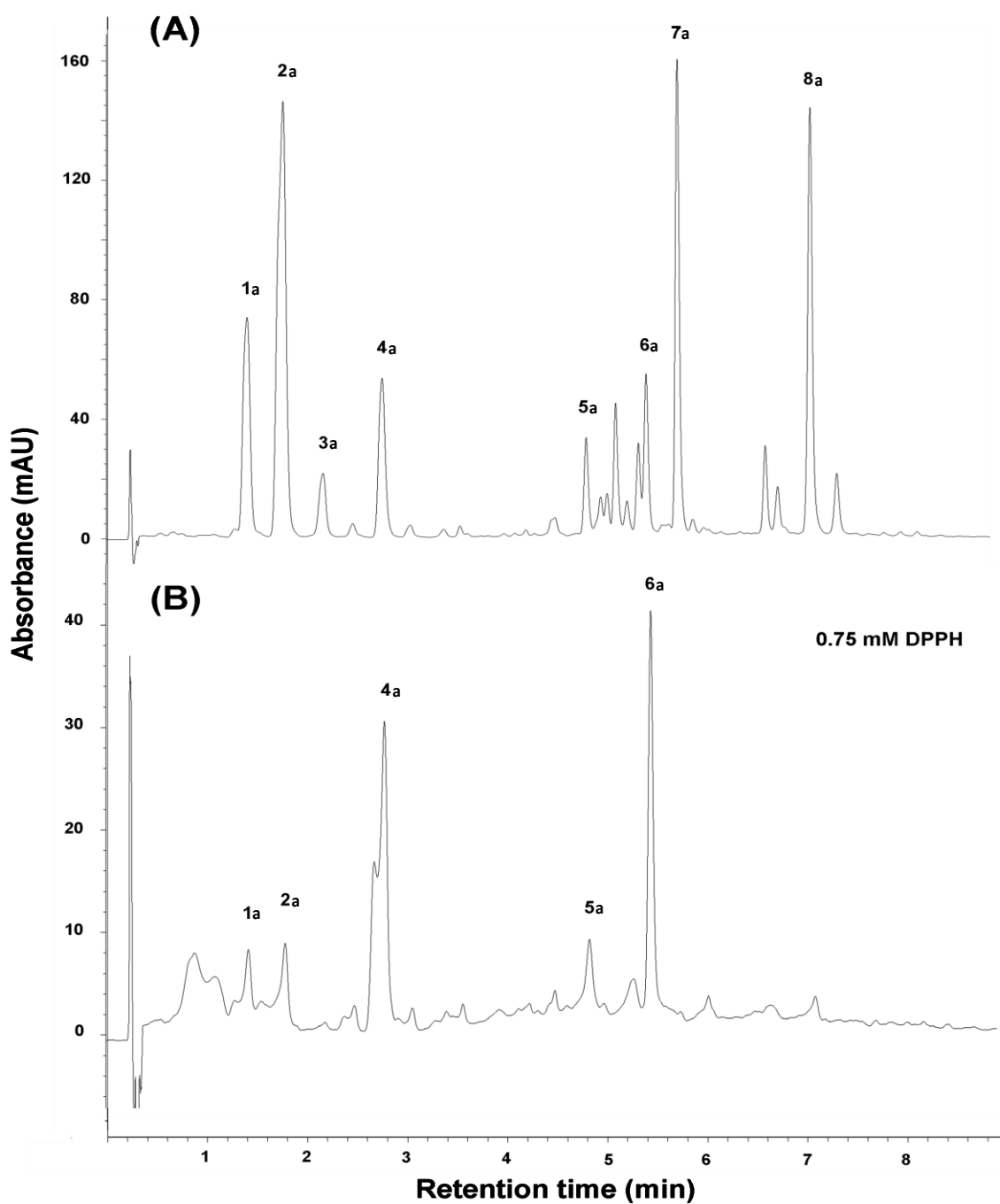


Figure 22. HPLC-DAD chromatogram of fraction VI of methanolic extract of *A. gmelinii* before (A) and after reacted with 0.75 mM DPPH radical obtained at 320 nm (B). The index **a** in compound numbering denotes for the origin *Artemisia*. Key to peak identity is presented in Table 2.

Table 2. Retention times and chemical structures of the identified (**1a-6a**) and isolated (**7a, 8a**) compounds in the fraction VI of methanolic extract of *A. gmelinii*.

Peak	t _R (min)	Compound	
1a	1.43	caffeic acid	
2a	1.80	chlorogenic acid	
3a	2.21	4- <i>O</i> -caffeoylquinic acid	
4a	2.81	scopoletin	
5a	4.88	luteolin-7- <i>O</i> -glucoside	
6a	5.49	apigenin-7- <i>O</i> -glucoside	
7a	5.81	3,5- <i>O</i> -dicaffeoylquinic acid	
8a	7.16	ethyl-3,5- <i>O</i> -dicaffeoylquinic acid	

The decreasing trend of the IC₅₀ values in Table 3 shows clearly that the radical scavenger components of *A. gmelinii* were enriched in the methanolic extract, especially in the last (VI) eluting fraction obtained by column chromatography. The isolated

DCQA's (**7a**, **8a**) possess great antioxidant capacities, which indirectly verified the efficiency of the DPPH-HPLC spiking assay. The IC₅₀ values of compounds **7a** and **8a** were significantly lower than that of the positive control trolox, and were at a similar level as the outstanding activity of quercetin. The observed superior reactivity of the two DCQA derivatives toward the DPPH radical is in accordance with the findings of Saito et al. [173], who described the contribution of an intramolecular interaction of the two caffeoyl residues. Moreover, after comparing the IC₅₀ values of compound **7a** and **8a** to the value of cynarin it can be supposed that the radical scavenging potential of these species is not affected by the difference in the observed stereochemistry of the quinic acid core moiety.

Table 3. DPPH radical scavenging activities of *A. gmelinii* extracts and isolated compounds.

Sample	IC ₅₀ ($\mu\text{g/mL}$)
CHCl ₃ extract	> 300
70% (v/v) aqueous MeOH extract:	76.6 \pm 4.9
• Fraction I of 70% (v/v) aqueous MeOH extract	> 300
• Fraction II of 70% (v/v) aqueous MeOH extract	> 300
• Fraction III of 70% (v/v) aqueous MeOH extract	109.9 \pm 9.9
• Fraction IV of 70% (v/v) aqueous MeOH extract	53.7 \pm 7.4
• Fraction V of 70% (v/v) aqueous MeOH extract	49.9 \pm 4.1
• Fraction VI of 70% (v/v) aqueous MeOH extract:	38.1 \pm 4.2
○ Compound 7a (3,5- <i>O</i> -dicaffeoylquinic acid)	8.7 \pm 0.9
○ Compound 8a (ethyl-3,5- <i>O</i> -dicaffeoylquininate)	10.63 \pm 1.1
cynarin	10.1 \pm 1.1
trolox	17.9 \pm 1.1
quercetin	9.4 \pm 0.6

4.4. HPLC-based peroxynitrite scavenging activity profiling of *Salvia* spp.

4.4.1. Introduction

The aim of this study was to adopt the pyrogallol red bleaching test [110] for LC-DAD which is capable of characterizing chemical constituents and ONOO⁻ scavenging activity of a large number of plant extracts in parallel without interference with pigments. The hypothesis is that upon reaction with ONOO⁻, the peak areas of compounds with potential radical scavenging activity in the LC chromatograms will significantly reduce or disappear. Confirming the usefulness of our methodology we designed a model mixture of 17 phenolic reference compounds, which is representative for alcoholic extracts of *Salvia* species.

The criteria of the marker compound selection were multilateral. First of all, they had to occur in alcoholic extracts of *Salvia* species as analytical or chemotaxonomic markers. Second, they had to be ubiquitous in plant extracts covering possibly wide lipophilicity range and finally they should be commercially available. Based on the literature we identified 17 phenolic compounds (Fig. 23) fulfilling these criteria including gallic acid (**1s**), caffeic acid (**3s**) and its derivatives (caftaric acid (**2s**), scopoletin (**4s**), sinapic acid (**5s**), rosmarinic acid (**9s**), salvianolic acid A (**12s**), salvianolic acid B (**10s**)) [158, 159], flavonoid aglycones (quercetin (**11s**), apigenin (**13s**), kaempferol (**14s**), chrysin (**15s**), 5-hydroxyflavone (**16s**)), flavonoid glycosides (rutin (**6s**), luteolin 7-*O*-glucoside (**7s**), apigenin 7-*O*-glucoside (**8s**)) and one major diterpene marker carnosol (**17s**) [160].

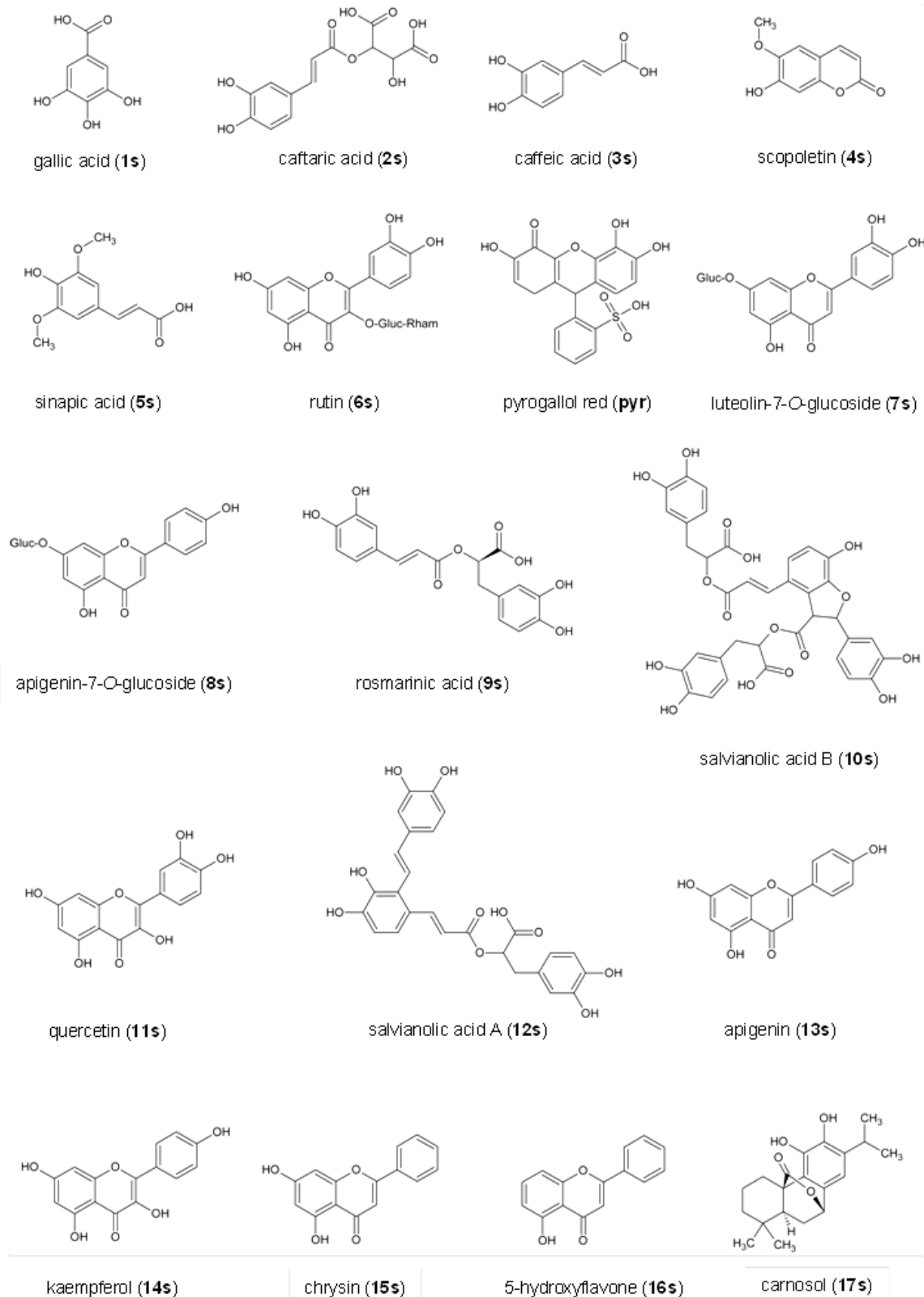


Figure 23. The chemical structures of typical *Salvia* marker compounds including the substrate of the assay pyrogallol red (**pyr**). The index s in compound numbering denotes for the origin *Salvia*.

Table 4 shows the chromatographic calibration data for all tested compounds. Calibration curves were constructed in six concentrations between 1-600 μM in triplicate. All the obtained calibration plots showed acceptable linearity ($R^2=0.998-0.999$) within the investigated concentration range. Limit of detection (LOD) was determined based upon the signal to noise ratio ($S/N=3$) of each analyte. The LOD for the 17 phenolic reference compounds ranged from 0.81 to 6.67 $\mu\text{g/mL}$. The amount of the marker compounds in scavenging activity measurements was calculated from these regression equations.

Table 4. Components of the model marker mixture in polarity order and their retention time, detection wavelength, linear calibration equation and limits of detection (LOD). In the regression equation $y = ax + b$, y is the peak area (mAU*s), x is the concentration of the analyte ($\mu\text{g/mL}$), a is the slope and b is the intercept.

No.	Compound name	t_R (min)	λ (nm)	Regression equation	R^2	LOD ($\mu\text{g/mL}$)
1s	gallic acid	0.646	220	$y = 23.179x - 19.138$	0.9997	0.90
2s	caftaric acid	2.223	320	$y = 11.478x - 9.486$	0.9995	1.25
3s	caffeic acid	2.566	320	$y = 14.306x - 8.041$	0.9994	0.81
4s	scopoletin	3.386	320	$y = 7.822x - 14.735$	0.9994	1.93
5s	sinapic acid	3.563	320	$y = 12.758x - 11.296$	0.9995	1.01
6s	rutin	3.866	320	$y = 2.967x - 19.389$	0.9995	6.67
pyr	pyrogallol red	3.999	470	$y = 12.183x - 1.859$	0.9996	0.46
7s	luteolin 7-glucoside	4.127	320	$y = 7.07x - 15.084$	0.9995	2.19
8s	apigenin-7-glucoside	4.746	320	$y = 15.803x - 24.908$	0.9993	1.60
9s	rosmarinic acid	4.966	320	$y = 7.226x - 24.117$	0.999	3.39
10s	salvianolic acid B	5.318	320	$y = 3.666x - 6.293$	0.9998	1.83
11s	quercetin	5.461	320	$y = 5.124x - 28.186$	0.9984	5.58
12s	salvianolic acid A	5.508	320	$y = 7.08x - 9.525$	0.9985	1.40
13s	apigenin	5.904	320	$y = 14.801x - 15.214$	0.9991	1.05
14s	kaempferol	5.981	320	$y = 6.782x - 9.544$	0.9994	1.47
15s	chrysin	7.420	320	$y = 8.789x - 9.181$	0.9996	1.10
16s	5-hydroxyflavone	9.578	320	$y = 6.153x - 27.306$	0.9993	4.50
17s	carnosol	9.781	220	$y = 9.187x - 19.12$	0.9998	2.12

After validating assay parameters with the above described model mixture we applied the reported method to a real *Salvia* sample. Since *S. miltiorrhiza* is one of the most studied and widely used medicinal *Salvia* species containing representative antioxidant polyphenolic components [175], we chose the methanolic extract of its herb to demonstrate the benefits of the developed method.

4.4.2. Optimization of the chromatographic conditions

In the first step, we optimized the LC separation conditions and the UV-vis detection wavelengths for the selective detection of the test substrate pyrogallol red (**pyr**). Depending on the acidity of the solution, pyrogallol red can occur in six different ionized forms with significantly different spectrophotometric characters [176]. Therefore, in order to minimize the interference between the phenolic markers and pyrogallol red, UV-vis spectra of chemically representative compounds (caffeic acid (**3s**), luteolin 7-*O*-glucoside (**7s**), rosmarinic acid (**9s**), salvianolic acid A (**12s**), kaempferol (**14s**)) were recorded and analyzed at different pH values (pH=1.90 0.1% (v/v) TFA; pH=4.00 0.1 M citric acid/Na-citrate; pH=6.80 0.1 M AcOH/NH₄OAc). The representative UV-vis spectra at pH=1.90 are shown in Fig. 24 below.

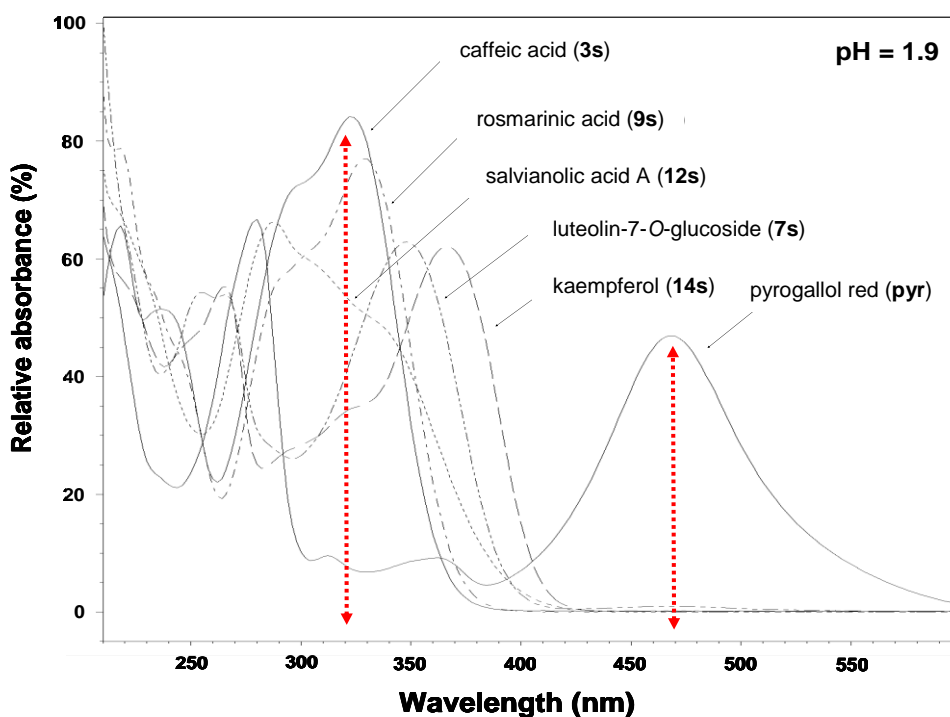


Figure 24. UV-vis spectra of five representative marker compounds (**3s**, **7s**, **9s**, **12s**, **14s**) and the substrate of the assay (**pyr**) at pH=1.90 acquired by the DAD detector in the HPLC runs (190-600 nm).

We found that at the most acidic pH the studied phenolic marker compounds had UV-vis maxima between 300-360 nm where pyrogallol red has minimum and *vice versa* at 470 nm. Moreover, low pH was the most favourable for separation of

compounds containing phenolic functional groups, while at neutral pH the peaks of the used compounds became broad and tailed. Therefore, the pH of the eluents was adjusted with trifluoroacetic acid to pH=1.90 and phenolic markers were monitored at 220 and 320 nm while pyrogallol red was detected selectively at 470 nm.

As the model mixture contained several chemical analogues (e.g. luteolin 7-glucoside (**7s**) – apigenin 7-glucoside (**8s**); salvianolic acid A (**12s**) – salvianolic acid B (**10s**); apigenin (**13s**) – kaempferol (**14s**)), two isocratic parts were integrated into the gradient elution profile (the first with 15% and the second with 35% of eluent B). Furthermore, at the design of the gradient program, we considered that in the case of real samples the method must have “extra retention time windows” for other common compounds which can occur in alcoholic *Salvia* extracts.

4.4.3. Calibration for pyrogallol red

After the analysis of the UV-vis spectra of representative marker compounds (Fig. 24), we chose the detection wavelength of 470 nm for quantification of pyrogallol red (**pyr**). The four chromatograms on the right side of Fig. 25 showed that there was no interference with typical phenolic compounds and with the major degradation products of pyrogallol red after reaction with ONOO^- . We found that the optimum injection volume for 100 μM pyrogallol red solution was 6 μL . The peak symmetry factors of pyrogallol red decreased below 0.85 at higher (8 and 10 μL) injection volumes. On the other hand, smaller (2 and 4 μL) injection volumes caused significant loss in detection range. Calibration curve for pyrogallol red was constructed under the optimized conditions in eight concentrations between 1-100 μM in triplicate. The calculated calibration equation was $Peak\ Area = 12.183 \times [PR] - 1.859$ with a correlation coefficient value 0.9996. The LOD and LOQ values were 0.46 and 1.52 $\mu\text{g/mL}$, respectively.

The repeatability and reproducibility of the analytical method was confirmed from the retention times and peak areas of the pyrogallol blank solution (100 μM). Results listed in Table 5 indicate excellent repeatability and inter-day precision with very low RSD (<2.3 RSD%). Therefore, we concluded that the LC-DAD method is robust and sensitive enough to quantify pyrogallol red in biological matrixes such as alcoholic plant extracts.

Table 5. Repeatability and reproducibility of the retention time and peak area of pyrogallol red (pyr) blank (100 μ M) solution (n=6).

	t_R (min)	RSD%	Peak Area (mAU*s) 100 μ M	RSD%
Day 1	4.026 \pm 0.008	0.19	496.0 \pm 11.4	2.31
Day 2	3.995 \pm 0.010	0.25	491.6 \pm 5.6	1.15
Day 3	4.018 \pm 0.290	0.29	493.6 \pm 7.2	1.45
Mean	4.013 \pm 0.016	0.40	493.7 \pm 2.2	0.45

4.4.4. Validation of the assay with a *Salvia* specific model mixture

Fig. 25 summarizes the overlaid UV chromatograms of the model mixture of *Salvia* markers and the degradation products after treated with increasing concentration of ONOO⁻. All of the eight chromatograms (four runs) contain base-line separated and sharp peaks which demonstrate the excellent resolving power of the analytical method and enable simultaneous quantification of the constituents of the mixture. It can be obviously seen that areas of certain peaks named **4s**, **7s**, **8s**, **13s**, **15s** and **16s** (marked with ●) did not change significantly after treating the model mixture with increasing concentration of the radical reagent. On the other hand, peaks with number **2s**, **5s**, **6s** and **17s** (marked with ●) significantly reduced whereas peaks **1s**, **3s**, **9s**, **10s**, **11s**, **12s** and **14s** (marked with ●) disappeared or almost disappeared in the chromatograms detected at the highest concentration of ONOO⁻.

Simultaneously, the concentration of the substrate pyrogallol red decreased gradually, which trend could be followed by the *I*% (inhibition percentages) on the right side of Fig. 25. These results indicate that the 17 phenolic components protected pyrogallol red from “bleaching” by ONOO⁻ in a competitive and concentration dependent manner. Some minor degradation products (marked with * on Fig. 25C) could be seen in the retention time ranges between the signed peaks (between peak **1s** and **2s**, **3s-4s**, **12s-13s**, and after **17s**) but their appearance did not disturb the detection of the marker compounds significantly.

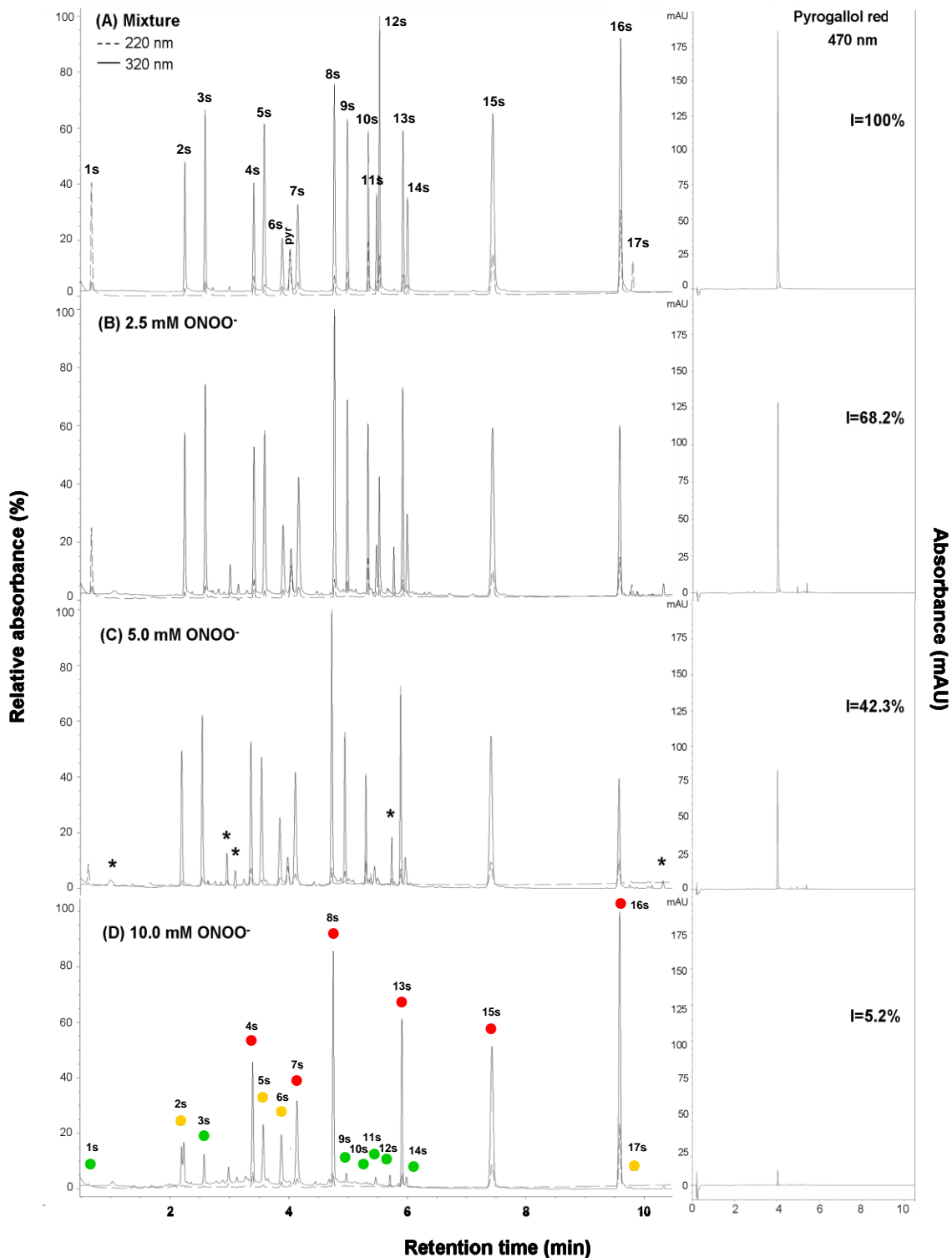


Figure 25. Left side: The overlaid UV-chromatograms of the model mixture of *Salvia* markers (A), and the reaction products after treated with increasing concentrations of ONOO^- (B-D); Right side: The decreasing peak areas of pyrogallol red (**pyr**) in the same run and the calculated percentage of inhibition. Peak names, retention times and detection wavelengths are listed in Table 4. Activity categories: ● active/great degradation, ● moderate activity/moderate degradation, ● inactive/no degradation, * degradation products.

4.4.4.1. Comparison of degradation kinetics in mixture to individual scavenging activities

Table 6 summarizes the obtained degradation kinetics parameters of the 17 compounds in equimolar mixture and their individual scavenging activities. The values of regression parameter $a \cdot 10^3$ could be interpreted as the apparent stoichiometries. The b values of the regression equations are proportional to the standard deviation of the given measurements while n shows the number of concentrations used for linear curve fitting. Reciprocal IC_{50} values were reported for easier data analysis.

Table 6. Components of the model marker mixture in polarity order and their degradation kinetics parameters after reaction with increasing concentrations of $ONOO^-$ (0, 0.5, 1.5, 2.5, 5, 10 mM) and their individual scavenging activities ($n=3$). Activity categories: ● active/great degradation, ● moderate activity/moderate degradation, ● inactive/no degradation.

Peak	Compound name	Degradation kinetic in mixture Linear regression parameters*				Individual scavenging activity		Activity categories
		$a \cdot 10^3$	b	n	R^2	IC_{50} (μ M)	$10^3/IC_{50}$	
1s	gallic acid	16.54	-	5	0.988	88 ± 18	11.4	●
2s	caftaric acid	5.90	-	6	0.906	1686 ± 211	0.6	●
3s	caffeic acid	8.24	-	6	0.981	238 ± 19	4.2	●
4s	scopoletin	0.35	5.58	5	0.901	n.a.	n.a.	●
5s	sinapic acid	5.32	17.76	5	0.997	1225 ± 195	0.8	●
6s	rutin	2.28	-	6	0.907	3058 ± 250	0.3	●
pyr	pyrogallol red	9.86	-	6	0.986	-	-	-
7s	luteolin-7-glucoside	1.75	2.66	6	0.821	n.a.	n.a.	●
8s	apigenin-7-glucoside	0.34	-	4	0.880	n.a.	n.a.	●
9s	rosmarinic acid	9.07	-	6	0.972	134 ± 14	7.4	●
10s	salvianolic acid B	10.11	-	6	0.997	73 ± 10	13.6	●
11s	quercetin	16.79	-	5	0.938	49 ± 9	20.3	●
12s	salvianolic acid A	18.78	-	5	0.952	25 ± 3	40.3	●
13s	apigenin	0.57	10.27	5	0.877	n.a.	n.a.	●
14s	kaempferol	14.12	-	5	0.988	96 ± 6	10.5	●
15s	chrysin	1.91	32.39	4	0.905	n.a.	n.a.	●
16s	5-hydroxyflavone	3.82	51.14	4	0.836	n.a.	n.a.	●
17s	carnosol	19.11	-	5	0.966	490 ± 111	2.0	●

In the regression equation $Y = aX + b$; Y is $\Delta[S]/[S]_0 - [S]$ where S is the concentration of the single compounds and X is $[ONOO^-]$; n is the number of data points used for regression and R^2 is the squared correlation coefficient; IC_{50} is the concentration which protects 50% of pyrogallol red against 500 μ M $ONOO^-$; n.a. = not active. *: Note that F-test and normal probability distribution of residuals was checked and fulfilled for every compound in the course of the regression analysis.

4.4.4.2. Validation of the assay parameters with structure – activity relationships

The resulted apparent stoichiometries and individual scavenging activities are listed in Table 6. Compounds without catechol moiety, namely scopoletin (**4s**), sinapic acid (**5s**), apigenin 7-glucoside (**8s**), apigenin (**13s**), chrysin (**15s**) and 5-hydroxyflavone (**16s**) were virtually inactive. In addition, phenolic compounds with one catechol function, gallic acid (**1s**), caftaric acid (**2s**), caffeic acid (**3s**), rutin (**6s**), kaempferol (**14s**) and carnosol (**17s**) showed strong ONOO⁻ scavenging properties. The most active compounds (rosmarinic acid (**9s**), salvianolic acid B (**10s**), quercetin (**11s**), salvianolic acid A (**12s**)), however, contain two or three catechol groups per molecule. In the case of flavonols with hydroxyl group at position 3 and 5 (quercetin (**11s**) and kaempferol (**14s**) in our study) an intramolecular rearrangement could take place forming a catechol-like structure in ring C (see Fig. 9 on p. 23) [177]. The above described trend in structure - ONOO⁻ scavenging activity relationship shows unambiguously the essential role of the catechol subunit. This relationship was thoroughly studied earlier [112, 177] and now confirms the new methodology reported here.

4.4.5. Demonstration of the assay performance on the methanolic extract of *Salvia miltiorrhiza*

Fig. 27 represents the overlaid UV chromatograms of *S. miltiorrhiza* extract and the protected amount of pyrogallol red in the same runs after treated with increasing concentration of ONOO⁻. Six major compounds were tentatively identified in the mixture based on retention time and UV spectra (caffeic acid (**3s**), rutin (**6s**), apigenin 7-glucoside (**8s**), rosmarinic acid (**9s**), salvianolic acid B (**10s**), salvianolic acid A (**12s**)).

Among the identified components of the extract, the peak areas of salvianolic acid A (**12s**), salvianolic acid B (**10s**) and rosmarinic acid (**9s**) decreased significantly, while the loss of caffeic acid (**3s**) and rutin (**6s**) was moderate and the amount of apigenin 7-glucoside (**8s**) did not change due to the increasing concentration of ONOO⁻.

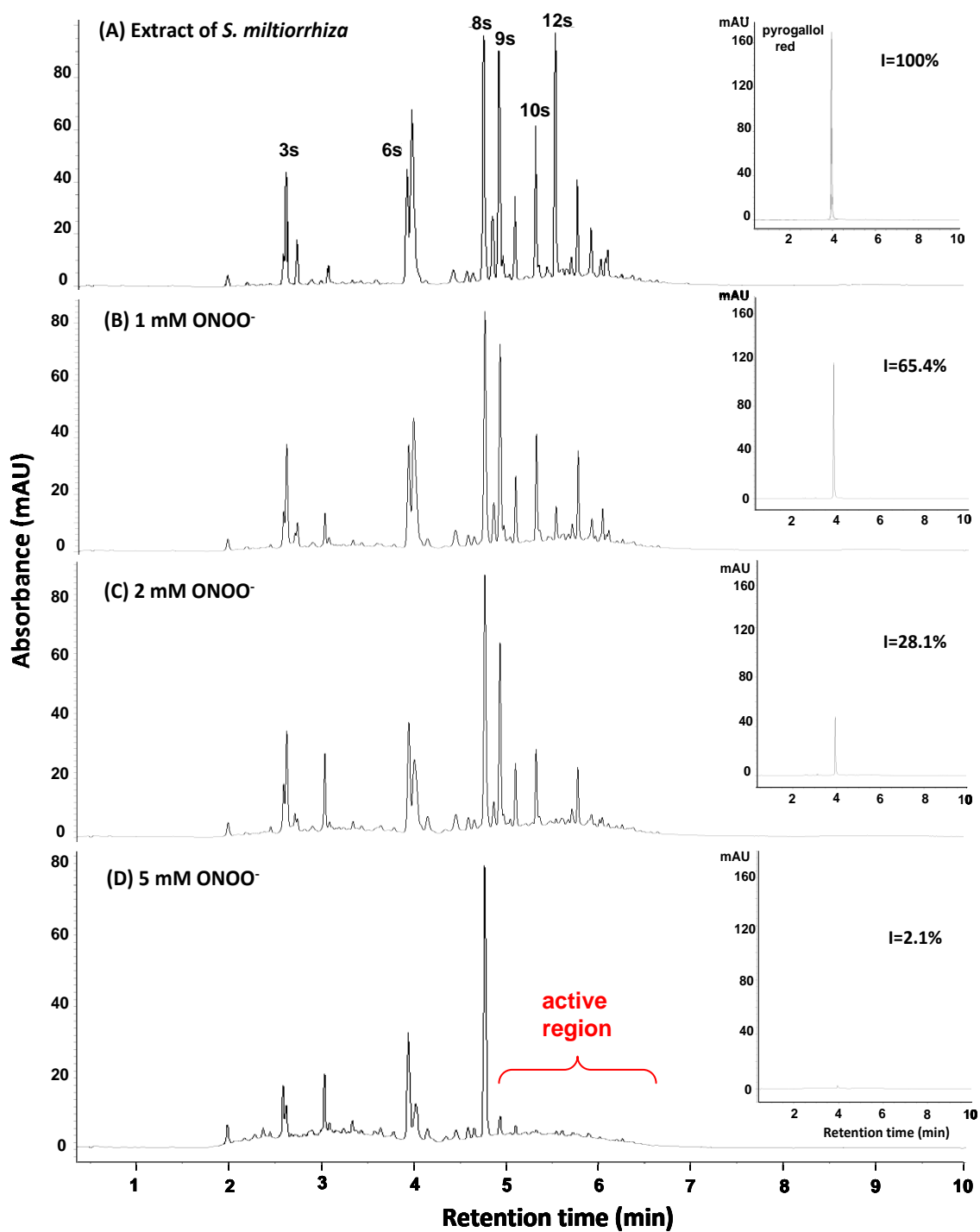


Figure 27. ONOO⁻ scavenging activity profile of *S. miltiorrhiza* methanolic extract (2.0 mg/mL final concentration). (A) The UV-chromatogram of *S. miltiorrhiza* methanolic extract, and (B-D) the reaction products after treated with increasing concentrations of ONOO⁻ acquired at 320 nm; Right side: The decreasing peak areas of pyrogallol red (**pyr**) in the same run acquired at 470 nm and the calculated percentage of inhibition. Key to peak identity as in Fig. 23.

In general, the peaks with retention times greater than 4.7 min showed an unambiguous response to the radical reagent and therefore were considered as the ONOO⁻ scavenger constituents of *S. miltiorrhiza* (i.e., active region). This experiment also showed that the screening dose of ONOO⁻ should be higher than 1 mM but lower than 5 mM against *Salvia* extracts with concentration of 2.0 mg/mL in order to be able to differentiate effectively between active and inactive components.

4.5. Blood-brain barrier (BBB) permeability screening and HPLC-based hit profiling

4.5.1. Introduction

While numerous natural products possess activity on central nervous system (CNS) targets, there has been no analytical approach to effectively identify compounds with high brain penetration potential in complex mixtures at the early stage of drug discovery. To overcome this issue, the performance of the *in vitro* PAMPA-BBB assay for NPs and for plant extracts has been validated and characterized.

Initially, a check was made on the predictive power of the PAMPA-BBB assay using a NP compound set, because this assay was developed originally with commercial drugs and validated on in-house compounds by Di and co-workers [131]. In contrast, the present validation set contained solely natural product drugs and natural product-like drugs [categorized as in 178] possessing experimental log BB values (the logarithmic value of brain tissue to plasma concentration ratio of a given drug) ranging evenly from -2.0 to 1.0 in value. Test compound selection was performed to ensure high chemical diversity and the predominance of alkaloids, representing the major phytochemical compound class known to act at the CNS [139]. In parallel, ubiquitous marker compounds of major NP compound classes were tested in order to characterize the “phytochemical selectivity” of the PAMPA-BBB system.

Next, the non-cytotoxic plant extract sublibrary was screened with the validated PAMPA-BBB assay and the resulting primary hits were confirmed and characterized by LC-MS. Moreover, as NMR spectroscopy has become an indispensable technique in the modern NP dereplication process [179], assay parameters were modified in order to obtain samples from permeability experiments directly suitable for NMR measurements, making the overall procedure more rapid and compact. Advantages and

limitations of this sequential approach were demonstrated in the case of four different types of representative plant extract hits (crude extracts; i.e., highly complex mixtures of 80-100 components in the case of *Tanacetum parthenium* and *Vinca major*, and semipurified (fractionated) extracts, i.e., less complex mixtures of 30-40 components in the case of *Salvia officinalis* and *Corydalis cava*), which emerged from the screening study.

4.5.2. Validation of the PAMPA-BBB assay for natural products

Experimentally determined effective permeability values ($\log P_e$) for a diverse compound set correlated quite well with corresponding $\log BB$ values taken from the literature (Fig. 28, for details on $\log BB$ data see Table A2, Appendix). Moreover, it could be seen that the arbitrary cut-off value of -6.0 for $\log P_e$ discriminated effectively between compounds possessing $\log BB$ values greater (considered as BBB+) and less than -0.5 (considered as BBB-).

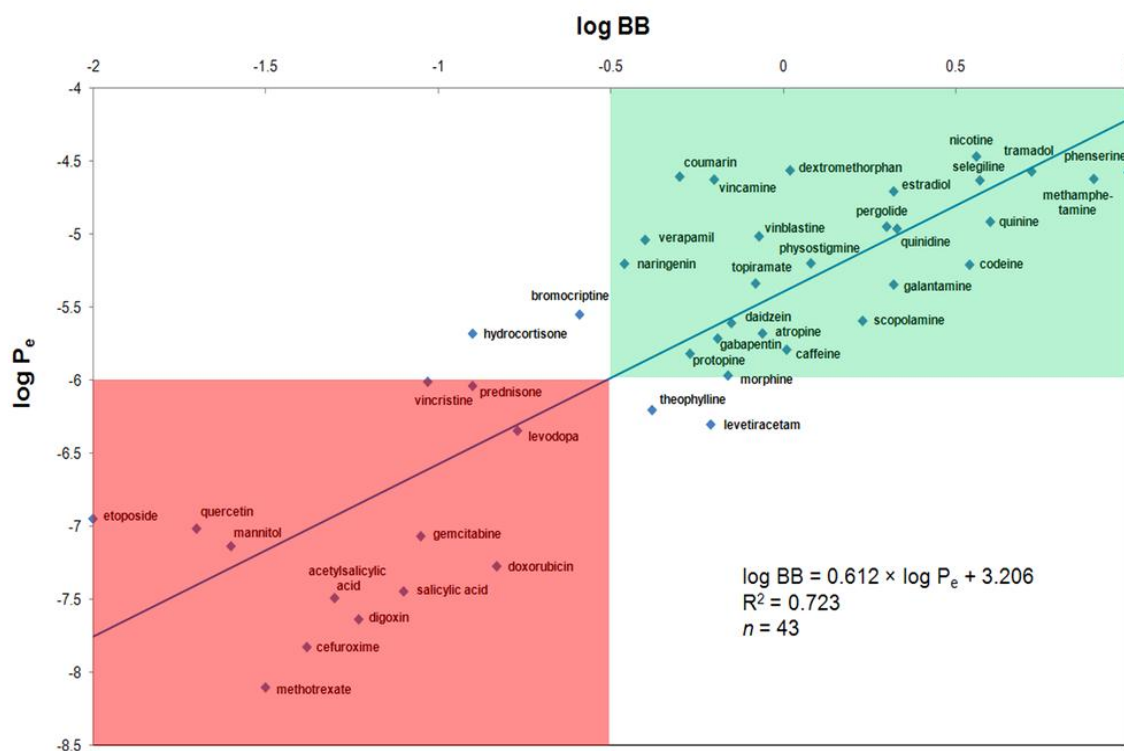


Figure 28. Correlation between experimental $\log BB$ values and effective permeabilities determined by the PAMPA-BBB assay for the validation set, consisting of 23 NP and 20 NP-like drugs. Compounds in the red zone are considered as BBB-, while the green zone shows predicted BBB+ compounds. SE values, all being under 0.1 log unit are not shown for clarity (for numerical values see Table A2, Appendix).

These findings were in good agreement with the log P_e ranges published by Li et al., classifying CNS drug candidates with high, moderate, and low BBB permeation potential [131]. Thus, it was concluded that the PAMPA-BBB assay preserved its predictive power in the case of NPs and is a valid physicochemical screening approach to study solely NP-containing plant extracts.

4.5.3. Characterization of the effective BBB-permeability potential of major phytochemical compound classes

The available pharmacokinetic information on the brain distribution of several NPs and herbal medicines addressing targets in the CNS is limited and mostly not very comparable [180]. Therefore, prior to screening plant extracts with the PAMPA-BBB assay, we sought to characterize the BBB permeability potential of major metabolite classes, that can occur in plant extracts. Fig. 29 shows the results of the 72 tested marker compounds. The analytical and calculated physicochemical data of the test set are summarized in Table A3 (Appendix). As our aim was to explore the general BBB permeability potential of compound classes, individual results and rank orders within groups are not discussed in detail.

Glycosides with sugar moieties and reference compounds containing a free carboxyl group showed a very low effective permeability potential and fell in the BBB-region ($\log P_e < -6.0$). However, it must be noted that the $\log P_e$ values for the majority of these compounds (marked with asterisks) were calculated with the corresponding limit of quantification (LOQ) values, because the test compound concentration in the acceptor side fell below the detection limit. These results are consistent with the basic concepts used by medicinal chemists regarding physicochemical properties that are prerequisites for brain penetration [181, 182]: glycosides due to their hydrophilic nature (high polar surface area, negative $\log D_{7.4}$ value, relatively high MW) are unable to pass across lipid bilayers by passive diffusion, while the apparent exclusion of free carboxylic acid group-bearing compounds (acidic pK_a values ranging from 2 to 4) from the acceptor phase reflect on the fact that the ionization state affects BBB permeability adversely in the case of negatively charged species [183].

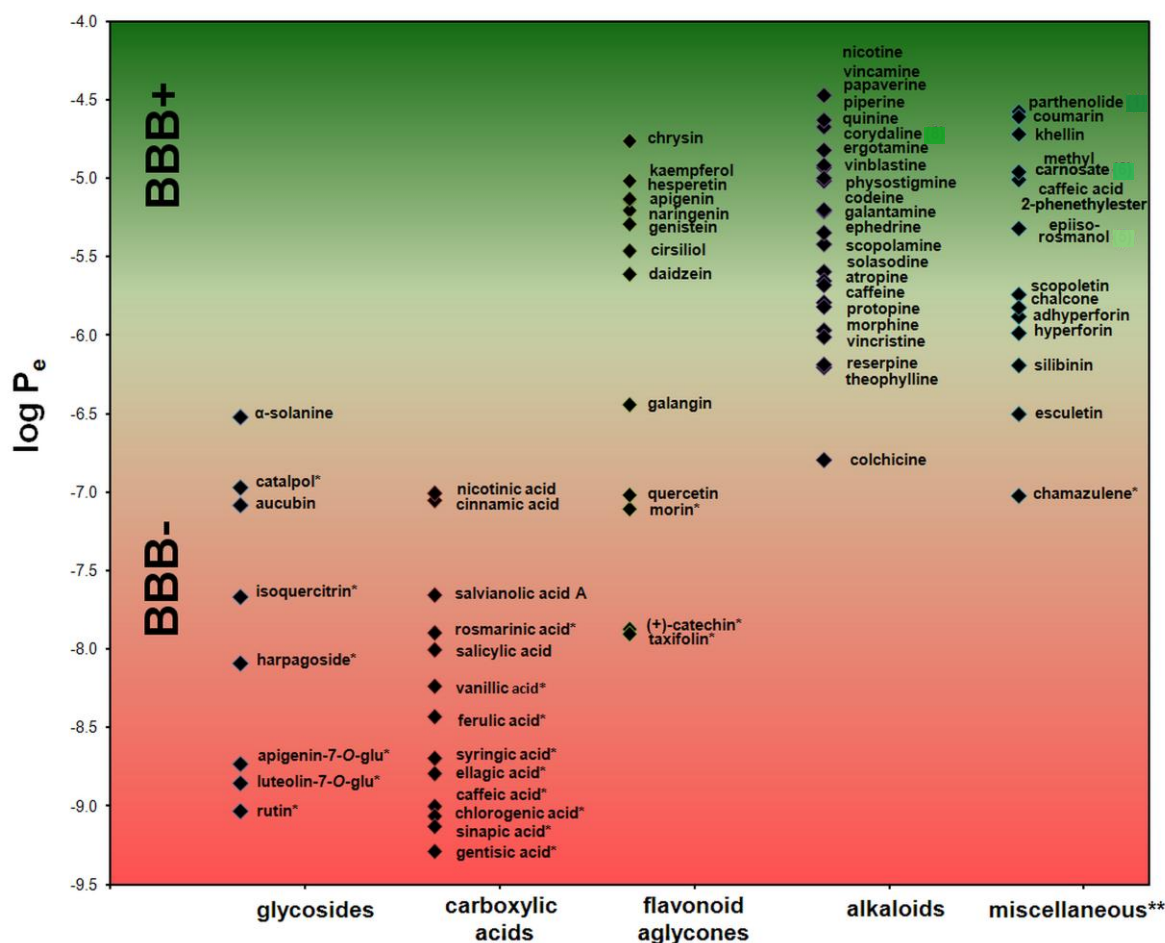


Figure 29. Effective BBB permeability profile of major phytochemical compound classes (* test compound was not detected in acceptor side; $\log P_e$ values were calculated with LOQ values (LC-MS UV/SIM measurements; see Table A3 in Appendix). ** Not measurable due to very low aqueous solubility: stigmaterol, lupeol, betulin).

In contrast, representative molecules of flavonoids (as aglycones) fell in the moderate or high permeability range (BBB+), confirming the results of several *in vitro* and *in vivo* pharmacokinetic observations and studies [123, 180, 184, 185]. As could be generally expected from their significant CNS activity (even toxicity in some cases) [186], alkaloids fell uniformly in the high or extremely high BBB permeability range. Moreover, the group of miscellaneous compounds including terpenoids and coumarins showed significant BBB permeability potential, although some representatives of these groups were not measurable due to their extremely low aqueous solubility. Nevertheless, the observed trend and gradation on a logarithmic scale in Fig. 29 indicated high “phytochemical selectivity” of the PAMPA-BBB system for the

compound classes investigated. The overall profile of this permeability map was consistent with the findings of Gomes et al. [139], who evaluated phytochemical compound classes responsible for the CNS activity of 84 plants (alkaloids 38%, flavonoids 16%, terpenoids 11%), and with the conclusions of Kennedy and Wightman [187], who reviewed human brain-affecting plant chemicals, thereby supporting the relevance of the present approach. This result prompted us to screen plant extracts in order to evaluate whether the 3-4 orders of magnitude difference in $\log P_e$ values of BBB+ and BBB- constituents could be exploited.

4.5.4. Co-solvent retention profile of the PAMPA-BBB assay

First, to select the most suitable co-solvent for the screening study, blank runs were performed with different starting volume ratios of DMSO and MeOH in the donor side. Gas chromatography with flame-ionization detector (GC-FID) analysis of the resulting co-solvent concentrations in the acceptor side revealed that the PBL membrane is practically impermeable for both organic solvents, although DMSO was significantly better retained (Fig. 30).

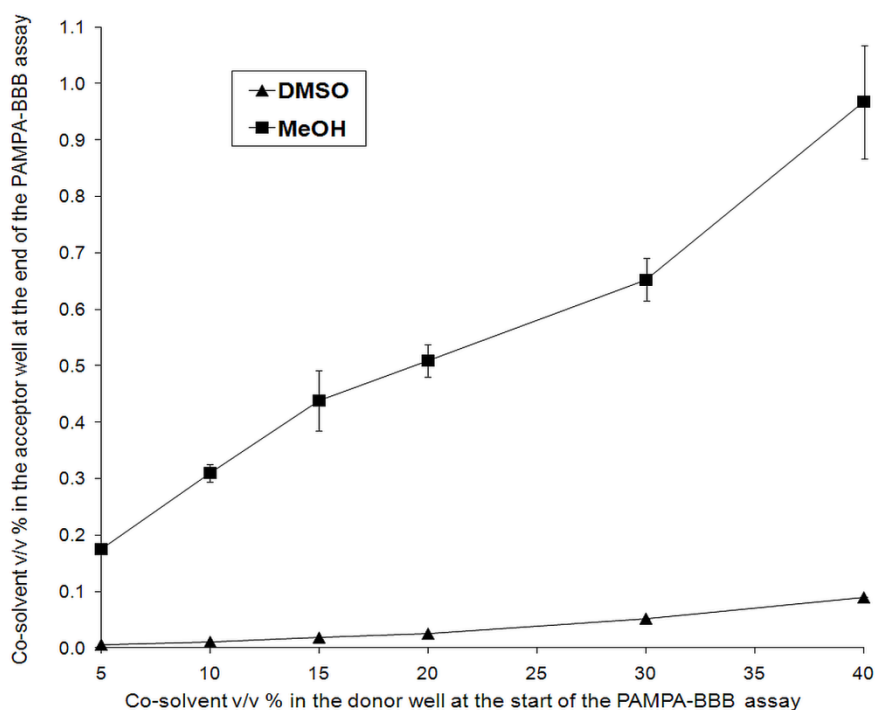


Figure 30. Co-solvent retention profile of the PAMPA-BBB assay measured by GC-FID.

Performing the PAMPA-BBB assay with 10 v/v % co-solvent content in the donor side resulted in 0.01 and 0.31 v/v % final nominal concentrations for DMSO and MeOH in the acceptor side, respectively. This phenomenon has important theoretical and methodological consequences: (i) $\log P_e$ is basically a kinetic parameter, however, it depends significantly on the aqueous solubility of test compounds, as the co-solvent content of the acceptor side is negligibly low during the assay. (ii) The co-solvent ratio of the acceptor and donor side creates practically an “anti-sink” condition (for definition of “sink” see [161]), making the assay setup physicochemically more strict. (iii) The co-solvent content of the donor side and thereby the sample dose could be elevated without significantly interfering with spectroscopic detections, e.g., using even 10 v/v % DMSO in the donor side enabled sensitive UV detection of the acceptor wells at 240 nm during the screening experiments (for NMR applicability see below; for the effect of DMSO content upon UV detection see Table 7).

Table 7. Effect of the DMSO co-solvent content of the donor side upon the UV-detectability of the acceptor side of the PAMPA-BBB assay. Absorbance values are expressed in arbitrary units.

wavelength (nm)	DMSO v/v% in the donor side at the start of the PAMPA-BBB assay						
	0	5	10	15	20	30	40
Absorbance of the acceptor side at the end of the PAMPA-BBB assay							
210	0.583	1.126	1.857	4.000	4.000	4.000	4.000
220	0.166	0.315	0.469	0.643	0.857	1.416	3.384
230	0.082	0.093	0.104	0.118	0.137	0.175	0.235
240	0.080	0.079	0.080	0.080	0.082	0.082	0.086
250	0.073	0.072	0.072	0.071	0.071	0.071	0.072
260	0.063	0.062	0.062	0.061	0.061	0.060	0.062
270	0.056	0.056	0.055	0.055	0.054	0.054	0.055
280	0.050	0.049	0.049	0.049	0.048	0.048	0.049
290	0.045	0.043	0.044	0.044	0.043	0.044	0.045
300	0.043	0.042	0.043	0.043	0.041	0.042	0.043

4.5.5. Screening of the plant extract library and tentative physicochemical characterization of BBB+ and BBB- plant extracts by LC-MS

Bearing these results in mind, the non-cytotoxic plant extract sublibrary consisting of 1760 individual samples was screened with the validated PAMPA-BBB assay at a 1.0 mg/mL concentration (with 10 v/v % DMSO as co-solvent) using an UV-vis reader. The campaign resulted in a hit rate of 7.1% which also showed the strict nature of the PAMPA-BBB assay and suggest its practicality as an effective HTS tool.

Primary hits (BBB+ extracts) were validated by LC-MS and the tentative physicochemical characterization of randomly selected BBB+ and BBB- compounds was performed by means of the logarithmic value of the apparent chromatographic retention factor ($\log k_0$ as an estimation of compound lipophilicity by gradient RP-HPLC [162, 188]) as well as the detected molecular weight (Fig. 31).

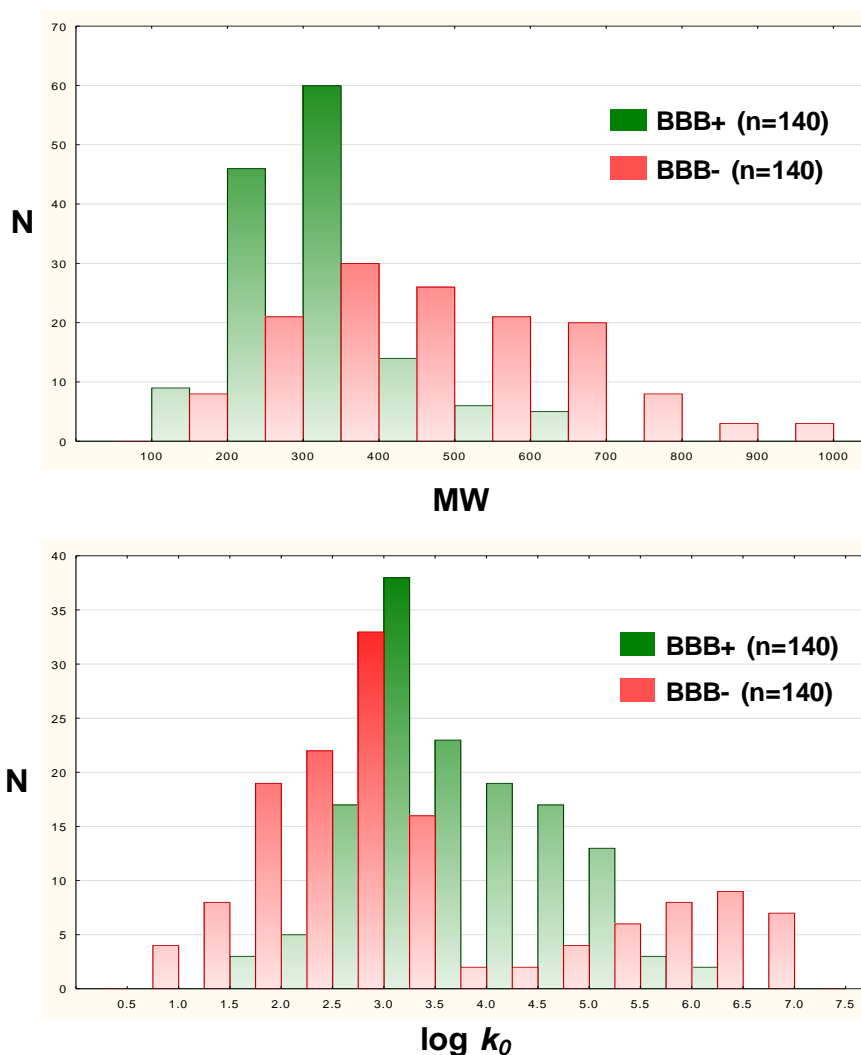


Figure 31. Physicochemical parameter histograms of randomly selected unique compounds from BBB+ and BBB- plant extracts measured by LC-MS.

In the case of both parameters, BBB+ compounds showed a significantly narrower distribution compared to the BBB- group. MW distribution of BBB+ compounds peaked out in the drug-like range of 200-400 daltons, but slightly extended to the 400-600 dalton range. In contrast, the MW distribution of BBB- compounds was more even in the tested MW range. Comparing the $\log k_0$ distributions of the two groups

revealed that compounds with moderate polarity ($\log k_0$ 2.5-5.0) enriched significantly in the BBB+ group while NP's with extremely low ($\log k_0 < 2.5$) or extremely high lipophilicity ($\log k_0 > 5.0$) were totally eliminated from the brain permeable group. This result suggests that brain penetrable compounds detected by the PAMPA-BBB assay from complex plant extracts were showing drug-like properties.

4.5.6. Application of the PAMPA-BBB/LC-MS/NMR procedure to four BBB+ plant extracts

In order to study the performance of the PAMPA-BBB system in detail, four typical BBB+ plant extracts were chosen from the validated hits of the PAMPA-BBB screen: *T. parthenium* and *V. major* were used as crude mixtures, while samples of *S. officinalis* and *C. cava* were selected to represent partially fractionated extracts. LC-DAD-ESI-MS/MS analysis of the starting stock solutions and the PAMPA-BBB-derived acceptor solutions were performed and compared (Fig. 32).

As the chromatographic profiles of Fig. 32A and B indicate, the sample complexity of crude extracts was alleviated due to the selective “filtering” effect of the PAMPA-BBB assay. Thus, BBB+ components of the mixtures were enriched in the acceptor side, while BBB- ingredients did not diffuse well and were practically eliminated from the samples. In contrast, in the case of the fractionated BBB+ extracts, the purifying effect was less pronounced (Fig. 32C and D). Identification (dereplication) of brain-penetrable components in acceptor samples could not be completed with high confidence solely on the basis of the acquired LC-DAD-ESI-MS/MS data, but revealed that in all four cases the detected BBB+ peaks corresponded to (very) closely related analogues (similar CID fragmentation patterns were detected). Hence, sesquiterpene lactones occurred in *T. parthenium*, indole alkaloids in *V. major*, phenolic diterpenes in *S. officinalis*, and isoquinoline alkaloids in *C. cava* (see Appendix for UV and MS characteristics of the most abundant BBB+ compounds).

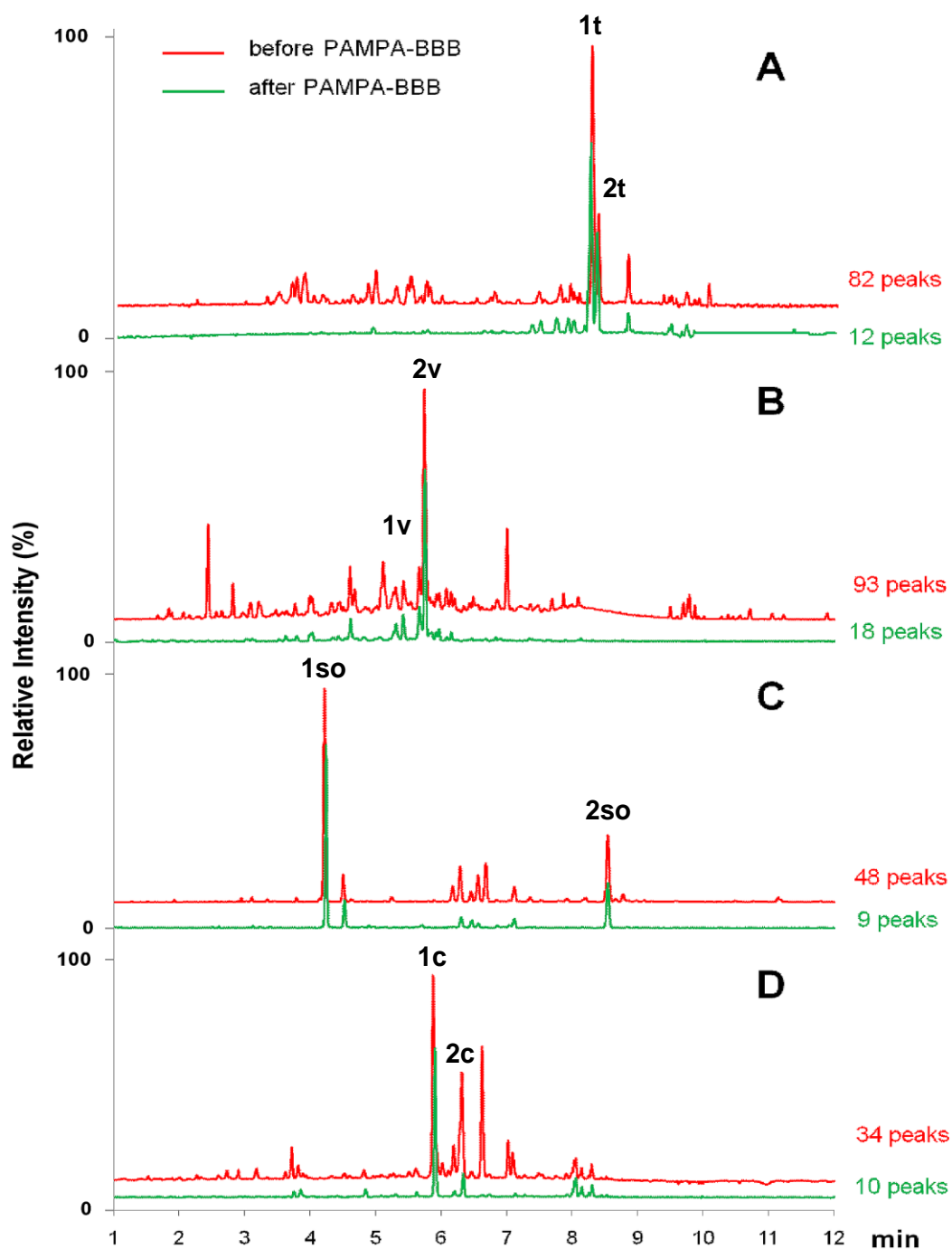


Figure 32. LC-MS chromatograms of four representative BBB+ extracts: stock solution before (red) and acceptor solution after the PAMPA-BBB experiment (green), (A) *Tanacetum parthenium* (ESI+ total ion chromatogram), (B) *Vinca major* (UV trace at 220 nm), (C) *Salvia officinalis* (UV trace at 220 nm), and (D) *Corydalis cava* (UV trace at 220 nm). Compound identities are presented in Table 8 and in Fig. 33.

Instead of isolating the above-mentioned BBB+ compounds, a NMR spectroscopic study was undertaken to investigate whether modifications in the assay design could provide samples directly suitable for NMR measurement. First, this was achieved by changing only the assay medium from a protic to a deuterio PBS buffer and subsequently conducting the assay with the most concentrated plant extracts possible (for experimental conditions see Chapter 3.8.1.), without prefiltering the donor samples to maximize the concentration of the targeted BBB+ compounds in the acceptor wells. It was found that the assay preserved its selectivity and filtering efficiency also in deuterated milieu with elevated plant extract doses. Second, as a consequence of the applied co-solvents in the donor wells, the most intense features in the ^1H NMR spectra were the singlets at 3.34 and 2.71 ppm belonging to MeOH and to DMSO, respectively (see Chapter 4.5.4.). Fortunately, the suppression of these signals was not necessary.

LC-DAD-MS data showed that, besides the numerous low-level components, each PAMPA-BBB “filtered” sample contained at least two major brain-penetrating (BBB+) components with individual concentrations ranging from 2.5 to 78.5 $\mu\text{g/mL}$ (Table 8). Even though these concentrations were smaller than those in the starting plant extracts, the “reduced” sample complexity offered more structural information based on which the identification/confirmation (dereplication) of the major BBB+ components became possible (for the observed difference in complexity of NMR spectra see Figure A1, Appendix). Although the effect of the “purification” is evident in this comparison, it should be noted that signal overlaps caused by the presence of two structurally similar components in comparable concentration make the identification of the components more difficult (see below) especially when no reference data are available in a given medium. The four BBB+ extracts examined represented four different scenarios from an NMR perspective. Since all of the components discussed below (Fig. 33) have been identified earlier, NMR assignments are presented in the Appendix.

Table 8. Summary of analytical and effective BBB permeability data of the four studied BBB+ plant extracts obtained by the PAMPA-BBB/LC-MS/NMR cascade.

Plant extract (HPLC profile)	Identified BBB+ compound	t _R (min)	log P _e ± SE	Concentration in acceptor solution subjected to NMR (µg/mL)	Information obtained by direct NMR
crude extract of <i>T. parthenium</i> herb (Fig. 32A)	parthenolide (1t)	8.23	-4.58 ± 0.05	78.5	complete ¹ H, almost complete ¹³ C assignment
	11,13-dihydro-parthenolide (2t)	8.34	-4.55 ± 0.04	14.4	complete ¹ H assignment
semicrude extract of <i>V. major</i> herb (Fig. 32B)	vincamajine (1v)	5.36	-4.99 ± 0.01	9.7	¹ H assignment of characteristic structural moieties
	majdine (2v)	5.69	-5.05 ± 0.02	65.7	¹ H assignment of characteristic structural moieties
fractionated extract of <i>S. officinalis</i> folium (Fig. 32C)	epiisorosmanol (1so)	4.18	-5.32 ± 0.05	56.7	complete ¹ H assignment
	methyl carnosate (2so)	8.68	-4.96 ± 0.02	18.8	complete ¹ H assignment
fractionated extract of <i>C. cava</i> tuber (Fig. 32D)	tetrahydropalmatine (1c)	5.92	-4.70 ± 0.01	14.3	complete ¹ H assignment
	corydaline (2c)	6.30	-4.93 ± 0.06	2.5	partial ¹ H assignment

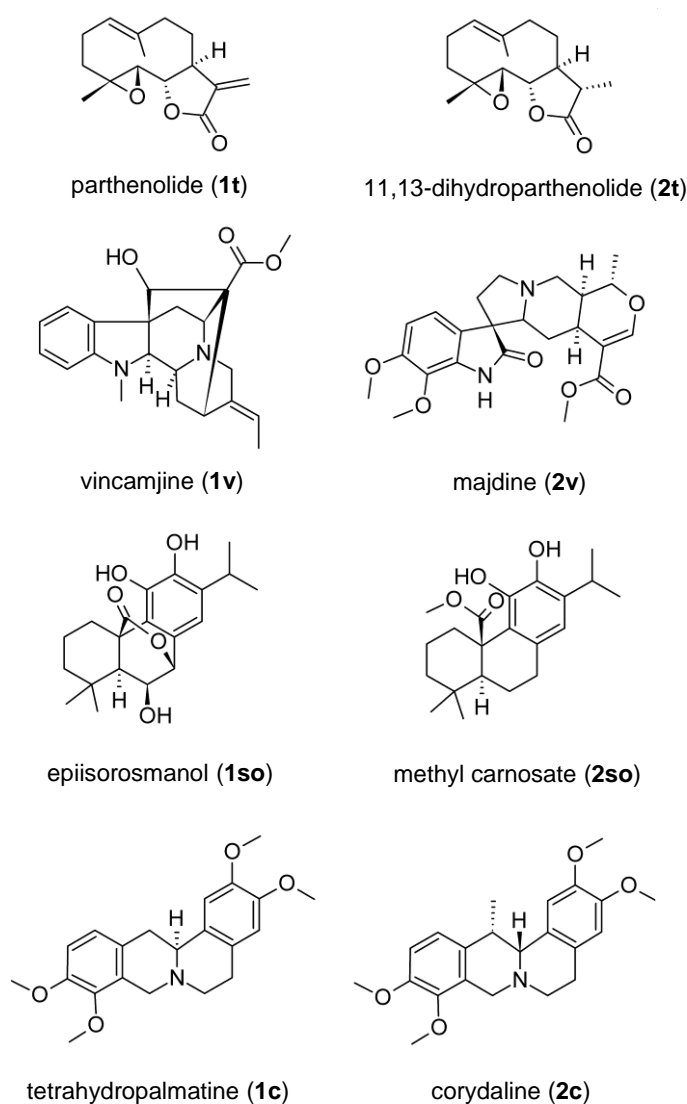


Figure 33. Chemical structures of the identified BBB+ compounds. In the case of compounds **1c** and **2c** only one enantiomer is shown for clarity. The indexes **t**, **v**, **so**, and **c** in compound numbering denote for origin *Tanacetum parthenium*, *Vinca major*, *Salvia officinalis* and *Corydalis cava*, respectively.

The most concentrated samples were obtained in the case of *T. parthenium*. Comparison of the LC-MS/MS data with available literature [189] suggested that the two main BBB+ components were two sesquiterpene lactone type compounds, parthenolide (**1t**) and 11,13-dihydroparthenolide (**2t**), in a ca. 4.5 to 1 molar ratio. Even if NMR assignments were not available in PBS buffer or D₂O as solvents (in CDCl₃ see [190]) for these two compounds, the suggested structures could be easily confirmed. The relatively high sample concentration enabled the acquisition of a ¹H-PreSat, a 2D-

ZTOCSY and a HSQCAD spectrum during a 12-h measurement time. For the major component parthenolide (**1t**), these data enabled the complete ^1H and the almost complete ^{13}C NMR assignments.⁴¹ Although the ^{13}C NMR assignment was not possible for the minor component, the complete ^1H NMR assignment obtained proved that it was 11,13-dihydroparthenolide (**2t**).

Besides the low concentration, signal overlapping due to the presence of structurally similar compounds could burden the identification/confirmation of BBB+ components. This drawback was most pronounced for the *V. major* extract sample, where the two main components, vincamajine (**1v**) and majdine (**2v**), were present in comparable amounts. In the absence of heteronuclear correlation data, analysis of the collected Presat and ZTOCSY spectra enabled only the ^1H NMR assignments of the characteristic structural moieties (Table A5, Appendix). Nevertheless, in comparison with the literature [191, 192], these assignments confirmed the structures of the main components suggested by the LC-MS/MS analysis.

In the case of *S. officinalis* sample, LC-MS/MS data alone did not enable the unambiguous identification of the two main BBB+ components. Without a more detailed discussion, these data allowed only narrowing the most likely structures to a number of phenolic diterpene isomers (such as rosmanol, methyl carnosate, and isorosmanol), having the same molecular mass and similar fragmentation patterns [193]. Thus, for this extract, ^1H NMR measurement based on the collected ^1H -Presat and ZTOCSY spectra was necessary not only for the confirmation of a given structural proposition but for the unambiguous identification of the appropriate isomer. Based on the complete ^1H NMR assignment (Table A6, Appendix) including a coupling constant analysis the two main BBB+ components in this case were identified as epiisosmanol (**1so**) and methyl carnosate (**2so**). These data were in accordance with the NMR data reported for these components in MeOH as the solvent [194].

The least concentrated sample was the extract of *C. cava*. In this case, LC-MS/MS data suggested that the two major BBB+ compounds were tetrahydropalmatine (**1c**) and corydaline (**2c**), at ca. 14 and 3 μM concentrations, respectively. Unfortunately, heteronuclear correlation data could not be collected in an appropriate time scale. Nevertheless, identification of the two alkaloids could still be performed. Based on the ^1H -Presat and the two-dimensional homonuclear correlation data, complete ^1H NMR

assignments were obtained for the major component, tetrahydropalmatine (**1c**), while for corydaline (**2c**) only a partial ^1H assignment was possible (Table A7, Appendix). This was due to its low concentration, and to signal overlapping in the aliphatic region caused by its close structural similarity to the major component. Nevertheless, in combination with available literature [195], and the MS/MS data [196], corydaline (**2c**) was identified reliably. This could have been overcome by sample concentration (evaporation or the application of solid phase extraction).

4.5.7. Evaluating the CNS-activity of the identified BBB+ compounds

T. parthenium has been used as a prophylactic remedy for the treatment of migraine, and the anti-migraine effect is ascribed mainly to parthenolide (**1t**) [197, 198]. In contrast, pharmacokinetic data regarding the brain penetrability of the constituents of *T. parthenium* are lacking [199]. Regarding *V. major* and its constituents (**1v**, **2v**), interestingly no CNS-related bioactivity has been reported to date [200]. The BBB+ identified phenolic diterpenes (**1so**, **2so**) in *S. officinalis* may support a belief that sage extracts possess beneficial effects on memory disorders [201, 202]. In the case of *C. cava*, the reported sedative and analgesic effect [195], and also brain penetrability [203] of the alkaloids present (**1c**, **2c**) are in accordance with the present results.

5. Discussion

Since the methodological and phytochemical aspects of the results were discussed in detail in the previous chapter, general findings and novelties of the three case studies are summarized shortly in the following.

5.1. HPLC-based antioxidant activity profiling of the methanolic extract of *Artemisia gmelinii*

The applied off-line coupling of the DPPH assay to the LC-MS analysis allowed the effective identification/isolation of the most active constituents in the mixture. We have firstly identified chlorogenic acid (**2a**), 4-*O*-caffeoylquinic acid (**3a**), luteolin-7-*O*-glucoside (**5a**), apigenin-7-*O*-glucoside (**6a**), 3,5-*O*-dicaffeoylquinic acid (**7a**) and its ethyl ester derivative (**8a**) in *Artemisia gmelinii*.

In addition, the identified constituents of *A. gmelinii*, namely caffeic acid, chlorogenic acid, luteolin-7-*O*-glucoside (cynaroside), and caffeoyl derivatives were described previously as the major hepatoprotective compounds of artichoke (*Cynara scolymus* L.) [174]. This similitude suggests that the identified phenylpropanoids and flavonoids may contribute *via* their free radical scavenging potential to the pharmacological effect of *A. gmelinii*, especially in inflammatory liver conditions.

5.2. HPLC-based peroxynitrite scavenging activity profiling of *Salvia* spp.

In this study we reported the successful adoption of a colorimetric ONOO⁻ scavenging assay to LC-DAD. The assay parameters were optimized and validated with a model mixture of seventeen phenolic *Salvia* markers. A methanolic extract of *S. miltiorrhiza* was used successfully to demonstrate the applicability of the assay. The outstanding ONOO⁻ scavenging activities of salvianolic acid A (**12s**) and B (**10s**) are reported here for the first time. Our results indicated that the individual depletion kinetics of compounds measured in mixture correlates moderately with the individual scavenging activities. Thus the apparent degradation stoichiometry, measured in complex mixtures, is suitable for ranking the components by individual scavenging activities. In addition, the established LC method covers wide lipophilicity range of phenolic compounds but

separates the analogues effectively. It enables baseline separation of 18 phenolic compounds in less than 10.5 minutes, hereby could be used as an excellent starting point for chemical fingerprint studies of *Salvia* species. The proposed LC coupled antioxidant assay could be applied to rapid and efficient screening for natural antioxidants derived from alcoholic extracts of *Salvia* species. Since the way of detecting ONOO⁻ mediated effects differs from that of the tyrosine nitration assay [106], our LC based assay represents an alternative method from mechanistic point of view. The reported analytical approach is rapid and standardizable, thus well adoptable for other free radicals and plant species.

5.3. Blood-brain barrier (BBB) permeability screening and HPLC-based hit profiling

Recent approaches that endeavor to re-establish natural products in the modern, HTS-based lead discovery paradigm, have focused on early compound selection driven by physicochemical properties associated with lead- and drug-likeness [204, 205]. In parallel with this concept, the presented PAMPA-BBB assay-based protocol incorporates two absorption-limiting physicochemical parameters, namely, solubility and BBB permeability. By mean of the presented relevance, selectivity and purifying effect, it was concluded that the PAMPA-BBB assay is worthy of being integrated in a CNS-targeted HTS workflow in two steps (Fig. 34).

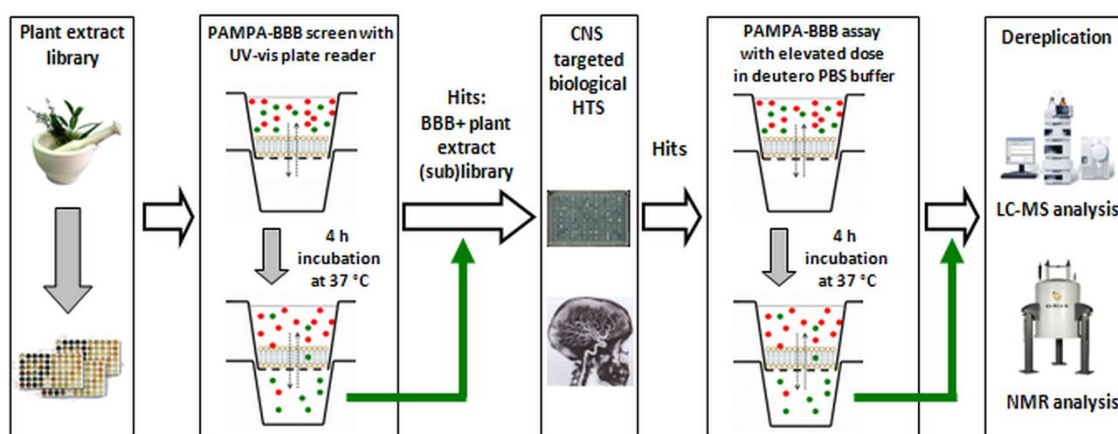


Figure 34. Flowchart of the proposed PAMPA-BBB assay/LC-MS/NMR screening cascade in a HTS-based CNS drug discovery environment.

In the first step, after collecting the plant extract hits from a simple screen, the PAMPA-BBB assay affords a BBB+ NP screening set (sub-library), enriched in compounds with moderate to high solubility and brain penetrability. Moreover, as the LC-MS analysis revealed that the resulted concentrations of major BBB+ compounds ranged in the 10 to 100 μM (typical screen concentration of HTS), these samples could be transferred directly to an HTS campaign. In the second step, after screening this set in a CNS-targeted HTS, dereplication of the resulting plant extract leads (primarily major components) is also feasible using the PAMPA-BBB assay without the need for lengthy isolation procedures. It must be noted here that, cell-based assays would be inadequate for this purpose under such conditions (i.e., conducted in deuterated milieu with elevated dose of multi-component samples). Testing the active transport potential of PAMPA-BBB positive, isolated, and biologically validated leads is, however, recommended at the mid-to-late stage of drug discovery. Finally, beyond the methodological aspects, the present study has provided important *in vitro* information regarding the brain penetrability of several pharmacologically active NPs.

6. Conclusions

Today's drug discovery relies basically on the HTS-based approach and operates at an accelerated pace. To meet the demand of this industrial environment, innovative methods focusing on the improvement and acceleration of the NP-based lead generation have emerged and been implemented recently. Among those, HPLC-coupled assays used for both chemical and biological profiling of complex NP extracts have shown potential to significantly increase the efficiency of or even to fully substitute time-consuming bioactivity-guided fractionation procedures. The essence and simultaneously the greatest challenge in the development of such HPLC-based profiling assays, beyond instrumentation issues, is the valid and efficient interfacing of biological data with chemo-analytical information.

The work described in this thesis is a contribution focusing on the methodological improvement of two distinctive, but therapeutically highly relevant NP research areas.

In the first part, a cytotoxicity and an antioxidant (DPPH) screening of a plant extract library were successfully designed and performed. It was found that more than the half of the library (57%) possessed cytotoxic activity, whereas the percent of samples with considerable antioxidant activity was only 5.7%. Moreover, we demonstrated that both the cytotoxic and the antioxidant activity were significantly dependent on the type of the solvent extraction procedure: samples extracted with chloroform were twice as likely to show cytotoxicity than samples originated from alcoholic extraction, whereas radical scavenging activity was more pronounced among samples extracted with methanol. These general findings underpin retrospectively the impact of targeted extraction procedures on the plant extract library design.

Afterwards, in course of a case study, a DPPH-HPLC method was developed for the antioxidant-activity guided phytochemical investigation of a methanolic plant extract hit, namely *Artemisia gmelinii*.

Methodological conclusions and novel findings: It was demonstrated that the off-line coupling of the DPPH assay with the LC method enabled the rapid and reliable identification of the free radical scavenger molecules in the mixture. This proved to be a

key advantage, since after the dereplication of 6 major constituents by LC-MS, the preparative HPLC purification was only targeted toward the isolation of the two most active compounds (3,5-*O*-dicaffeoylquinic acid (**7a**) and ethyl-3,5-*O*-dicaffeoylquinic acid (**8a**)). It must be noted, however, that the structure elucidation of the isolated DCQAs turned out to be an unexpectedly difficult task due to literature ambiguities.

Phytochemical and pharmacological conclusions and novel findings: Out of the eight identified compounds (**1a-8a**) six, namely chlorogenic acid (**2a**), 4-*O*-caffeoylquinic acid (**3a**), luteolin-7-*O*-glucoside (**5a**), apigenin-7-*O*-glucoside (**6a**), and the two DCQAs (**7a**, **8a**) were first described in *A. gmelinii*. Moreover, based on the high degree of phytochemical similitude with major hepatoprotective compounds of artichoke, it was speculated that the identified phenylpropanoids and flavonoids may confirm by their antioxidant potential the ethnopharmacological usage of *A. gmelinii* in inflammatory liver conditions.

Next, the same off-line coupling concept was realized in the case of another radical species. The colorimetric pyrogallol red bleaching assay used for ONOO⁻ scavenging assessment was successfully adopted for HPLC.

Methodological conclusions and novel findings: We proved the theory by a thorough validation study that upon reaction with ONOO⁻, the peak areas of compounds in complex mixtures with radical scavenging potential will significantly decrease or disappear in the chromatograms. Aspecific degradation of carnosol (**17s**) represented the inherent limitation of the assay. Thus, it was demonstrated that the developed assay enabled simultaneously and reliably the rapid chemical characterization and the ONOO⁻ scavenging activity profiling of alcoholic extracts of *Salvia* species.

Phytochemical and pharmacological conclusions and novel findings: By studying the ONOO⁻ scavenging activity of 17 phenoloid marker compounds of the genus *Salvia*, it was found that gallic acid (**1s**), caffeic acid (**3s**), rosmarinic acid (**9s**), salvianolic acid B (**10s**), quercetin (**11s**), salvianolic acid A (**12s**), and kaempferol (**14s**) possessed outstanding activity against ONOO⁻. Moreover, application of the developed assay on the methanolic extract of *S. miltiorrhiza* revealed that basically the phenylpropanoid constituents (**9s**, **10s**, **12s**) were responsible for the significant ONOO⁻ scavenging activity of this widely used medicinal herb.

In the second part of our work, to narrow the gap between NP research and the demand of early stage CNS drug discovery, applicability of the PAMPA-BBB assay to NPs and plant extracts was thoroughly demonstrated.

Methodological conclusions and novel findings: It was found that the PAMPA-BBB assay preserved its predictive power in the case of NPs and provided high phytochemical selectivity, which enabled its use as a unique filtering tool in terms of selecting brain penetrable compounds from plant extracts. We took advantage of the single mechanism-based (passive diffusion) as well as the *in vitro* nature of the PAMPA-BBB assay: it was demonstrated that simple modifications in the assay design (i.e., performed in deuterated milieu with an elevated dose of multicomponent extracts) allowed the direct (at-line) use of PAMPA-BBB filtered samples in a dereplication process, as performed by NMR and LC-MS. Finally, it was concluded that the developed PAMPA-BBB/LC-MS/NMR cascade is worthy of being integrated in a HTS-based, NP-utilizing CNS drug discovery environment (see Fig. 34).

Phytochemical and pharmacological conclusions and novel findings: By studying the effective BBB permeability profile of major phytochemical compound classes, it was revealed that, in accordance with basic concepts, glycosides and carboxylic acids were unable to pass across lipid bilayers by passive diffusion, whereas representative compounds of flavonoids (as aglycones), alkaloids, terpenes and coumarins showed moderate or considerable BBB permeability potential. Moreover, our work provided important *in vitro* evidences regarding the brain penetrability of the pharmacologically active constituents of *T. parthenium*, *V. major*, *S. officinalis*, and *C. cava*.

Based on the resolution and multi-dimensional information content provided by the presented HPLC-based profiling assays, we conclude that the marriage of advanced separation and spectroscopic techniques to robust bioassays is a viable and powerful approach to NP-based lead generation. In addition, the developed profiling assays could be superior for the quality, efficacy and safety assessment of medicinal plant extracts and herbal formulas. Finally, we believe that these novel approaches will be gradually naturalized also in the mainstream drug discovery.

7. Summary

In the NP-based drug discovery, the rapid and reliable identification of bioactive compounds in complex mixtures presents a key step and a great challenge as well. Coupled analytical approaches, integrating modern spectroscopic and separation techniques with robust bioassays could represent an efficient solution for this issue. In the first part of our work, the cytotoxicity and the antioxidant (DPPH) HTS of the plant extract library (N=4400) of Gedeon Richter Plc. were designed and successfully performed. It was found that the apolar samples prepared by chloroformic extraction had significantly higher potential to show cytotoxic activity than polar samples originated from alcoholic extraction. In contrast, radical scavenging activity were more pronounced among polar samples. Afterwards, the phytochemically less characterized extract of *Artemisia gmelinii* was selected from non-cytotoxic antioxidant hits and analyzed by an off-line coupled DPPH-HPLC assay. It was demonstrated by mean of the rapid and efficient HPLC-coupled assay, that caffeic acid derivatives were responsible for the experienced outstanding radical scavenging activity of the sample. For further analysis of antioxidant hits emerged from the genus *Salvia*, the ONOO⁻ scavenging assay based on pyrogallol red bleaching was successfully adopted for HPLC. Efficiency and validity of the developed off-line ONOO⁻-HPLC assay were deduced from the detailed analysis of a marker compound mixture of 17 phenoloids and of the extract of *Salvia miltiorrhiza*, respectively. In the second part of our work, applicability of the PAMPA-BBB system to plant extracts was thoroughly studied. It was found that the PAMPA-BBB assay preserved its predictive power in the case of NPs and provided high phytochemical selectivity. In addition, it was demonstrated that conducting the permeability assay in deuterated buffer with elevated sample doses could result in a filtrate, which was directly suitable for the dereplication of major brain penetrable compounds of the extracts, as performed by LC-MS and NMR. This perception of us was exemplified with the extracts of four hits emerged from the PAMPA-BBB screening of the plant extract library.

8. Összefoglalás

A természetes anyagokból kiinduló gyógyszerkutatás folyamatában, a hatásosnak talált komplex kivonatok vizsgálata során kulcslépés és egyúttal jelentős kihívás az adott biológiai hatásért felelős komponens(ek) gyors és megbízható azonosítása. Erre a célra hatékony megoldást kínálnak a modern elválasztástechnikákat, illetve szerkezetazonosítási eljárásokat biokémiai tesztekkel ötvöző, úgynevezett kapcsolt analitikai megközelítések. Munkánk első felében a Richter Gedeon Nyrt. növényi kivonat gyűjteményének (N=4400) nagy áteresztőképességű citotoxikus, illetve antioxidáns (DPPH) hatásra irányuló szűrővizsgálatát terveztük meg és végeztük el. Kimutattuk, hogy a kloroformos kivonattal készült (apoláros) minták esetén szignifikánsan nagyobb az esélye citotoxikus komponensek jelenlétének, mint a metanolos kivonattal nyert poláros minták esetén. Az antioxidáns hatás ezzel szemben jellemzően a poláros mintákhoz volt köthető. Ezt követően, a fokozott antioxidáns hatású, nem citotoxikus kivonatok (találatok) közül a fitokémiaileg kevésbé feltárt *Artemisia gmelinii* kivonatát elemeztük off-line módon kapcsolt DPPH-HPLC technikával. A HPLC-vel kapcsolt tesztrendszer révén gyorsan és megbízhatóan sikerült kimutatnunk, hogy különböző kávésav származékok feleltek a minta szabadgyök-fogó sajátosságáért. Az antioxidáns találatok közül a *Salvia* nemzetségbe tartozó kivonatok további vizsgálatának érdekében, a pirogallol vörös színkioltásán alapuló, ONOO⁻ semlegesítését mérő tesztet ültettük át HPLC-re. A kialakított off-line ONOO⁻-HPLC tesztrendszer hatékonyságát és validitását 17 fenoloid markervegyületből álló mesterséges keverék, illetve a *Salvia miltiorrhiza* kivonatának részletes elemzésével bizonyítottuk. Munkánk második felében a vér-agy gát permeabilitás mérésére szolgáló *in vitro* PAMPA-BBB tesztrendszer növényi kivonatokon történő alkalmazhatóságát vizsgáltuk. Bizonyítottuk, hogy a PAMPA-BBB teszt természetes anyagok esetén is megőrzi prediktív erejét, és jelentős szelektivitást mutat fitokémiai értelemben. Ezen felül kimutattuk, hogy a permeabilitási tesztet deuterált pufferben, megnövelt kivonat-koncentrációval végezve, LC-MS és NMR vizsgálatra közvetlenül alkalmas szűrlet nyerhető, amelyben a fő, potenciálisan agyi penetrációval bíró komponensek azonosíthatóvá válnak. E felismerésünket a kivonat gyűjtemény PAMPA-BBB szűrésekor talált 4 db aktív minta példáján mutattuk be.

9. References

- [1] Butler MS. (2004) The role of natural product chemistry in drug discovery. *J Nat Prod*, 67: 2141–2153.
- [2] Koehn FE, Carter GT. (2005) The evolving role of natural products in drug discovery. *Nat Rev Drug Discov*, 4: 206–220.
- [3] Lam KS. (2007) New aspects of natural products in drug discovery. *Trends Microbiol*, 15: 279–289.
- [4] Harvey AL. (2008) Natural products in drug discovery. *Drug Discov Today*, 13: 894–901.
- [5] Appendino G, Fontana G, Pollastro F. Natural products drug discovery. In: Mander L, Lui H-W (eds.), *Comprehensive Natural Products II; Chemistry and Biology*. Elsevier, Oxford, 2010: 205–236.
- [6] Burrill & Company. Analysis for Pharmaceutical Research and Manufacturers of America; PhRMA Annual Member Survey 2010 (Washington, DC: PhRMA, 2010)
- [7] Pammolli F, Magazzini L, Riccaboni M. (2011) The productivity crisis in pharmaceutical R&D. *Nat Rev Drug Discov*, 10: 428–438.
- [8] Solecki RS. (1975) Shanidar IV, a Neanderthal flower burial in northern Iraq. *Science*, 190: 880–881.
- [9] Newmann DJ, Cragg GM, Snader KM. (2000) The influence of natural products upon drug discovery. *Nat Prod Rep* 17: 215–234.
- [10] Newman DJ, Cragg GM. (2012) Natural products as sources of new drugs over the 30 years from 1981 to 2010. *J Nat Prod*, 75: 311–335.
- [11] Newman DJ, Cragg GM, Snader KM. (2003) Natural products as sources of new drugs over the period 1981-2002. *J Nat Prod*, 66: 1022–1037.
- [12] Avery VM, Camp D, Carroll AR, Jenkins ID, Quinn RJ. The identification of bioactive natural products by high throughput screening (HTS). In: Mander L, Lui H-W (eds.), *Comprehensive Natural Products II, Chemistry and Biology*. Elsevier, Oxford, 2010: 177–203.
- [13] Kingston DGI. (2011) Modern natural products drug discovery and its relevance to biodiversity conservation. *J Nat Prod*, 74: 496–511.

- [14] Zhu Y, Zhang Z, Zhang M, Mais DE, Wang M-W. (2010) High throughput screening for bioactive components from Traditional Chinese Medicine. *Comb Chem High T Scr*, 13: 837–848.
- [15] Arve L, Voigt T, Waldmann H. (2006) Charting biological and chemical space: PSSC and SCONP as guiding principles for the development of compound collections based on natural product scaffolds. *QSAR Comb Sci*, 25: 449–456.
- [16] Wess G, Urmann M, Sickenberger M. (2001) Medicinal chemistry: challenges and opportunities. *Angew Chem Int Ed Engl*, 40: 3341–3350.
- [17] Feher M, Schmidt JM. (2003) Property distributions: differences between drugs, natural products, and molecules from combinatorial chemistry. *J Chem Inf Comput Sci*, 43: 218–227.
- [18] Lachance H, Wetzel S, Kumar K, Waldmann H. (2012) Charting, navigating, and populating natural product chemical space for drug discovery. *J Med Chem*, 55: 5989–6001.
- [19] Quinn RJ, Carroll AR, Pham NB, Baron P, Palframan ME, Suraweera L, Pierens GK, Muresan S. (2008) Developing a drug-like natural product library. *J Nat Prod*, 71: 464–468.
- [20] Evans BE, Rittle KE, Bock MG, DiPardo RM, Freidinger RM, Whitter WL, Lundell GF, Veber DF, Anderson PS, Chang RSL, Lotti VJ, Cerino DJ, Chen TB, Kling PJ, Kunkel KA, Springer JP, Hirshfield J. (1988) Methods for drug discovery: development of potent, selective, orally effective cholecystokinin antagonists. *J Med Chem*, 31: 2235–2246.
- [21] Strege MA. (1999) High-performance liquid chromatographic-electrospray ionization mass spectrometric analyses for the integration of natural products with modern high-throughput screening. *J Chromatogr B*, 725: 67–78.
- [22] Bax A, Aszalos A, Dinya Z, Sudo K. (1986) Structure elucidation of the antibiotic desertomycin through the use of new two-dimensional NMR techniques. *J Am Chem Soc*, 108: 8056–8063.
- [23] Olson DL, Norcross JL, O’Neil-Johnson M, Molitor PF, Detlefsen DJ, Wilson AG, Peck TL. (2004) Microflow NMR: concepts and capabilities. *Anal Chem*, 76: 2966–2974.

- [24] Breton RC, Reynolds WF. (2013) Using NMR to identify and characterize natural products. *Nat Prod Rep*, 30: 501–524.
- [25] Schmid I, Sattler I, Grabley S, Thiericke R. (1999) Natural products in high throughput screening: automated high-quality sample preparation. *J Biomol Screen*, 4: 15–25.
- [26] Bindseil KU, Jakupovic J, Wolf D, Lavayre J, Leboul J, van der Pyl D. (2001) Pure compound libraries; a new perspective for natural product based drug discovery. *Drug Discov Today* 6: 840–847.
- [27] Tu Y, Jeffries C, Ruan H, Nelson C, Smithson D, Shelat AA, Brown KM, Li X-C, Hester JP, Smillie T, Khan IA, Walker L, Guy K, Yan B. (2010) Automated high-throughput system to fractionate plant natural products for drug discovery. *J Nat Prod*, 73: 751–754.
- [28] Avery VM, Camp D, Carroll AR, Jenkins ID, Quinn RJ. The identification of bioactive natural products by high throughput screening (HTS). In: Mander L, Lui H-W (eds.), *Comprehensive Natural Products II; Chemistry and Biology*. Elsevier, Oxford, 2010: 190.
- [29] Danz H, Stoyanova S, Wippich P, Brattstrom A, Hamburger M. (2001) Identification and isolation of the cyclooxygenase-2 inhibitory principle in *Isatis tinctoria*. *Planta Med*, 67: 411–416.
- [30] Dittmann K, Riese U, Hamburger M. (2004) HPLC-based bioactivity profiling of plant extracts: a kinetic assay for the identification of monoamine oxidase-A inhibitors using human recombinant monoamine oxidase-A. *Phytochemistry*, 65: 2885–2891.
- [31] Zaugg J, Eickmeier E, Rueda DC, Hering S, Hamburger M. (2011) HPLC-based activity profiling of *Angelica pubescens* roots for new positive GABA_A receptor modulators in *Xenopus oocytes*. *Fitoterapia*, 82: 434–440.
- [32] Hou Y, Cao X, Dong L, Wang L, Cheng B, Shi Q, Luo X, Bai G. (2012) Bioactivity-based liquid chromatography-coupled electrospray ionization tandem ion trap/time of flight mass spectrometry for β_2 AR agonist identification in alkaloidal extract of *Alstonia scholaris*. *J Chromatogr A*, 1227: 203–209.
- [33] Yu F, Kong L, Zou H, Lei X. (2010) Progress on the screening and analysis of bioactive compounds in Traditional Chinese Medicines by biological fingerprinting analysis. *Comb Chem High T Scr*, 13: 855–868.

- [34] Xu N, Yang H, Cui M, Wan C, Liu S. (2012) High-performance liquid chromatography-electrospray ionization-mass spectrometry ligand fishing assay: a method for screening triplex DNA binders from natural plant extracts. *Anal Chem*, 84: 2562–2568.
- [35] Guo M, Su X, Kong L, Li X, Zou H. (2006) Characterization of interaction property of multicomponents in Chinese herb with protein microdialysis combined with HPLC. *Anal Chim Acta*, 556: 183–188.
- [36] Su XY, Kong L, Li X, Chen XG, Guo M, Zou HF. (2005) Screening and analysis of bioactive compounds with biofingerprinting chromatogram analysis of traditional Chinese medicines targeting DNA by microdialysis/HPLC. *J Chromatogr A*, 1076: 118–126.
- [37] Lei X, Kong L, Su X, Guo M, Zou H. (2008) Biological fingerprinting analysis of interaction between taxoids in taxus and microtubule protein by microdialysis coupled with high-performance liquid chromatography/mass spectrometry for screening antimicrotubule agents. *Chem Res Chinese Univ*, 24: 411–419.
- [38] Maciuk A, Moaddel R, Haginaka J, Wainer IW. (2008) Screening of tobacco smoke condensate for nicotinic acetylcholine receptor ligands using cellular membrane affinity chromatography columns and missing peak chromatography. *J Pharm Biomed Anal*, 48: 238–246.
- [39] Mao X, Kong L, Luo Q, Li X, Zou H. (2002) Screening and analysis of permeable compounds in *Radix Angelica Sinensis* with immobilized liposome chromatography. *J Chromatogr B*, 779: 331–339.
- [40] Wang HL, Zou HF, Ni JY, Kong L, Gao S, Guo BC. (2000) Fractionation and analysis of *Artemisia capillaries Thunb.* by affinity chromatography with human serum albumin as stationary phase. *J Chromatogr A*, 870: 501–510.
- [41] Wang L, Ren J, Sun M, Wang S. (2010) A combined cell membrane chromatography and online HPLC/MS method for screening compounds from *Radix Caulophylli* acting on the human α_{1A} -adrenoceptor. *J Pharm Biomed Anal*, 51: 1032–1036.
- [42] Shi SY, Zhou HH, Zhang YP, Jiang XY, Chen XQ, Huang KL. (2009) Coupling HPLC to on-line, post-column (bio)chemical assays for high-resolution screening of bioactive compounds from complex mixtures. *Trends Anal Chem*, 28: 865–877.

- [43] Kool J, Giera M, Irth H, Niessen WMA. (2011) Advances in mass spectrometry-based post-column bioaffinity profiling of mixtures. *Anal Bioanal Chem*, 399: 2655–2668.
- [44] Niederländer HAG, van Beek TA, Bartasiute A, Koleva II. (2008) Antioxidant activity assays on-line with liquid chromatography. *J Chromatogr A*, 1210: 121–134.
- [45] Malherbe CJ, de Beer D, Joubert E. (2012) Development of on-line high performance liquid chromatography (HPLC)-biochemical detection methods as tools in the identification of bioactives. *Int J Mol Sci*, 13: 3101–3133.
- [46] Moaddel R, Wainer IW. (2009) The preparation and development of cellular membrane affinity chromatography columns. *Nat Protoc*, 4: 197–205.
- [47] Wolfender JL, Queiroz EF, Hostettmann K. Development and application of LC-NMR techniques to the identification of bioactive natural products. In: Colegate SM, Molyneux RJ (eds.): *Bioactive Natural Products - Detection, Isolation, and Structural Determination*. CRC Press/Taylor & Francis, Boca Raton, 2008: 143–190.
- [48] Funari CS, Eugster PJ, Martel S, Carrupt PA, Wolfender JL, Silva DH. (2012) High resolution ultra high pressure liquid chromatography-time-of-flight mass spectrometry dereplication strategy for the metabolite profiling of Brazilian *Lippia* species. *J Chromatogr A*, 1259: 167–178.
- [49] Wu H, Guo J, Chen S, Liu X, Zhou Y, Zhang X, Xu X. (2013) Recent developments in qualitative and quantitative analysis of phytochemical constituents and their metabolites using liquid chromatography-mass spectrometry. *J Pharm Biomed Anal*, 72: 267–291.
- [50] <http://www.napralert.org>
- [51] <http://dnp.chemnetbase.com>
- [52] <http://www.sigmaaldrich.com/life-science/nutrition-research/learning-center/plant-profiler>
- [53] Raudonis R, Raudone L, Jakstas V, Janulis V. (2012) Comparative evaluation of post-column free radical scavenging and ferric reducing antioxidant power assays for screening of antioxidants in strawberries. *J Chromatogr A*, 1233: 8–15.
- [54] Potterat O, Hamburger M. (2013) Concepts and technologies for tracking bioactive compounds in natural product extracts: generation of libraries, and hyphenation of analytical processes with bioassays. *Nat Prod Rep*, 30: 546–564.

- [55] Bachi A, Dalle-Donne I, Scaloni A. (2013) Redox proteomics: chemical principles, methodological approaches and biological/biomedical promises. *Chem Rev*, 113: 596–698.
- [56] Halliwell B, Gutteridge JMC. *Free radicals in biology and medicine*. Oxford University Press, Oxford, 1999.
- [57] Valko M, Leibfritz D, Moncol J, Cronin MT, Mazur M, Telser J. (2007) Free radicals and antioxidants in normal physiological functions and human disease. *Int J Biochem Cell Biol*, 39: 44–84.
- [58] Halliwell B. (2007) Oxidative stress and cancer: have we moved forward? *Biochem J*, 401: 1–11.
- [59] Eberhardt MK. *Reactive oxygen metabolites: chemistry and medical consequences*. CRC Press, Boca Raton, 2001.
- [60] Giacco F, Brownlee M. (2010) Oxidative stress and diabetic complications. *Circ Res*, 107: 1058–1070.
- [61] Bonomini F, Tengattini S, Fabiano A, Bianchi R, Rezzani R. (2008) Atherosclerosis and oxidative stress. *Histol Histopathol*, 23: 381–390.
- [62] Li X-J, Gao N, Zhang H-Y. (2009) Natural inspirations for antioxidant drug discovery. *Drug Discov Today*, 14: 910–912.
- [63] Giles GI, Fry FH, Tasker KM, Holme AL, Peers C, Green KN, Klotz L-O, Sies H, Jacob C. (2003) Evaluation of sulfur, selenium and tellurium catalysts with antioxidant potential. *Org Biomol Chem*, 1: 4317–4322.
- [64] Balogh GT, Vukics K, Könczöl Á, Kis-Varga Á, Gere A, Fischer J. (2005) Nitron derivatives of trolox as neuroprotective agents. *Bioorg Med Chem Lett*, 15: 3012–3015.
- [65] Lee H, Lee K, Jung JK, Cho J, Theodorakis EA. (2005) Synthesis and evaluation of 6-hydroxy-7-methoxy-4-chromanone- and chroman-2-carboxamides as antioxidants. *Bioorg Med Chem Lett*, 15: 2745–2748.
- [66] Sárbu C, Casoni D. (2013) Comprehensive evaluation of biogenic amines and related drugs' antiradical activity using reactive 2,2-diphenyl-1-picrylhydrazyl (DPPH) radical. *Centr Eur J Chem*, 11: 679–688.
- [67] Betigeri S, Thakur A, Raghavan K. (2005) Use of 2,2'-azobis(2-amidinopropane) dihydrochloride as a reagent tool for evaluation of oxidative stability of drugs. *Pharm Res*, 22: 310–317.

- [68] Lee SK, Mbwapbo ZH, Chung H, Luyengi L, Gamez EJ, Mehta RG, Kinghorn AD, Pezzuto JM. (1998) Evaluation of the antioxidant potential of natural products. *Comb Chem High Throughput Screen*, 1: 35–46.
- [69] Maldonado PD, Rivero-Cruz I, Mata R, Pedraza-Chaverri J. (2005) Antioxidant activity of A-type proanthocyanidins from *Geranium niveum* (Geraniaceae). *J Agric Food Chem*, 23: 1996–2001.
- [70] Chen CH, Shaw CY, Chen CC, Tsai YC. (2002) 2,3,4-Trimethyl-5,7-dihydroxy-2,3-dihydrobenzofuran, a novel antioxidant, from *Penicillium citrinum* F5. *J Nat Prod*, 65: 740–741.
- [71] Papas AM. Antioxidant status, diet, nutrition, and health. CRC Press, Boca Raton, 1999.
- [72] Silva, CG, Herdeiro RS, Mathias CJ, Panek AD, Silveira CS, Rodrigues VP, Rennó MN, Falcao DQ, Cerqueira DM, Minto ABM, Nogueira FLP, Quaresma CH, Silva JFM, Menezes FS, Eleutherio ECA. (2005) Evaluation of antioxidant activity of Brazilian plants. *Pharmacol Res*, 52: 229–233.
- [73] Conforti F, Sosa S, Marrelli M, Menichini F, Statti GA, Uzunov D, Tubaro A, Menichini F, Loggia RD. (2008) In vivo anti-inflammatory and in vitro antioxidant activities of Mediterranean dietary plants. *J Ethnopharmacol*, 116: 144–151.
- [74] Fenglin H, Ruili L, Bao H, Liang M. (2004) Free radical scavenging activity of extracts prepared from fresh leaves of selected Chinese medicinal plants. *Fitoterapia*, 75: 14–23.
- [75] Trouillas P, Calliste C-A, Allais D-P, Simon A, Marfak A, Delage C, Duroux J-L. (2003) Antioxidant, antiinflammatory and antiproliferative properties of sixteen water plant extracts used in the Limousin countryside as herbal teas. *Food Chem*, 80: 399–407.
- [76] Katalinic V, Milos M, Kulisic T, Jukic M. (2006) Screening of 70 medicinal plant extracts for antioxidant capacity and total phenols. *Food Chem*, 94: 550–557.
- [77] Kumari A, Kakkar P. (2008) Screening of antioxidant potential of selected barks of Indian medicinal plants by multiple in vitro assays. *Biomed Environ Sci*, 21: 24–29.
- [78] Goldsmith S, Renn K. (1922) *Chem Ber*, 55: 628–643.
- [79] Blois MS. (1958) Antioxidant determination by the use of a stable free radical. *Nature*, 181: 1199–1200.

- [80] Kedare SB, Singh RP. (2011) Genesis and development of DPPH method of antioxidant assay. *J Food Sci Technol*, 48: 412–422.
- [81] Menichetti S, Aversa MC, Cimino F, Contini A, Viglianisi C, Tomaino A. (2005) Synthesis and "double-faced" antioxidant activity of polyhydroxylated 4-thiaflavans. *Org Biomol Chem*, 3: 3066–3072.
- [82] Gong J, Huang K, Wang F, Yang L, Feng Y, Li H, Li X, Zeng S, Wu X, Stöckigt J, Zhao Y, Qu J. (2009) Preparation of two sets of 5,6,7-trioxygenated dihydroflavonol derivatives as free radical scavengers and neuronal cell protectors to oxidative damage. *Bioorg Med Chem*, 17: 3414–3425.
- [83] Glavind J, Holmer G. (1967) Thin-layer chromatographic determination of antioxidants by the stable free radical α, α' -diphenyl- β -picrylhydrazyl. *J Am Oil Chem Soc*, 44: 539–542.
- [84] Cieśla Ł, Kryszewski J, Stochmal A, Oleszek W, Waksmundzka-Hajnos M. (2012) Approach to develop a standardized TLC-DPPH• test for assessing free radical scavenging properties of selected phenolic compounds. *J Pharm Biomed Anal*, 70:126–135.
- [85] Yamaguchi T, Takamura H, Matoba T, Terao J. (1998) HPLC method for evaluation of the free radical-scavenging activity of foods by using 1,1-diphenyl-2-picrylhydrazyl. *Biosci Biotechnol Biochem*, 62: 1201–1204.
- [86] Boudier A, Tournebize J, Bartosz G, El Hani S, Bengueddour R, Sapin-Minet A, Leroy P. (2012) High-performance liquid chromatographic method to evaluate the hydrogen atom transfer during reaction between 1,1-diphenyl-2-picryl-hydrazyl radical and antioxidants. *Anal Chim Acta*, 711: 97–106.
- [87] Tang D, Li HJ, Chen J, Guo CW, Li P. (2008) Rapid and simple method for screening of natural antioxidants from Chinese herb *Flos Lonicerae Japonicae* by DPPH-HPLC-DAD-TOF/MS. *J Sep Sci*, 31: 3519–3526.
- [88] Helmja K, Vaher M, Püssa T, Kaljurand M. (2009) Analysis of the stable free radical scavenging capability of artificial polyphenol mixtures and plant extracts by capillary electrophoresis and liquid chromatography-diode array detection-tandem mass spectrometry. *J Chromatogr A*, 1216: 2417–2423.

- [89] Koleva II, Niederländer HA, van Beek TA. (2000) An on-line HPLC method for detection of radical scavenging compounds in complex mixtures. *Anal Chem*, 72: 2323–2328.
- [90] Niederländer HA, van Beek TA, Bartasiute A, Koleva II. (2008) Antioxidant activity assays on-line with liquid chromatography. *J Chromatogr A*, 1210: 121–134.
- [91] Nuengchamnong N, de Jong CF, Bruyneel B, Niessen WM, Irth H, Ingkaninan K. (2005) HPLC coupled on-line to ESI-MS and a DPPH-based assay for the rapid identification of anti-oxidants in *Butea superba*. *Phytochem Anal*, 16: 422–428.
- [92] Bandoniene D, Murkovic M. (2002) The detection of radical scavenging compounds in crude extract of borage (*Borago officinalis* L.) by using an on-line HPLC-DPPH method. *J Biochem Biophys Methods*, 53: 45–49.
- [93] Niu Y, Yin L, Luo S, Dong J, Wang H, Hashi Y, Chen S. (2013) Identification of the anti-oxidants in *Flos Chrysanthemi* by HPLC-DAD-ESI/MS⁽ⁿ⁾ and HPLC coupled with a post-column derivatisation system. *Phytochem Anal*, 24: 59–68.
- [94] Zhang YP, Shi SY, Xiong X, Chen XQ, Peng MJ. (2012) Comparative evaluation of three methods based on high-performance liquid chromatography analysis combined with a 2,2'-diphenyl-1-picrylhydrazyl assay for the rapid screening of antioxidants from *Pueraria lobata* flowers. *Anal Bioanal Chem*, 402: 2965–2976.
- [95] Zhang Y, Shi S, Wang Y, Huang K. (2011) Target-guided isolation and purification of antioxidants from *Selaginella sinensis* by offline coupling of DPPH-HPLC and HSCCC experiments. *J Chromatogr B Analyt Technol Biomed Life Sci*, 879: 191–196.
- [96] Shi S, Zhou H, Zhang Y, Huang K. (2008) Hyphenated HSCCC-DPPH for rapid preparative isolation and screening of antioxidants from *Selaginella moellendorffii*. *Chromatographia*, 68: 173–178.
- [97] Shi S, Ma Y, Zhang Y, Liu L, Liu Q, Peng M, Xiong X. (2012) Systematic separation and purification of 18 antioxidants from *Pueraria lobata* flower using HSCCC target-guided by DPPH-HPLC experiment. *Sep Purif Technol*, 89: 225–233.
- [98] Dai X, Huang Q, Zhou B, Gong Z, Liu Z, Shi S. (2013) Preparative isolation and purification of seven main antioxidants from *Eucommia ulmoides* Oliv. (Du-zhong) leaves using HSCCC guided by DPPH-HPLC experiment. *Food Chem*, 139:563–570.

- [99] Hu C, Kitts DD. (2005) Dandelion (*Taraxacum officinale*) flower extract suppresses both reactive oxygen species and nitric oxide and prevents lipid oxidation in vitro. *Phytomed*, 12: 588–597.
- [100] Pacher P, Beckman JS, Liaudet L. (2007) Nitric oxide and peroxynitrite in health and disease. *Physiol Rev*, 87: 315–424.
- [101] Szabó C, Ischiropoulos H, Radi R. (2007) Peroxynitrite: biochemistry, pathophysiology and development of therapeutics. *Nat Rev Drug Discov*, 6: 662–680.
- [102] Pietraforte D, Minetti M. (1997) Direct ESR detection of peroxynitrite-induced tyrosine-centred protein radicals in human blood plasma. *Biochem J*, 325: 675–684.
- [103] Radi R, Peluffo G, Alvarez MN, Naviliat M, Cayota A. (2001) Unraveling peroxynitrite formation in biological systems. *Free Radic Biol Med*, 30: 463–488.
- [104] Sun ZN, Wang HL, Liu FQ, Chen Y, Tam PK, Yang D. (2009) BODIPY-based fluorescent probe for peroxynitrite detection and imaging in living cells. *Org Lett*, 11: 1887–1890.
- [105] Sieracki NA, Gantner BN, Mao M, Horner JH, Ye RD, Malik AB, Newcomb ME, Bonini MG. (2013) Bioluminescent detection of peroxynitrite with a boronic acid-caged luciferin. *Free Radic Biol Med*, 61C: 40–50.
- [106] van der Vliet A, O'Neill CA, Halliwell B, Cross CE, Kaur H. (1994) Aromatic hydroxylation and nitration of phenylalanine and tyrosine by peroxynitrite. Evidence for hydroxyl radical production from peroxynitrite. *FEBS Lett*, 339: 89–92.
- [107] Pannala AS, Razaq R, Halliwell B, Singh S, Rice-Evans CA. (1998) Inhibition of peroxynitrite dependent tyrosine nitration by hydroxycinnamates: nitration or electron donation? *Free Radic Biol Med*, 24: 594–606.
- [108] Hughes MN, Nicklin HG. (1968) The chemistry of pernitrites. Part I. Kinetics of decomposition of pernitrous acid. *J Chem Soc A*, 450–452.
- [109] Kooy NW, Royall JA, Ischiropoulos H, Beckman JS. (1994) Peroxynitrite-mediated oxidation of dihydrorhodamine 123. *Free Radic Biol Med*, 16: 149–156.
- [110] Balavoine GGA, Geletii YV. (1999) Peroxynitrite Scavenging by Different Antioxidants. Part I: Convenient Assay. *Nitric Oxide*, 3: 40–54.
- [111] Robaszkiewicz A, Bartosz G. (2009) Estimation of antioxidant capacity against pathophysiologically relevant oxidants using Pyrogallol Red. *Biochem Biophys Res Commun*, 390: 659–661.

- [112] Pannala AS, Singh S, Rice-Evans C. [19] Flavonoids as peroxynitrite scavengers in vitro. In: Methods in enzymology. Vol. 299. Academic Press, New York, 1999: 207–235.
- [113] Pavlovic R, Santaniello E. (2007) Peroxynitrite and nitrosoperoxy carbonate, a tightly connected oxidizing-nitrating couple in the reactive nitrogen-oxygen species family: new perspectives for protection from radical-promoted injury by flavonoids. *J Pharm Pharmacol*, 59: 1687–1695.
- [114] Niwa T, Doi U, Kato Y, Osawa T. (1999) Inhibitory mechanism of sinapinic acid against peroxynitrite-mediated tyrosine nitration of protein in vitro. *FEBS Lett*, 459: 43–46.
- [115] Kim JE, Kim AR, Chung HY, Han SY, Kim BS, Choi JS. (2003) In vitro peroxynitrite scavenging activity of diarylheptanoids from *Curcuma longa*. *Phytother Res*, 17: 481–484.
- [116] Pannala AS, Rice-Evans C, Sampson J, Singh S. (1998) Interaction of peroxynitrite with carotenoids and tocopherols within low density lipoprotein. *FEBS Lett*, 423: 297–301.
- [117] Pavlovic R, Santaniello E. (2007) Peroxynitrite and nitrosoperoxy carbonate, a tightly connected oxidizing-nitrating couple in the reactive nitrogen-oxygen species family: new perspectives for protection from radical-promoted injury by flavonoids. *J Pharm Pharmacol*, 59: 1687–1695.
- [118] Kim AR, Zou YN, Park TH, Shim KH, Kim MS, Kim ND, Kim JD, Bae SJ, Choi JS, Chung HY. (2004) Active components from *Artemisia iwayomogi* displaying ONOO(•) scavenging activity. *Phytother Res*, 18: 1–7.
- [119] Hyun SK, Jung HA, Chung HY, Choi JS. (2006) In vitro peroxynitrite scavenging activity of 6-hydroxykynurenic acid and other flavonoids from *Ginkgo biloba* yellow leaves. *Arch Pharm Res*, 29: 1074–1079.
- [120] Nugroho A, Lim SC, Byeon JS, Choi JS, Park HJ. (2013) Simultaneous quantification and validation of caffeoylquinic acids and flavonoids in *Hemistepta lyrata* and peroxynitrite-scavenging activity. *J Pharm Biomed Anal*, 76: 139–144.
- [121] Davson H, Segal MB. Physiology of the CSF and Blood-Brain Barriers. CRC Press, Boca Raton, FL, 1995.

- [122] Abbott NJ, Patabendige AA, Dolman DE, Yusof SR, Begley DJ. (2010) Structure and function of the blood-brain barrier. *Neurobiol Dis*, 37: 13–25.
- [123] Youdim KA, Qaiser MZ, Begley DJ, Rice-Evans CA, Abbott NJ. (2004) Flavonoid permeability across an *in situ* model of the blood-brain barrier. *Free Radic Biol Med*, 36: 592–604.
- [124] Pardridge WM. (2007) Blood-brain barrier delivery. *Drug Discov Today*, 12: 54–61.
- [125] Abbott NJ, Rönnbäck L, Hansson E. (2006) Astrocyte-endothelial interactions at the blood-brain barrier. *Nat Rev Neurosci*, 7: 41–53.
- [126] Di L, Kerns EH, Carter GT. (2008) Strategies to assess blood-brain barrier penetration. *Expert Opin Drug Discov*, 3: 677–687.
- [127] Abbott NJ. (2004) Prediction of blood-brain barrier permeation in drug discovery from *in vivo*, *in vitro* and *in silico* models. *Drug Discov Today Tech*, 1: 407–416.
- [128] Mensch J, Oyarzabal J, Mackie C, Augustijns P. (2009) *In vivo*, *in vitro* and *in silico* methods for small molecule transfer across the BBB. *J Pharm Sci*, 98: 4429–4468.
- [129] Summerfield SG, Dong KC. (2013) *In vitro*, *in vivo* and *in silico* models of drug distribution into the brain. *J Pharmacokinet Pharmacodyn*, 40: 301–314.
- [130] Kansy M, Senner F, Gubernator K. (1998) Physicochemical high throughput screening: parallel artificial membrane permeation assay in the description of passive absorption processes. *J Med Chem*, 41: 1007–1010.
- [131] Di L, Kerns EH, Fan K, McConnell OJ, Carter GT. (2003) High throughput artificial membrane permeability assay for blood-brain barrier. *Eur J Med Chem*, 38: 223–232.
- [132] Di L, Kerns EH, Bezar IF, Petusky SL, Huang Y. (2009) Comparison of blood-brain barrier permeability assays: *in situ* brain perfusion, MDR1-MDCKII and PAMPA-BBB. *J Pharm Sci*, 98: 1980–1991.
- [133] Naik P, Cucullo L. (2012) *In vitro* blood-brain barrier models: current and perspective technologies. *J Pharm Sci*, 101: 1337–1354.
- [134] McKenna DJ. (1996) Plant hallucinogens: springboards for psychotherapeutic drug discovery. *Behav Brain Res*, 73: 109–116.
- [135] Clement JA, Yoder BJ, Kingston DGI. (2004) Natural products as a source of CNS agents. *Mini-Rev Org Chem*, 1: 183–208.

- [136] Kumar V. (2006) Potential medicinal plants for CNS disorders: an overview. 20: 1023–1035.
- [137] Campos HC, da Rocha MD, Viegas FP, Nicastro PC, Fossaluzza PC, Fraga CA, Barreiro EJ, Viegas C Jr. (2011) The role of natural products in the discovery of new drug candidates for the treatment of neurodegenerative disorders I: Parkinson's disease. *CNS Neurol Disord Drug Targets*, 10: 239–250.
- [138] Williams P, Sorribas A, Howes MJ. (2011) Natural products as a source of Alzheimer's drug leads. *Nat Prod Rep*, 28: 48–77.
- [139] Gomes NG, Campos MG, Orfão JM, Ribeiro CA. (2009) Plants with neurobiological activity as potential targets for drug discovery. *Prog Neuropsychopharmacol Biol Psychiatry*, 33: 1372–1389.
- [140] Katritzky AR, Kuanar M, Slavov S, Dobchev DA, Fara DC, Karelson M, Acree WE Jr, Solov'ev VP, Varnek A. (2006) Correlation of blood-brain penetration using structural descriptors. *Bioorg Med Chem*, 14: 4888–4917.
- [141] Platts JA, Abraham MH, Zhao YH, Hersey A, Ijaz L, Butina D. (2001) Correlation and prediction of a large blood-brain distribution data set--an LFER study *Eur J Med Chem*, 36: 719–730.
- [142] Feher M, Schmidt JM. (2003) Property distributions: differences between drugs, natural products, and molecules from combinatorial chemistry. *J Chem Inf Comput Sci*, 43: 218–227.
- [143] Lachance H, Wetzel S, Kumar K, Waldmann H. (2012) Charting, navigating, and populating natural product chemical space for drug discovery. *J Med Chem*, 55: 5989–6001.
- [144] Avdeef A, Strafford M, Block E, Balogh MP, Chambliss W, Khan I. (2001) Drug absorption in vitro model: filter-immobilized artificial membranes. 2. Studies of the permeability properties of lactones in *Piper methysticum* Forst. *Eur J Pharm Sci*, 14: 271–280.
- [145] Balimane PV, Pace E, Chong S, Zhu M, Jemal M, Pelt CK. (2005) A novel high-throughput automated chip-based nanoelectrospray tandem mass spectrometric method for PAMPA sample analysis. *J Pharm Biomed Anal*, 2005 39: 8–16.

- [146] Carrara S, Reali V, Misiano P, Dondio G, Bigogno C. (2007) Evaluation of in vitro brain penetration: optimized PAMPA and MDCKII-MDR1 assay comparison. *Int J Pharm*, 345: 125–133.
- [147] Mensch J, Noppe M, Adriaensen J, Melis A, Mackie C, Augustijns P, Brewster ME. (2007) Novel generic UPLC/MS/MS method for high throughput analysis applied to permeability assessment in early drug discovery. *J Chromatogr B Analyt Technol Biomed Life Sci*, 847: 182–187.
- [148] Zhang J, Maloney J, Drexler DM, Cai X, Stewart J, Mayer C, Herbst J, Weller H, Shou WZ. (2012) Cassette incubation followed by bioanalysis using high-resolution MS for in vitro ADME screening assays. *Bioanalysis*, 4: 581–593.
- [149] Tarragó T, Kichik N, Claasen B, Prades R, Teixidó M, Giralt E. (2008) Baicalin, a prodrug able to reach the CNS, is a prolyl oligopeptidase inhibitor. *Bioorg Med Chem*, 16: 7516–7524.
- [150] Kumar J, Mishra GP, Naik PK, Murkute AA, Srivastava RB. (2011) Genomic DNA isolation from *Artemisia* species grown in cold desert high altitude of India. *Afr J Biotechnol*, 10: 7303–7307.
- [151] <http://www.plantasia.de/salvia-miltiorrhiza-chinesischer-salbei-rotwurzelsalbei.html>
- [152] <http://flickeflu.com/set/72157607306097923>
- [153] http://hu.wikipedia.org/wiki/Odvas_keltike
- [154] <http://www.flickr.com/photos/verzo/4727719901/lightbox/>
- [155] <http://www.floravascular.com/index.php?spp=Vinca%20major>
- [156] <http://www.promega.com>
- [157] Zhang JH, Chung TDY, Oldenburg KR. (1999) Simple statistical parameter for use in evaluation and validation of high throughput screening assays. *J Biomol Screen*, 4: 67–73.
- [158] Jiang RW, Lau KM, Hon PM, Mak TC, Woo KS, Fung KP. (2005) Chemistry and biological activities of caffeic acid derivatives from *Salvia miltiorrhiza*. *Curr Med Chem*, 12: 237–246.
- [159] Li YG, Song L, Liu M, Hu ZB, Wang ZT. (2009) Advancement in analysis of *Salviae miltiorrhizae* Radix et Rhizoma (Danshen). *J Chromatogr A*, 1216: 1941–1953.

- [160] Kenjerić D, Mandić ML, Primorac L, Čačić F. (2008) Flavonoid pattern of sage (*Salvia officinalis* L.) unifloral honey. *Food Chem*, 110: 187–192.
- [161] Avdeef A. *Absorption and Drug Development: Solubility, Permeability and Charge State*, John Wiley & Sons, Hoboken, NJ, 2003: xxiv.
- [162] Snyder LR, Dolan JW. (1996) Initial experiments in high-performance liquid chromatographic method development I. Use of a starting gradient run. *J Chromatogr A*, 721: 3–14.
- [163] Leeson PD, Empfield JR. (2010) Reducing the risk of drug attrition associated with physicochemical properties. *Annu Rep Med Chem*, 45: 393–407.
- [164] Waring MJ. (2010) Lipophilicity in drug discovery. *Expert Opin Drug Discov*, 5: 235–248.
- [165] Wong C-C, Li H-B, Cheng K-W, Chen F. (2006) A systematic survey of antioxidant activity of 30 Chinese medicinal plants using the ferric reducing antioxidant power assay. *Food Chem*, 97: 705–711.
- [166] *Medicinal Plants in the Republic of Korea* compiled by Natural Products Research Institute Seoul National University, Manila: World Health Organization, Regional Office for the Western Pacific. 1998: 37.
- [167] Ballabh B, Chaurasia OP. (2007) Traditional medicinal plants of cold desert Ladakh-Used in treatment of cold, cough and fever. *J Ethnopharmacol*, 112: 341–349.
- [168] Ghimire SK, Lama YC, Tripathi GR, Schmitt S, Aumeeruddy-Thomas Y. Conservation of plant resources, community development and training in applied ethnobotany at Shey-Phoksundo national park and its buffer zone, Dolpa. Report Series No. 41, WWF Nepal Program, Kathmandu, Nepal, 2001.
- [169] Manandhar NP. *Plants and People of Nepal*. Timber Press Inc., Portland, Oregon, 2002.
- [170] Chemesova II, Belenovskaya LM, Markova LP. (1987) Phenolic compounds of *Artemisia gmelinii*. *Chem Nat Compd*, 19: 364–365.
- [171] Greger H, Zdero C, Bohlmann F. (1986) Eudesman-12,8 β -olides and other terpenes from *Artemisia* species. *Phytochemistry* 25: 891–897.
- [172] Khanina MA, Serykh EA, Pokrovsky LM, Tkachev AV. (2000) Results of chemical study of *Artemisia gmelinii* Web. et Stechm. from Siberia. *Chem Plant Raw Mater*, 3: 77–84.

- [173] Saito S, Kurakane S, Seki M, Takai E, Kasai T, Kawabata J. (2005) Radical scavenging activity of dicaffeoylcyclohexanes: Contribution of an intramolecular interaction of two caffeoyl residues. *Bioorg Med Chem*, 13: 4191–4199.
- [174] Gebhardt R, Fausel M. (1997) Antioxidant and hepatoprotective effects of artichoke extracts and constituents in cultured rat hepatocytes. *Toxicol in Vitro* 11: 669–672.
- [175] Lu Y, Foo LY. (2002) Polyphenolics of *Salvia* - a review. *Phytochemistry*, 59: 117–140.
- [176] Ivanov VM, Mamedov AM. (2006) 3,4,5-Trihydroxyfluorones as analytical reagents. *J Anal Chem*, 61: 1040–1062.
- [177] Heijnen CG, Haenen GR, van Acker FA, van der Vijgh WJ, Bast A. (2001) Flavonoids as peroxynitrite scavengers: the role of the hydroxyl groups. *Toxicol In Vitro*, 15: 3–6.
- [178] Bade R, Chan HF, Reynisson J. (2010) Characteristics of known drug space. Natural products, their derivatives and synthetic drugs. *Eur J Med Chem*, 45: 5646–5652.
- [179] Lang G, Mayhudin NA, Mitova MI, Sun L, van der Sar S, Blunt JW, Cole AL, Ellis G, Laatsch H, Munro MH. (2008) Evolving trends in the dereplication of natural product extracts: new methodology for rapid, small-scale investigation of natural product extracts. *J Nat Prod*, 71: 1595–1599.
- [180] Rangel-Ordóñez L, Nöldner M, Schubert-Zsilavec M, Wurglics M. (2010) Plasma levels and distribution of flavonoids in rat brain after single and repeated doses of standardized *Ginkgo biloba* extract EGb 761®. *Planta Med*, 76: 1683–1690.
- [181] Clark DE. (2003) In silico prediction of blood-brain barrier permeation. *Drug Discov Today*, 8: 927–933.
- [182] Ghose AK, Herberz T, Hudkins RL, Dorsey BD, Mallamo JP. (2012) Knowledge-based, central nervous system (CNS) lead selection and lead optimization for CNS drug discovery. *ACS Chem Neurosci*, 3: 50–68.
- [183] Liu X, Tu M, Kelly RS, Chen C, Smith BJ. (2004) Development of a computational approach to predict blood-brain barrier permeability. *Drug Metab Dispos*, 32: 132–139.

- [184] Youdim KA, Dobbie MS, Kuhnle G, Proteggente AR, Abbott NJ, Rice-Evans C. (2003) Interaction between flavonoids and the blood-brain barrier: in vitro studies. *J Neurochem*, 85: 180–192.
- [185] Singh SP, Wahajuddin, Tewari D, Patel K, Jain GK. (2011) Permeability determination and pharmacokinetic study of nobiletin in rat plasma and brain by validated high-performance liquid chromatography method. *Fitoterapia*, 82: 1206–1214.
- [186] Wink M. Interference of alkaloids with neuroreceptors and ion channels. In: Attar-Rahman (ed.), *Bioactive Natural Products (Part B)*, Elsevier, Amsterdam, 2000: 3–122.
- [187] Kennedy DO, Wightman EL. (2011) Herbal extracts and phytochemicals: plant secondary metabolites and the enhancement of human brain function. *Adv Nutr*, 2: 32–50.
- [188] Kaliszan R. In: Brown PR, Grushka E. (eds.) *Advances in Chromatography*. Marcel Dekker, New York, 1993: 147–154.
- [189] Fishedick JT, Standiford M, Johnson DA, De Vos RC, Todorović S, Banjanac T, Verpoorte R, Johnson JA. (2012) Activation of antioxidant response element in mouse primary cortical cultures with sesquiterpene lactones isolated from *Tanacetum parthenium*. *Planta Med*, 78: 1725–1730.
- [190] Milosavljevic S, Juranic I, Aljancic I, Vajs V, Todorovic N. (2003) Conformational analysis of three germacranolides by the PM3 semi-empirical method. *J Serb Chem Soc*, 68: 281–289.
- [191] Yagudaev MR, Abdurakhimova N, Yunusov SY. (1968) The structure of majdine *Chem Nat Compd*, 4: 170–171.
- [192] Yu J, Wearing XZ, Cook JM. (2005) A general strategy for the synthesis of vincamajine-related indole alkaloids: stereocontrolled total synthesis of (+)-dehydrovoachalotine, (-)-vincamajinine, and (-)-11-methoxy-17-epivincamajine as well as the related quebrachidine diol, vincamajine diol, and vincarinol. *J Org Chem*, 70: 3963–3979.
- [193] Miliauskas G. Screening, Isolation and Evaluation of Antioxidative Compounds from *Geranium macrorrhizum*, *Potentilla fruticosa* and *Rhaponticum carthamoides*; Ph.D. Thesis, Wageningen University, Wageningen, The Netherlands, 2006: 109.

- [194] Pukalskas A, van Beek TA, de Waard P. (2005) Development of a triple hyphenated HPLC-radical scavenging detection-DAD-SPE-NMR system for the rapid identification of antioxidants in complex plant extracts. *J Chromatogr A*, 1074: 81–88.
- [195] Halbsguth C, Meissner O, Häberlein H. (2003) Positive cooperation of protoberberine type 2 alkaloids from *Corydalis cava* on the GABA(A) binding site. *Planta Med*, 69: 305–309.
- [196] Ding B, Zhou T, Fan G, Hong Z, Wu Y. (2007) Qualitative and quantitative determination of ten alkaloids in traditional Chinese medicine *Corydalis yanhusuo* W.T. Wang by LC-MS/MS and LC-DAD. *J Pharm Biomed Anal*, 45: 219–226.
- [197] Heptinstall S, Awang DV, Dawson BA, Kindack D, Knight DW, May J. (1992) Parthenolide content and bioactivity of feverfew (*Tanacetum parthenium* (L.) Schultz-Bip.). Estimation of commercial and authenticated feverfew products. *J Pharm Pharmacol*, 44: 391–395.
- [198] Tassorelli C, Greco R, Morazzoni P, Riva A, Sandrini G, Nappi G. (2005) Parthenolide is the component of tanacetum parthenium that inhibits nitroglycerin-induced Fos activation: studies in an animal model of migraine. *Cephalalgia*, 25: 612–621.
- [199] European Medicines Agency, 2011. Assessment Report on *Tanacetum parthenium* (L.) Schulz Bip., Herba (EMA/HMPC/587579/2009).
- [200] Rajput MS, Nair V, Chauhan A, Jawanjali H, Dange V. (2011) Evaluation of antidiarrheal activity of aerial parts of *Vinca major* in experimental animals. *Middle East J Sci Res*, 7: 784–788.
- [201] Kavvadias D, Monschein V, Sand P, Riederer P, Schreier P. (2003) Constituents of sage (*Salvia officinalis*) with in vitro affinity to human brain benzodiazepine receptor. *Planta Med*, 69: 113–117.
- [202] Perry NS, Bollen C, Perry EK, Ballard C. (2003) *Salvia* for dementia therapy: review of pharmacological activity and pilot tolerability clinical trial. *Pharmacol Biochem Behav*, 75: 651–659.
- [203] Wang C, Wang S, Fan G, Zou H. (2010) Screening of antinociceptive components in *Corydalis yanhusuo* W.T. Wang by comprehensive two-dimensional liquid chromatography/tandem mass spectrometry. *Anal Bioanal Chem*, 396: 1731–1740.

[204] Camp D, Davis RA, Campitelli M, Ebdon J, Quinn RJ. (2012) Drug-like properties: guiding principles for the design of natural product libraries. *J Nat Prod*, 75: 72–81.

[205] Quinn RJ, Carroll AR, Pham NB, Baron P, Palframan ME, Suraweera L, Pierens GK, Muresan S. (2008) Developing a drug-like natural product library. *J Nat Prod*, 71: 464–468.

10. List of Publications

10.1. Publications related to the thesis

Articles

Könczöl Á, Kéry Á, Keserű GM, Balogh GT. (2010) LC determination of peroxynitrite scavenging activity of phenols from *Salvia* spp. *Chromatographia*, 71(S1): 51-59. IF: 1.075

Balogh GT, **Könczöl Á**. (2011) Plant extracts in drug discovery: Traditional considerations, novel chances [Növényi extraktumok az eredeti gyógyszerkutatásban: Tradicionális érvek, új lehetőségek]. *Acta Pharm Hung*, 81: 5-17. IF:-

Könczöl Á, Béni Z, Sipos MM, Rill A, Háda V, Hohmann J, Máthé I, Szántay C, Keserű GM, Balogh GT. (2012) Antioxidant activity-guided phytochemical investigation of *Artemisia gmelinii* Webb. ex Stechm.: Isolation and spectroscopic challenges of 3,5-*O*-dicaffeoyl (epi?) quinic acid and its ethyl ester. *J Pharm Biom Anal*, 59: 83-89. IF: 2.967

Könczöl Á, Müller J, Földes E, Béni Z, Végh K, Kéry Á, Balogh GT. (2013) Applicability of a Blood-Brain Barrier Specific Artificial Membrane Permeability Assay at the Early Stage of Natural Product-Based CNS Drug Discovery. *J Nat Prod*, 76: 655-663. IF: 3.128

Book chapter

Balogh GT, **Könczöl Á**. Növényi eredetű hatóanyagok helye és szerepe az eredeti gyógyszerkutatásban (chapter IV.1.1.) In: Balázs A, Blázovics A, Kéry Á, Kursinszki L, Lemberkovics É, Szőke É, Then M, Farmakognózia – Fitokémia. Gyógynövények alkalmazása. Szőke É. (ed.) (2013) ISBN 978-963-9129-87-0.

10.2. Further scientific publications

Könczöl Á. (2004) Glükózaminoglikánok antioxidáns hatásának összehasonlító vizsgálata [Comparative study of the antioxidative effect of glycosaminoglycans]. *Period Polytech Chem Eng*, 48:137.

Balogh GT, Vukics K, **Könczöl Á**, Kis-Varga Á, Gere A, Fischer J. (2005) Nitronne derivatives of trolox as neuroprotective agents. *Bioorg Med Chem Lett*, 15: 3012-3015. IF: 2.478

Kiss R, Kiss B, **Könczöl Á**, Szalai F, Jelinek I, László V, Noszál B, Falus A, Keseru GM. (2008) Discovery of novel human histamine H4 receptor ligands by large-scale structure-based virtual screening. *J Med Chem* 51: 3145-3153. IF: 4.898

Balogh GT, **Könczöl Á**, Sándor M. (2011) Új megoldások az eredeti gyógyszerkutatás szintézistámogató analitikájában. *Magyar Kémikusok Lapja LXVI évf. 12*: 378-382.

Balogh GT, Müller J, **Könczöl Á**. (2013) pH-gradient PAMPA-based *in vitro* model assay for drug-induced phospholipidosis in early stage of drug discovery. *Eur J Pharm Sci* 49: 81-89. IF: 3.212

11. Acknowledgements

The presented work was performed entirely in the Drug Discovery and Compound Profiling Laboratories of Gedeon Richter Plc.

First and foremost, I would like to express my deepest gratitude to my supervisor **Dr. György T. Balogh** for his persistent professional and human support and inspiration. He became my closest friend over the years. Thank you so much “Darth Plagueis”!

I wish to thank my consultant **Prof. Ágnes Kéry** for her guidance in pharmacognosy and phytotherapy. Our consultations have highly inspired my professional thinking.

I acknowledge the former and present management of Gedeon Richter Plc., **Prof. György M. Keserű** and **Dr. István Greiner**, who made it possible for me to carry out research beside my daily routine work.

I owe special thanks to my dear colleagues: **Dr. Zoltán Béni** for excellent NMR measurements and helpful discussions, **Márta Sipos Meszlényiné** for introducing me in the world of HPLC, **Dr. Attila Rill** for preparative HPLC isolations, **Dr. Viktor Háda** for HRMS measurements, **Dr. András Visegrády** for the cytotoxicity screening, **Zsuzsanna Huszárné**, **Marika Csomontányiné**, and **Zsuzsanna Gyulai** for the excellent technical assistance, **Judit Müller** PhD student fellow for conducting PAMPA experiments, and **László Kiss** for proofreading this manuscript.

I am grateful to **Prof. Éva Szőke**, **Prof. Éva Lemberkovics**, **Dr. Ágnes Alberti**, **Dr. Rita Engel**, **Prof. Judit Hohmann** and **Prof. Imre Máthé** for their botanical and phytochemical support and collaboration.

Finally, I would like to thank all my family for the endless support and patience they have provided me through my entire life and, in particular, I must acknowledge my parents, my beloved wife Kata, and my sister Sara.

My dear Grandma, this work would not have been finalized without the motivation you instilled me. This thesis is dedicated principally to you.

12. Appendix

Table A1. ^1H and ^{13}C chemical shifts for compounds **7a**, **8a** and cynarin in DMSO-*d*₆.

Table A2. Experimental log BB values taken from the literature and log P_e values measured by the PAMPA-BBB assay for the validation set of 23 NP and 20 NP-like drugs. **References of Table A2.**

Table A3. Measured effective BBB permeability values and calculated physicochemical properties of the tested marker compounds of major NP classes.

Figure A1. Demonstration of the purifying effect of PAMPA-BBB in NMR.

Table A4. NMR assignment of parthenolide (**1t**) and 11,13-dihydroparthenolide (**2t**) in deuterio PBS buffer at 800 MHz. UV and MS characteristics parthenolide (**1t**) and 11,13-dihydroparthenolide (**2t**).

Table A5. Partial assignment of vincamajine (**1v**) and majdine (**2v**) in deuterio PBS buffer at 800 MHz. UV and MS characteristics of vincamajine (**1v**) and majdine (**2v**).

Table A6. NMR assignment of epiisorosmanol (**1so**) and methyl carnosate (**2so**) in deuterio PBS buffer at 800 MHz. UV and MS characteristics of epiisorosmanol (**1so**) and methyl carnosate (**2so**).

Table A7. NMR assignment of tetrahydropalmatine (**1c**) and corydaline (**2c**) in deuterio PBS buffer at 800 MHz. UV and MS characteristics of tetrahydropalmatine (**1c**) and corydaline (**2c**).

Table A1. ^1H and ^{13}C chemical shifts for compounds **7a**, **8a** and cynarin in DMSO- d_6 .

Position	7a		8a		cynarin	
	^1H (ppm)	^{13}C (ppm)	^1H (ppm)	^{13}C (ppm)	^1H (ppm)	^{13}C (ppm)
1	-	72.4	-	72.4		79.3
2	1.97 m	34.6	2.00 m	34.4	2.27 m	31.7
2	2.15 m		2.20 m		2.50 m	
3	5.20 m	70.5	5.18 m	69.9	5.29 q	71.0
4	3.84 br	67.4	3.84 m	66.5	3.49 m	72.8
5	5.12 m	70.9	5.08 m	70.9	4.00 t	65.8
6	1.98 m	34.6	2.00 m	34.4	1.71 m	
6	2.15 m		2.20 m		2.29 m	39.4
7	-	175.2	-	173.2		172.4
1'	-	166.1	-	166.0		166.0
2'	6.26 d	114.7	6.26 d	114.5	6.05 d	114.4
3'	7.48 d	144.8	7.49 d	144.9	7.39 d	144.8
4'	-	125.6	-	125.4		125.2
5'	7.06 d	114.8	7.04 d	114.6	6.90 br	115.7
6'	-	148.3	-	148.5		148.0
7'	-	145.6	-	145.6		145.3
8'	6.78 d	115.8	6.78 d	115.8	6.52 br d	115.8
9'	7.01 dd	121.4	6.99 dd	121.2	6.61 br d	119.9
1''	-	165.5	-	165.3		165.2
2''	6.16 d	114.1	6.13 d	113.6	6.20 d	113.9
3''	7.45 dd	145.1	7.43 dd	145.3	7.42 d	145.5
4''	-	125.6	-	125.3		125.3
5''	7.04 d	114.8	7.03 d	114.6	7.01 d	115.3
6''	-	148.4	-	148.3		148.5
7''	-	145.6	-	145.6		145.6
8''	6.77 d	115.7	6.77 d	115.9	6.66 d	115.8
9''	7.00 dd	121.2	6.98 dd	121.3	6.87 br d	120.9
4-OH	5.31	-	5.40 br		5.00 d	
5-OH	5.51 br	-	5.74 br		4.95 br	
O-CH ₂ -CH ₃	-	-	3.99 m	60.4		
O-CH ₂ -CH ₃			4.07 m			
O-CH ₂ -CH ₃	-	-	1.15 t	13.8		
COOH	12.49 br	-	-		12.91 br	
6'-OH	9.17 s	-	9.18 s		9.10 s	
7'-OH	9.56 s	-	9.61 s		9.43 s	
6''-OH	9.17 s	-	9.18 s		9.14 s	
7''-OH	9.60 s	-	9.61 s		9.56 s	

Table A2. Experimental log BB values taken from the literature and log P_e values measured by the PAMPA-BBB assay for the validation set of 23 NP and 20 NP-like drugs.

Natural product drugs	log BB	log P_e^a	SE	Number of reference
atropine	-0.06	-5.68	0.02	[A1]
caffeine	0.01	-5.79	0.06	[A2]
coumarin	-0.30	-4.61	0.02	[A3]
daidzein	-0.15	-5.61	0.02	[A4]
digoxin	-1.23	-7.64	0.00	[A5]
estradiol	0.32	-4.71	0.03	[A6]
galantamine	0.32	-5.35	0.02	[A7]
hydrocortisone	-0.90	-5.68	0.02	[A5]
levodopa	-0.77	-6.35	0.01	[A8]
mannitol	-1.60	-7.14	0.02	[A9]
morphine	-0.16	-5.97	0.02	[A10]
naringenin	-0.46	-5.20	0.03	[A11]
nicotine	0.56	-4.47	0.03	[A12]
physostigmine	0.08	-5.20	0.04	[A13]
protopine	-0.27	-5.82	0.10	[A14]
quercetin	-1.70	-7.02	0.08	[A5]
quinine	0.60	-4.92	0.04	[A15]
salicylic acid	-1.10	-7.45	0.09	[A16]
scopolamine	0.23	-5.59	0.01	[A17]
theophylline	-0.38	-6.20	0.03	[A18]
vinblastine	-0.07	-5.02	0.06	[A5]
vincamine	-0.20	-4.63	0.04	[A19]
vincristine	-1.03	-6.01	0.06	[A5]
Natural product-like drugs	log BB	log P_e	SE	Number of reference
acetylsalicylic acid	-1.30	-7.49	0.10	[A20]
bromocriptine	-0.59	-5.55	0.05	[A21]
cefuroxime	-1.38	-7.83	0.08	[A22]
codeine	0.54	-5.21	0.03	[A10]
dextromethorphan	0.02	-4.56	0.01	[A23]
doxorubicin	-0.83	-7.27	0.04	[A5]
etoposide	-2.00	-6.95	0.05	[A1]
gabapentin	-0.19	-5.71	0.03	[A24]
gemcitabine	-1.05	-7.07	0.01	[A25]
levetiracetam	-0.21	-6.30	0.07	[A26]
methamphetamine	0.90	-4.62	0.01	[A27]
methotrexate	-1.50	-8.10	0.10	[A28]
pergolide	0.30	-4.95	0.05	[A1]
phenserine	1.00	-4.58	0.01	[A29]
prednisone	-0.90	-6.04	0.03	[A30]
quinidine	0.33	-4.96	0.04	[A31]
selegiline	0.57	-4.63	0.07	[A30]
topiramate	-0.08	-5.34	0.01	[A32]
tramadol	0.72	-4.57	0.01	[A32]
verapamil	-0.40	-5.04	0.01	[A33]

References of Table A2.

- [A1] Garg P, Verma J. (2006) In silico prediction of blood brain barrier permeability: an Artificial Neural Network model. *J Chem Inf Model*, 46: 289–297.
- [A2] Kaplan GB, Greenblatt DJ, LeDuc BW, Thompson ML, Shader RI. (1989) Relationship of plasma and brain concentrations of caffeine and metabolites to benzodiazepine receptor binding and locomotor activity. *J Pharm Exp Therapeutics* 248: 1078–1083.
- [A3] Ritschel WA, Hardt TJ. (1983) Pharmacokinetics of coumarin, 7-hydroxycoumarin and 7-hydroxycoumarin glucuronide in the blood and brain of gerbils following intraperitoneal administration of coumarin. *Arzneimittelforschung*, 33: 1254–1258.
- [A4] Yueh TL, Chu HY. (1977) The metabolic fate of daidzein. *Sci Sin*, 20: 513–521.
- [A5] Tsinman O, Tsinman K, Sun N, Avdeef A. (2011) Physicochemical selectivity of the BBB microenvironment governing passive diffusion--matching with a porcine brain lipid extract artificial membrane permeability model. *Pharm Res*, 28: 337–363.
- [A6] Crivori P, Cruciani G, Carrupt PA, Testa B. (2000) Predicting blood-brain barrier permeation from three-dimensional molecular structure. *J Med Chem*, 43: 2204–2216.
- [A7] Kewitz H. (1997) Pharmacokinetics and metabolism of galanthamine. *Drugs Today*, 33: 265–272.
- [A8] ChemSilico; CSBBB External Validation Set Compounds; http://www.chemsilico.com/CS_prBBB/BBBExValcomp.html.
- [A9] Oldendorf WH. (1972) Distribution of various classes of radiolabeled tracers in plasma, scalp, and brain. *J Nucl Med*, 13: 681–685.
- [A10] Dambisya YM, Chan K, Wong CL. (1992) Dispositional study of opioids in mice pretreated with sympathomimetic agents. *J Pharmacy Pharmacol*, 44: 687–690.
- [A11] Youdim KA, Qaiser MZ, Begley DJ, Rice-Evans CA, Abbott N. (2004) Flavonoid permeability across an in situ model of the blood-brain barrier. *J Free Radic Biol Med*, 36: 592–604.
- [A12] Romano C, Goldstein A, Jewell NP. (1981) Characterization of the receptor mediating the nicotine discriminative stimulus. *Psychopharmacology*, 74: 310–315.
- [A13] Hurh E, Lee EJ, Kim YG, Kim SY, Kim SH, Kim YC, Lee MG. (2000) Effects of physostigmine on the pharmacokinetics of intravenous parathion in rats. *Biopharm Drug Dispos*, 21: 331–338.
- [A14] Wang C, Wang S, Fan G, Zou H. (2010) Screening of antinociceptive components in *Corydalis yanhusuo* W.T. Wang by comprehensive two-dimensional liquid chromatography/tandem mass spectrometry. *Anal Bioanal Chem*, 396: 1731–1740.
- [A15] Avdeef A. Absorption and drug development. Wiley Interscience, New York. 2003: 116–246.
- [A16] Salminen T, Pulli A, Taskinen JJ. (1997) Relationship between immobilised artificial membrane chromatographic retention and the brain penetration of structurally diverse drugs. *J Pharm Biomed Anal*, 15: 469–477.
- [A17] Hirose H, Aoki I, Kimura T, Fujikawa T, Numazawa T, Sasaki K, Sato A, Hasegawa T, Nishikibe M, Mitsuya M, Ohtake N, Mase T, Noguchi K. (2001) Pharmacological properties of (2R)-N-[1-(6-aminopyridin-2-ylmethyl)piperidin-4-yl]-2-[(1R)-3,3-difluorocyclopentyl]-2-hydroxy-2-phenylacetamide: a novel muscarinic antagonist with M(2)-sparing antagonistic activity. *J Pharm Exp Therapeutics*, 297: 790–797.

- [A18] Wilkinson JM, Pollard I. (1993) Accumulation of theophylline, theobromine and paraxanthine in the fetal rat brain following a single oral dose of caffeine. *Dev Brain Res*, 75: 193–199.
- [A19] Juan YP, Tsai TH. (2005) Measurement and pharmacokinetics of vincamine in rat blood and brain using microdialysis. *J Chromatogr A*, 1088: 146–151.
- [A20] Miyagi N, Kondoh H, Sakurai E, Hikichi N, Niwa H. Effect of concanavalin A on the aspirin concentration and distribution in the brain and plasma of rats. *J Pharmacobio-Dyn*, 9: 704–714.
- [A21] Granveau-Renouf S, Valente D, Durocher A, Grognet J-M, Ezan E. (2000) Microdialysis study of bromocriptine and its metabolites in rat pituitary and striatum. *Eur J Drug Metab Ph*, 25: 79–84.
- [A22] Tsai TH, Cheng FC, Chen KC, Chen YF, Chen CF. (1999) Simultaneous measurement of cefuroxime in rat blood and brain by microdialysis and microbore liquid chromatography. Application to pharmacokinetics. *J Chromatogr B Biomed Sci Appl*, 735: 25–31.
- [A23] Uhr M, Namendorf C, Grauer MT, Rosenhagen M, Ebinger M. (2004) P-glycoprotein is a factor in the uptake of dextromethorphan, but not of melperone, into the mouse brain: evidence for an overlap in substrate specificity between P-gp and CYP2D6. *J Psychopharmacol*, 18: 509–515.
- [A24] Wang Y, Welty DF. (1996) The simultaneous estimation of the influx and efflux blood-brain barrier permeabilities of gabapentin using a microdialysis-pharmacokinetic approach. *Pharm Res*, 13: 398–403.
- [A25] Apparaju SK, Gudelsky GA, Desai PB. (2008) Pharmacokinetics of gemcitabine in tumor and non-tumor extracellular fluid of brain: an in vivo assessment in rats employing intracerebral microdialysis. *Cancer Chemother Pharmacol*, 61: 223–229.
- [A26] Tong X, Patsalos PN. (2001) A microdialysis study of the novel antiepileptic drug levetiracetam: extracellular pharmacokinetics and effect on taurine in rat brain. *Br J Pharmacol*, 133: 867–874.
- [A27] Rivière GJ, Gentry WB, Owens SM. (2000) Disposition of methamphetamine and its metabolite amphetamine in brain and other tissues in rats after intravenous administration. *J Pharmacol Exp Ther*, 292: 1042–1047.
- [A28] Guerra A, Páez JA, Campillo NE. (2008) Artificial Neural Networks in ADMET Modeling: Prediction of Blood-Brain Barrier Permeation. *QSAR Combinat Sci*, 27: 586–594.
- [A29] Kunsman GW, Rohrig TP. (1993) Tissue distribution of ibuprofen in a fatal overdose. *Am J Forensic Med Pathol*, 14: 48–50.
- [A30] Doran A, et al. (2004) The impact of P-glycoprotein on the disposition of drugs targeted for indications of the central nervous system: evaluation using the MDR1A/1B knockout mouse model. *Drug Metab Dispos*, 33: 165–174.
- [A31] Yata N, Toyoda T, Murakami T, Nishiura A, Higashi Y. (1990) Phosphatidylserine as a determinant for the tissue distribution of weakly basic drugs in rats. *Pharm Res*, 7: 1019–1025.
- [A32] Fridén M, Winiwarter S, Jerndal G, Bengtsson O, Wan H, Bredberg U, Hammarlund-Udenaes M, Antonsson M. (2009) Structure-brain exposure relationships in rat and human using a novel data set of unbound drug concentrations in brain interstitial and cerebrospinal fluids. *J Med Chem*, 52: 6233–6243.
- [A33] Bart J. (2003) Quantitative assessment of P-glycoprotein function in the rat blood-brain barrier by distribution volume of [¹¹C]verapamil measured with PET. *Neuroimage*, 20: 1775–1782.

Table A3. Measured effective BBB permeability values and calculated physicochemical properties of the tested marker compounds of major NP classes (Marvin, ChemAxon v5.10.2). Red colored values violate the basic medchem rules of brain penetration: CNS-: MW > 450; PSA > 90 Å²; log $D_{7.4}$ < 1 or > 3; CNS+: MW < 450; PSA < 90 Å²; 1 < log $D_{7.4}$ < 3.

Compound class Test compound	Measured properties (by PAMPA-BBB/LC-MS)			Calculated properties (by Marvin)		
	log $P_e \pm SE$	quantified by	limit of quantification (LOQ) (ng/mL)	MW	polar surface area (Å ²)	cLog $D_{7.4}$
glycosides						
α -solanine	-6.52 ± 0.15	UV at 210 nm	23.4	868.1	240.7	-2.84
apigenin-7- <i>O</i> -glucoside*	-8.74	SIM m/z 433	3.8	432.4	166.1	-0.57
aucubin	-7.09 ± 0.01	SIM m/z 369	6.7	344.4	128.8	-1.98
catalpol*	-6.97	SIM m/z 385	13.5	362.3	161.6	-4.18
harpagoside*	-8.09	UV at 282 nm	2.4	494.5	175.4	-0.84
isoquercitrin*	-7.67	SIM m/z 488	7.4	464.4	206.6	-1.53
luteolin-7- <i>O</i> -glucoside*	-8.86	SIM m/z 449	6.7	448.4	186.4	-0.86
rutin*	-9.04	SIM m/z 303	17.1	610.5	265.5	-2.56
carboxylic acids						
caffeic acid*	-9.01	SIM m/z 179	0.9	180.2	77.8	-1.75
chlorogenic acid*	-9.07	SIM m/z 353	1.5	354.3	164.8	-3.47
cinnamic acid	-7.05 ± 0.04	UV at 280 nm	40.9	148.2	37.3	-0.25
ellagic acid*	-8.80	SIM m/z 301	2.2	302.2	133.5	1.03
ferulic acid*	-8.43	SIM m/z 193	1.6	194.2	66.8	-1.69
gentisic acid*	-9.29	SIM m/z 153	0.2	154.1	77.8	-2.01
nicotinic acid	-7.01	SIM m/z 124	2.4	123.1	50.2	-3.11
rosmarinic acid*	-7.90	SIM m/z 359	1.8	360.3	144.5	0.17
salicylic acid	-7.45 ± 0.09	SIM m/z 137	3.1	138.1	57.5	-1.70
salvianolic acid A	-7.65 ± 0.01	SIM m/z 493	9.5	494.4	185	2.31
sinapic acid*	-9.13	SIM m/z 223	0.8	224.2	76	-1.98
syringic acid*	-8.70	SIM m/z 197	0.4	198.2	76	-2.49
vanillic acid*	-8.24	SIM m/z 167	0.7	168.2	66.8	-2.08
flavonoid aglycons						
(+)-catechin*	-7.87	SIM m/z 291	0.7	290.3	110.4	1.79
apigenin	-5.14 ± 0.03	UV at 320 nm	7	270.2	87	1.74
chrysin	-4.76 ± 0.01	UV at 270 nm	2.6	254.2	66.8	2.04
cirsiliol	-5.46 ± 0.09	UV at 345 nm	3	330.3	105.5	1.59
daidzein	-5.61 ± 0.02	UV at 250 nm	2.9	254.2	66.8	2.82
galangin	-6.44 ± 0.04	UV at 220 nm	2	270.2	87	-0.51
genistein	-5.29 ± 0.01	UV at 220 nm	1.9	270.2	87	3.07
hesperetin	-5.13 ± 0.05	UV at 220 nm	1.1	302.3	96.2	2.02
kaempferol	-5.02 ± 0.05	UV at 360 nm	6.8	286.2	107.2	-0.89
morin*	-7.10	SIM m/z 303	5.3	302.2	127.5	-1.47
naringenin	-5.20 ± 0.03	UV at 280 nm	0.6	272.3	87	2.27
quercetin	-7.02 ± 0.08	SIM m/z 303	2.5	302.2	127.5	-1.31
taxifolin*	-7.90	SIM m/z 305	4	304.3	127.5	1.19
alkaloids						
atropine	-5.68 ± 0.02	UV at 210 nm	0.7	289.4	49.8	1.01
caffeine	-5.79 ± 0.06	UV at 210 nm	0.4	194.2	58.4	-0.79

codeine	-5.21 ± 0.03	UV at 210 nm	0.8	299.4	41.9	-0.53
colchicine	-6.80 ± 0.03	UV at 250 nm	0.9	399.4	83.1	1.08
corydaline (2c)	-4.93 ± 0.02	UV at 220 nm	1.1	369.5	40.2	2.99
ephedrine	-5.42 ± 0.03	UV at 210 nm	0.5	165.2	32.3	-0.80
ergotamine	-5.00 ± 0.03	UV at 220 nm	3.3	581.7	118.2	2.25
galantamine	-5.35 ± 0.02	UV at 220 nm	0.9	287.4	41.9	-0.44
morphine	-5.97 ± 0.02	UV at 220 nm	0.7	285.3	52.9	-0.57
nicotine	-4.47 ± 0.03	SIM m/z 163	0.04	162.2	16.1	0.1
papaverine	-4.67 ± 0.02	UV at 220 nm	0.5	339.4	49.8	2.71
physostigmine	-5.20 ± 0.04	UV at 250 nm	1.5	275.3	44.8	2.49
piperine	-4.82 ± 0.07	UV at 320 nm	0.6	285.3	38.8	2.97
protopine	-5.82 ± 0.10	UV at 220 nm	1.5	353.4	57.2	2.41
quinine	-4.92 ± 0.04	UV at 220 nm	0.3	324.4	45.6	0.67
reserpine	-6.19 ± 0.06	UV at 220 nm	10.8	608.7	117.8	2.61
scopolamine	-5.59 ± 0.01	UV at 210 nm	1.7	303.4	62.3	0.7
solasodine	-5.65 ± 0.11	SIM m/z 414	3.9	413.6	41.5	2.67
theophylline	-6.20 ± 0.03	UV at 280 nm	0.7	180.2	69.3	-1.03
vinblastine	-5.02 ± 0.06	UV at 220 nm	0.5	811	154.1	1.16
vincamine	-4.63 ± 0.04	UV at 220 nm	0.7	354.4	54.7	2.58
vincristine	-6.01 ± 0.01	UV at 220 nm	0.5	825	171.2	0.04
miscellaneous						
adhyperforin	-5.88 ± 0.11	SIM m/z 551	52.3	550.8	71.4	8.23
caffeic acid 2-phenethyl ester	-5.01 ± 0.05	UV at 320 nm	0.2	284.3	66.8	4.59
chalcone	-5.83 ± 0.03	UV at 320 nm	2.7	208.3	17.1	3.92
chamazulene*	-7.02	SIM m/z 185	0.9	184.3	0	4.85
coumarin	-4.61 ± 0.02	UV at 280 nm	0.5	146.1	26.3	1.52
epiisorosmanol (1so)	-5.32 ± 0.04	UV at 210 nm	9.8	346.4	87	3.65
esculetin	-6.50 ± 0.05	UV at 320 nm	0.5	178.1	66.8	0.94
hyperforin	-5.99 ± 0.09	SIM m/z 537	34.5	536.8	71.4	7.82
khellin	-4.72 ± 0.02	UV at 250 nm	0.4	260.2	57.9	1.47
methyl carnosate (2so)	-4.96 ± 0.02	UV at 210 nm	4	346.5	66.8	5.3
parthenolide (1t)	-4.58 ± 0.02	UV at 210 nm	0.6	248.3	38.8	2.85
scopoletin	-5.74 ± 0.02	UV at 320 nm	0.5	192.2	55.8	0.98
silibinin	-6.19 ± 0.02	UV at 220 nm	0.7	482.4	155.1	1.72
stigmasterol	-	Too low aqueous solubility		412.7	20.2	7.34
betulin	-			442.7	40.5	6.43
lupeol	-			426.7	20.2	7.73

* test compound was not detected in the acceptor side, log P_e values were calculated with corresponding LOQ values in this cases.

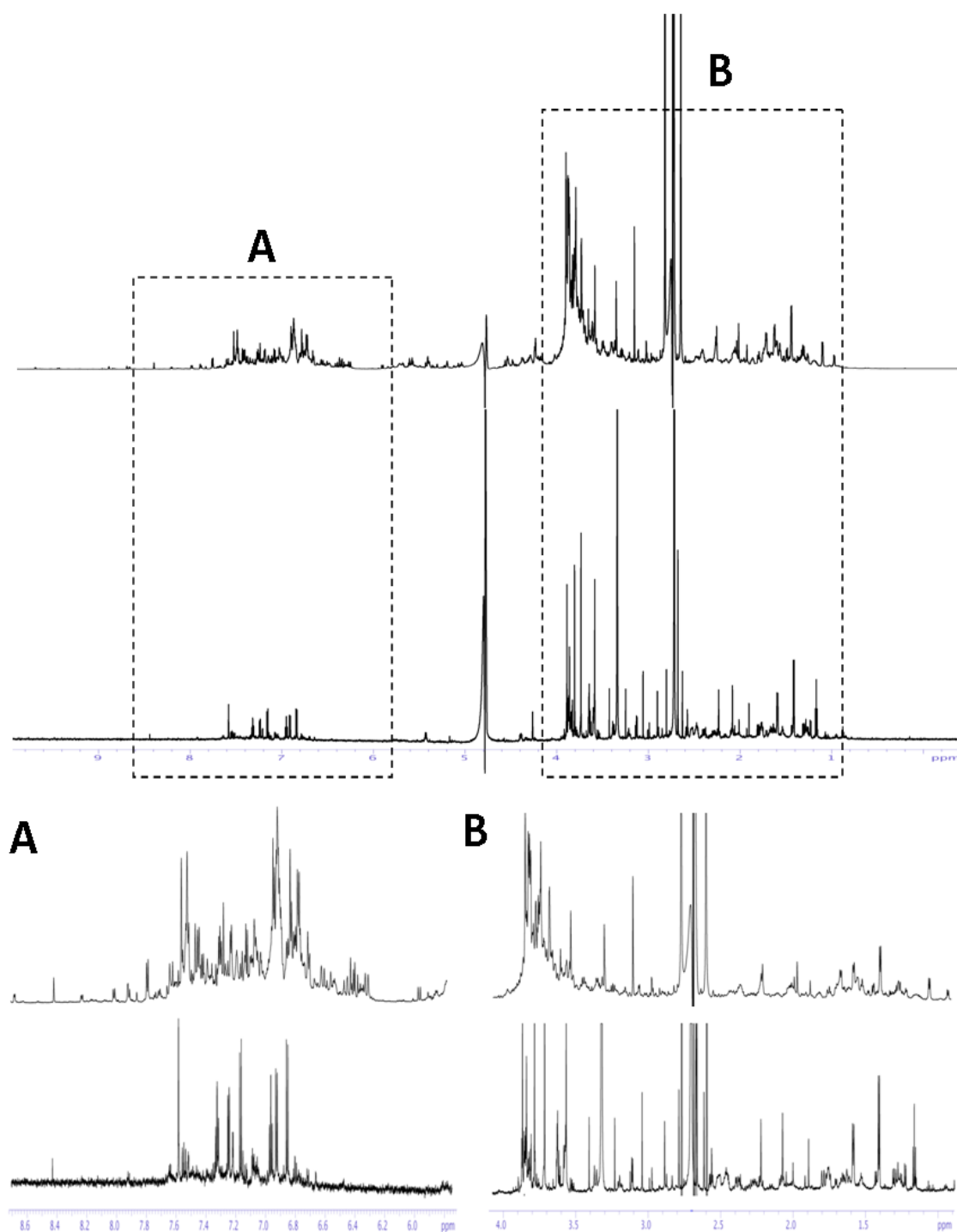


Figure A1. Demonstration of the purifying effect of PAMPA-BBB in NMR. Top: ^1H -Presat NMR spectrum (deutero PBS buffer, 800 MHz) of the crude extract of *V. major* before (top), and after PAMPA-BBB experiment (bottom). Bottom: aromatic (**A**) and aliphatic (**B**) region enlarged.

Table A4. NMR assignment of parthenolide (**1t**) and 11,13-dihydroparthenolide (**2t**) in deuterio PBS buffer at 800 MHz.

parthenolide (1t)			11,13-dihydroparthenolide (2t)		
Position	¹ H	¹³ C	¹ H	¹³ C	¹ H
1	5.31 dd (12.0, 2.9 Hz)	126.4	5.27 dd (12.0, 2.9 Hz)		
2	2.17 m	25.3	2.14 m		
	2.48 m		2.46 m		
3	1.26 m	37.3	1.22 m		
	2.17 m		2.14 m		
5	3.17 d (9 Hz)	68.8	3.08 d (9.4 Hz)		
6	4.23 t (8.8 Hz)	84.9	4.17 t (9.4 Hz)		
7	3.04 m	48.7	2.12 m		
8	1.83 m	31.5	1.77 m		
	2.17 m		2.26 m		
9	2.20 m	42.2	1.89 m		
	2.35 dd (13.0, 6.0 Hz)		2.08 m		
12	-	nd	2.56 dq (12.4, 6.9 Hz)		
13	5.84 d (3.3 Hz)	124.3	1.22 d (6.9 Hz)		
	6.29 dd (3.7, 0.3 Hz)				
14	1.71 s	17.9	1.70 s		
15	1.35 s	18.0	1.34 s		

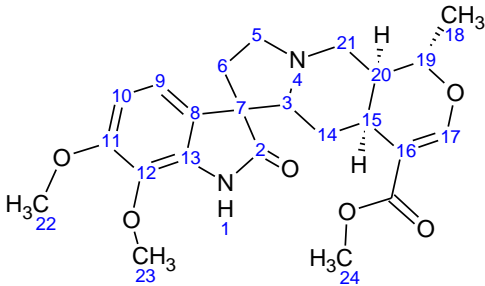
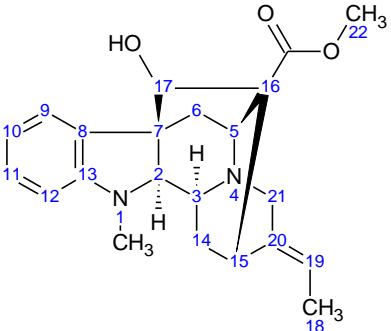
UV and MS characteristics

parthenolide (**1t**): UV (MeCN) λ_{\max} : 205 nm. MS ESI+ m/z (rel. int.): 249 (26%), 231 (100%), 213 (12%), 203 (17%), 195 (19%).

11,13-dihydroparthenolide (**2t**): UV:-. MS ESI+ m/z (rel. int.): 251 (30%), 233 (100%), 215 (12%), 205 (18%), 187 (18%).

QQQ-MS conditions: product ion mode, drying gas temperature 300 °C, nitrogen flow rate 13 L/min, nebuliser pressure 40 psi, quadrupole temperature 100 °C, capillary voltage 3000 V, fragmentor voltage 100 V, CID 2.

Table A5. Partial assignment of vincamajine (**3**) and majdine (**4**) in deuterio PBS buffer at 800 MHz.

	majdine (2v)	vincamajine (1v)
		
Position	¹ H	¹ H
9	7.16 d (8.3 Hz)	7.24 d (7.3 Hz)
10	6.84 d (8.3 Hz)	6.95 t (7.3 Hz)
11	-	7.32 t (7.3 Hz)
12	-	6.91 d (7.3 Hz)
17	7.58 s	4.26 s
18	1.41 d (6.2 Hz)	1.59 d (6.8 Hz)
19	4.43 dq (10.0, 6.2)	5.43 q (6.8 Hz)
20	1.77 dd (14.1, 9.7 Hz)	-
22	3.81 s	3.73 s
23	3.89 s	-
24	3.59 s	-
N-Me		2.66 s

UV and MS characteristics

vincamajine (**1v**): UV (MeCN) λ_{\max} : 246, 292 nm. MS ESI+ m/z (rel. int.): 367 (100%), 333 (15%), 182 (19%), 166 (11%), 158 (9%).

majdine (**2v**): UV 228 nm. MS ESI+ m/z (rel. int.): 429 (100%), 397 (79%), 220 (45%).

QQQ-MS conditions: product ion mode, drying gas temperature 350 °C, nitrogen flow rate 13 L/min, nebuliser pressure 40 psi, quadrupole temperature 100 °C, capillary voltage 4000 V, fragmentor voltage 135 V, CID 30 for vincamajine (**1v**) and CID 20 for majdine (**2v**).

Table A6. NMR assignment of epiisorosmanol (**1so**) and methyl carnosate (**2so**) in deuterio PBS buffer at 800 MHz.

	epiisorosmanol (1so)	methyl carnosate (2so)
Position	¹ H	¹ H
1	2.54 td (13.5, 4.4 Hz)	1.02 m
	2.70 m	3.20 m
2	1.65 m	1.57 m
	1.75 m	1.77 m
3	1.37 m	1.28 m
	1.51 m	1.47 m
5	1.41 d (4.2 Hz)	1.36 m
6	4.45 t (4.2 Hz)	1.83 m
		2.45 m
7	5.37 d (4.2 Hz)	2.80 m
14	6.92 s	6.71 s
15	3.21 m	3.17 m
16	1.19 d ()	1.17 d
17	1.21 d ()	1.18 d
20	-	3.73 s

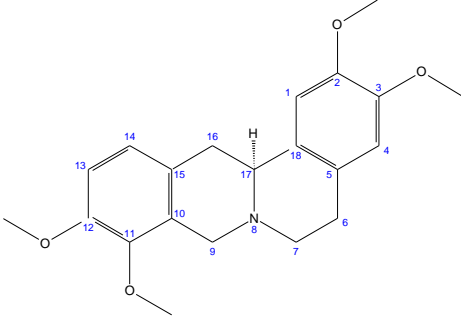
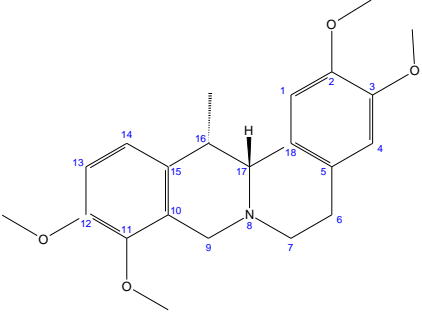
UV and MS characteristics

epiisorosmanol (**1so**): UV (MeCN) λ_{max} : 210, 230sh, 285 nm. MS ESI+ m/z (rel. int.): 345 (40%), 301 (100%), 283 (20%).

methyl carnosate (**2so**): UV (MeCN) λ_{max} : 210, 230sh, 285 nm. MS ESI+ m/z (rel. int.): 345 (100%), 301 (84%), 286 (36%).

QQQ-MS conditions: product ion mode, drying gas temperature 350 °C, nitrogen flow rate 13 L/min, nebuliser pressure 40 psi, quadrupole temperature 100 °C, capillary voltage 4000 V, fragmentor voltage 135 V, CID 10.

Table A7. NMR assignment of tetrahydropalmatine (**1c**) and corydaline (**2c**) in deuterio PBS buffer at 800 MHz.

	tetrahydropalmatine (1c)	corydaline (2c)
		
Position	¹ H	¹ H
1	6.91 s	6.91 s
4	6.99 s	6.95 s
6	2.86 m	nd
	3.10 m	nd
7	2.91 m	nd
	3.37 m	nd
9	3.82 br	nd
	4.31 d (15.8 Hz)	nd
13	7.06 m	7.10 d (9.1 Hz)
14	7.08 m	7.15 d (9.1 Hz)
16	2.83 dd (16.8, 11.8 Hz)	3.63 m
	3.58 dd (17.1, 3.5 Hz)	
17	3.93 m	nd
16-Me	-	0.92 d (7.0 Hz)
2-OMe	3.82 s	3.82 s
3-OMe	3.86 s	3.86 s
11-OMe	3.88 s	3.86 s
12-OMe	3.88 s	3.89 s

UV and MS characteristics

tetrahydropalmatine (**1c**): UV (MeCN) λ_{\max} : 235, 282 nm. MS ESI+ m/z (rel. int.): 356 (15%), 192 (100%), 165 (22%), 151 (9%).

corydaline (**2c**): UV (MeCN) λ_{\max} : 235, 282 nm. MS ESI+ m/z (rel. int.): 370 (75%), 192 (100%), 165 (65%), 151 (10%).

QQQ-MS conditions: product ion mode, drying gas temperature 350 °C, nitrogen flow rate 13 L/min, nebuliser pressure 40 psi, quadrupole temperature 100 °C, capillary voltage 4000 V, fragmentor voltage 135 V, CID 20.